

Project Review Committee

Each research project has an advisory committee appointed by the LTRC Director. The Project Review Committee (PRC) is responsible for assisting the LTRC Administrator or Manager in the development of acceptable research problem statements, requests for proposals, review of research proposals, oversight of approved research projects, and implementation of findings.

LTRC appreciates the dedication of the following Project Review Committee members in guiding this research study to fruition.

LTRC Administrator

Chris Abadie, P.E.
Materials Research Administrator

Members

Phil Arena, FHWA (Retired)
Gary Fitts, Formerly Asphalt Institute (AI)
Mike Boudreaux, LRTC
Bert Wintz, Geotechnical Investigation Engineer
Jay Collins, District 04 Lab Engineer
Don Weathers, LA Asphalt Pavement Assoc.
Jon Long, Carmeuse Lime and Stone

Directorate Implementation Sponsor

William H. Temple, LADOTD Chief Engineer

TECHNICAL REPORT STANDARD PAGE

1. Report No. FHWA/LA/432		2. Government Accession No.		3. Recipient's Catalog No.	
4. Title and Subtitle Evaluation of Superpave Mixtures Containing Hydrated Lime		5. Report Date July 2013			
		6. Performing Organization Code			
7. Author(s) Louay N. Mohammad, Ph.D., Md Sharear Kabir, Samuel Cooper, Jr., P.E., Amar Raghavendra, P.E.		8. Performing Organization Report No.			
9. Performing Organization Name and Address Louisiana Transportation Research Center 4101 Gourrier Avenue Baton Rouge, LA 70809		10. Work Unit No.			
		11. Contract or Grant No. State Project Number: 736-99-1358 LTRC Project Number: 05-1B			
12. Sponsoring Agency Name and Address Louisiana Transportation Research Center 4101 Gourrier Avenue Baton Rouge, LA 70809		13. Type of Report and Period Covered Final Report Period Covered: April 2006-June 2007			
		14. Sponsoring Agency Code			
15. Supplementary Notes					
16. Abstract <p>The use of hydrated lime in Hot-Mix Asphalt (HMA) mixtures can reduce permanent deformation, long-term aging, and moisture susceptibility of mixtures. In addition, hydrated lime increases the stiffness and fatigue resistance of mixtures. This study evaluated (1) the fundamental engineering properties of HMA mixtures containing hydrated lime as compared to conventional mixtures designed to meet the current Louisiana Superpave specifications and (2) the influence of the method of addition of hydrated lime on the mechanical properties of HMA mixtures. A Louisiana Superpave 19.0 mm Level II HMA mixture design was utilized. Siliceous limestone aggregates and three asphalt binders, a neat PG 64-22 and two Styrene-Butadiene (SB) polymer modified binders meeting Louisiana specifications for PG 70-22M and PG 76-22M were included. Based on the same mixture design, three conventional and six hydrated lime treated HMA mixtures were developed. The conventional mixtures contained no hydrated lime and the three aforementioned asphalt binders respectively. The lime treated mixtures were produced by incorporating hydrated lime into the HMA mixture in two ways: "slurry" or "paste" method when hydrated lime was mixed with the aggregate as slurry and "dry" or "no-paste" method when dry hydrated lime was blended with the asphalt binders. For each lime treatment method, three HMA mixtures were produced using the three identical asphalt cements (PG 64-22, PG 70-22M, and PG 76-22M) utilized in the three conventional mixtures. The overall results from mechanistic tests on HMA mixtures and rheological tests on asphalt binders indicated that the addition of hydrated lime improved the permanent deformation characteristics of the HMA mixtures. This improvement was substantial particularly at higher testing temperatures for mixtures containing polymer modified asphalt binders.</p>					
17. Key Words Hot-Mix Asphalt, Hydrated lime, Indirect Tensile Strength and Strain test, Semi-Circular Bend test Dissipated Creep Strain Energy test, Simple Performance Test(s), Hamburg Loaded Wheel Tracking test			18. Distribution Statement Unrestricted. This document is available through the National Technical Information Service, Springfield, VA 21161.		
19. Security Classif. (of this report) N/A		20. Security Classif. (of this page) N/A		21. No. of Pages 126	
				22. Price	

Evaluation of Superpave Mixtures Containing Hydrated Lime

by

Louay N. Mohammad, Ph.D.

Professor of Civil and Environmental Engineering
Director, Engineering Materials Characterization Research Facility

Md Sharear Kabir

Graduate Research Assistant
Department of Civil and Environmental Engineering
Louisiana State University

Samuel Cooper, Jr., P.E.

Associate Director, Technology Transfer and Training

Amar Raghavendra, P.E.

Applications Engineering Manager

Louisiana Transportation Research Center
4101 Gourrier Ave.
Baton Rouge, LA 70808

Louisiana Transportation Research Center

Research Project No. 05-1B

State Project No. 736-99-1358

The contents of this report reflect the views of the author/principal investigator who is responsible for the facts and accuracy of the data presented herein. The contents of this report do not necessarily reflect the views or policies of the Louisiana Department of Transportation and Development or the Louisiana Transportation Research Center. This report does not constitute a standard, specification, or regulation.

July 2013

ABSTRACT

The use of hydrated lime in Hot-Mix Asphalt (HMA) mixtures can reduce permanent deformation, long-term aging, and moisture susceptibility of mixtures. In addition, hydrated lime increases the stiffness and fatigue resistance of mixtures. This study evaluated (1) the fundamental engineering properties of HMA mixtures containing hydrated lime as compared to conventional mixtures designed to meet the current Louisiana Superpave specifications and (2) the influence of the method of addition of hydrated lime on the mechanical properties of HMA mixtures.

A Louisiana Superpave 19.0 mm Level II HMA mixture design was utilized in this study. Siliceous limestone aggregates and three asphalt binders, a neat PG 64-22 and two Styrene-Butadiene (SB) polymer modified binders meeting Louisiana specifications for PG 70-22M and PG 76-22M, were included in this study. Based on the same mixture design, three conventional and six hydrated lime treated HMA mixtures were developed. The conventional mixtures contained no hydrated lime and the three aforementioned asphalt binders, respectively. The lime treated mixtures were produced by incorporating hydrated lime into the HMA mixture in two ways: “slurry” or “paste” method when hydrated lime was mixed with the aggregate as slurry and “dry” or “no-paste” method when dry hydrated lime was blended with the asphalt binders. For each lime treatment method, three HMA mixtures were produced using the three identical asphalt cements (PG 64-22, PG 70-22M, and PG 76-22M) utilized in the three conventional mixtures.

Mechanistic tests namely, Indirect Tensile Strength (ITS), Semi-Circular Bend (SCB), Dissipated Creep Strain Energy (DSCE), Dynamic Modulus, Flow Number, Flow Time, and Loaded Wheel Tracking (LWT) tests were conducted to define the permanent deformation and endurance life of HMA mixtures with and without hydrated lime. In addition, physical and rheological tests on asphalt binders were performed. The overall results indicated that the addition of hydrated lime improved the permanent deformation characteristics of the HMA mixtures. This improvement was substantial particularly at higher testing temperatures for mixtures containing polymer modified asphalt binders.

ACKNOWLEDGEMENTS

The U.S. Department of Transportation, Federal Highway Administration (FHWA), the Louisiana Department of Transportation and Development (LADOTD), and the Louisiana Transportation Research Center (LTRC) financially supported this research project. The assistance of the asphalt laboratory staff at LTRC is greatly appreciated. The guidance of the Project Review Committee to this research project is also greatly appreciated.

IMPLEMENTATION STATEMENT

Based on the results of this study, specifications were developed and added to the LADOTD supplemental specifications for the HMA mixture and asphalt cement binder to allow the use of the hydrated lime in HMA mixtures. The hydrated lime treatment has shown excellent promise to improve the permanent deformation characteristics HMA pavements. Therefore, hydrated lime can be added to asphalt mixtures to construct HMA pavements. The use of hydrated lime in Louisiana's Superpave mixes should also provide for a longer life expectancy of the pavement structure.

Specifically, it is recommended that Louisiana specification for asphalt mixture section 502 be amended to state, "when adding hydrated lime, in accordance with section 503.5 of the standard specifications, to mixtures containing PG 70-22M binder then it may be substituted for mixtures containing PG 76-22M."

It is further recommended that this specification be promulgated at first regionally to those production facilities that are capable of the addition of hydrated lime to allow for the validation of the laboratory test results obtained from this study.

TABLE OF CONTENTS

ABSTRACT.....	iii
ACKNOWLEDGEMENTS.....	v
IMPLEMENTATION STATEMENT.....	vii
TABLE OF CONTENTS.....	ix
LIST OF TABLES.....	xi
LIST OF FIGURES.....	xiii
INTRODUCTION.....	1
OBJECTIVES.....	5
SCOPE.....	7
METHODOLOGY.....	9
Material Properties and Mixture Design.....	9
Aggregate Properties.....	9
Hydrated Lime.....	9
Asphalt Binder Characterization.....	10
Asphalt Mixture Design.....	11
HMA Specimen Preparation.....	12
Laboratory Tests for HMA Mixture Characterization.....	18
DISCUSSION OF RESULTS.....	21
Statistical Analysis Methods and Approaches.....	21
Asphalt Binder Test Results.....	23
Laboratory Characterization of Mixtures.....	27
Indirect Tensile Strength (ITS) Test Results.....	27
Semi-Circular Bend (SCB) Test Results.....	33
Dissipated Creep Strain Energy (DCSE) Test Results.....	35
Dynamic Modulus (E*) Test Results.....	40
Flow Number Test Results.....	48
Flow Time Test Results.....	52
Loaded Wheel Tracking (LWT) Test Results.....	55
Correlation between Test Results.....	59
Correlation between Binder and Mixture Properties.....	59
Correlation between Fatigue Related Properties of HMA Mixtures.....	61
Correlation between Permanent Deformation Properties of HMA Mixtures.....	63
CONCLUSIONS.....	67
RECOMMENDATIONS.....	69
REFERENCES.....	71

APPENDIX A.....	75
Descriptions of Test Procedures	75
Indirect Tensile Strength (ITS) Test.....	75
Semi-Circular Bend (SCB) Test	76
Dissipated Creep Strain Energy (DCSE) Test	78
Dynamic Modulus $ E^* $ Test.....	79
Flow Number Test	80
Flow Time Test.....	81
Loaded Wheel Tracking (LWT) Test	82
APPENDIX B.....	83
Individual Test Results of Binders.....	83

LIST OF TABLES

Table 1	Aggregate consensus properties.....	9
Table 2	Aggregate gradation for hydrated lime.....	10
Table 3	LADOTD performance graded asphalt cement specification.....	11
Table 4	Job mix formula.....	12
Table 5	Test factorial.....	18
Table 6	HMA mixture performance test conditions.....	19
Table 7	LADOTD performance graded asphalt cement specification and test results.....	24
Table 8	ITS test results at 25°C.....	31
Table 9	ITS test results at 40°C.....	32
Table 10	Summary of the DCSE test results.....	36
Table 11	DCSE test results for 64 HMA mixture group.....	37
Table 12	DCSE test results for 70 HMA mixture group.....	38
Table 13	DCSE test results for 76 HMA mixture group.....	38
Table 14	Comparison of DCSE results between mixtures 64LS, 64LM, and 70CO.....	39
Table 15	Comparison of DCSE results between mixtures 70LS, 70LM, and 76CO.....	39
Table 16	Comparison of DCSE results for conventional mixture group.....	39
Table 17	Statistical analyses on dynamic modulus test data.....	48
Table 18	Flow number test results for 64 HMA mixture group.....	49
Table 19	Flow number test results for 70 HMA mixture group.....	50
Table 20	Flow number test results for 76 HMA mixture group.....	50
Table 21	Comparison of flow number between 64LS, 64LM, and 70CO mixtures.....	51
Table 22	Comparison of flow number between 70LS, 70LM, and 76CO mixtures.....	51
Table 23	Comparison of flow number between conventional mixtures.....	52
Table 24	Flow time test results for 64 HMA mixture group.....	53
Table 25	Flow time test results for 70 HMA mixture group.....	53
Table 26	Flow time test results for 76 HMA mixture group.....	54
Table 27	Comparison of flow time between mixtures 64LS, 64LM, and 70CO.....	54
Table 28	Comparison of flow time between mixtures 70LS, 70LM, and 76CO.....	55
Table 29	Comparison of flow time between conventional HMA mixture groups.....	55
Table 30	LWT results for 64 HMA mixture group.....	57
Table 31	LWT results for 70 HMA mixture group.....	57
Table 32	LWT results for 76 HMA mixture group.....	58
Table 33	Comparisons of LWT results between 64LS, 64LM, and 70CO mixtures.....	58
Table 34	Comparisons of LWT results between 70LS, 70LM, and 76CO mixtures.....	59
Table 35	Comparisons of LWT results between conventional HMA mixture groups.....	59

Table 36	Criteria for goodness of fit statistical parameters	63
Table 37	Statistical measure of goodness of fit	65

LIST OF FIGURES

Figure 1 High-speed mixer	10
Figure 2 Aggregate gradation curves	14
Figure 3 Sample fabrication for the SCB test	14
Figure 5 Cored sample and waste ring	15
Figure 6 Grinding operation	16
Figure 7 Grinded specimen and its ends	16
Figure 8 Fixation of Metallic Studs on E* Specimen	16
Figure 9 Instrumentation for DCSE test specimen	17
Figure 10 Master curves for asphalt binders	25
Figure 11 Binder shear modulus isotherms	26
Figure 12 Binder phase angle isotherms	26
Figure 13 ITS strength results at 25°C	27
Figure 14 ITS strength results at 40°C	27
Figure 15 ITS results strain at 25°C	28
Figure 16 ITS strain results at 40°C	28
Figure 17 TI results at 25°C	29
Figure 18 TI results at 40°C	29
Figure 19 Aging index – from TI result	33
Figure 20 SCB test results	34
Figure 21 Aging indices computed from SCB test	35
Figure 22 DCSE test results for all mixtures	37
Figure 23 Dynamic modulus isotherms at low temperatures	40
Figure 24 Dynamic modulus isotherms at intermediate and high temperatures	41
Figure 25 Variation of phase angles with dynamic modulus	42
Figure 26 Phase angle isotherms at low temperatures	42
Figure 27 Phase angle isotherms at intermediate and high temperatures	43
Figure 28 Comparison of E* results between 70CO, 64LS, and 64LM mixtures	44
Figure 29 Comparison of E* results between 76CO, 70LS, and 70LM mixtures	45
Figure 30 Comparison of E* results between conventional mixtures	45
Figure 31 Rutting factor at 5 Hz and 54.4°C	46
Figure 32 Fatigue factor at 5 Hz and 25°C	47
Figure 33 Flow number test results for all mixtures	49
Figure 34 Flow time test results for all mixtures	53
Figure 35 LWT test results – rut depth	56
Figure 36 LWT test results – rut profile	56

Figure 37	Correlation – binder and mixture stiffness	60
Figure 38	Correlation – binder and mixture rut factor at 5 Hz and 54.4°C	61
Figure 39	Correlation – TI and J_c	62
Figure 40	Correlation – DCSE and TI.....	62
Figure 41	Correlation – DCSE and J_c	62
Figure 42	Correlation – fatigue factor and TI.....	63
Figure 43	Correlation – fatigue factor and J_c	63
Figure 44	Correlation – flow number and rut depth	64
Figure 45	Correlation – flow time and rut depth	64
Figure 46	Correlation – E^* and rut depth	64
Figure 47	Correlation – rut factor and rut depth	64

INTRODUCTION

In the mid-1990s LADOTD revised its HMA mixture specifications. Some of those major changes included requiring larger nominal maximum aggregate size in its aggregate structure and significant reduction in the amount of natural sands (fine aggregates) used in the HMA mixtures. Later, in 2003, LADOTD implemented the Superpave mixture design method [1, 2]. Under the Superpave system, most HMA mixtures are encouraged to use coarse gradations that pass below the maximum density line, which eventually leads to a reduction in the amount of fine aggregate materials from the aggregate structure. This lower fine aggregate content in combination with high Voids in the Mineral Aggregate (VMA) can result in Superpave mixtures with high permeability, less resistance to age hardening, and poor rut resistance [3]. The addition of quality filler materials can be a possible solution to these concerns. Fillers are considered as fine mineral particles smaller than about 75 μm (70 to 100 percent passing through a No. 200 sieve) in size [4]. In general, fillers improve the cohesion of the binder and increase the stiffness of HMA mixtures.

The use of fillers in Hot-Mix Asphalt (HMA) concrete is not a new concept. In general, fillers improve the cohesion of the binder and increase the stiffness of HMA mixtures. Puzinauskas [5] employed two theories to explain the stabilizing effects of fillers in HMA mixtures. According to the first theory, filler serves to fill out the voids between aggregate particles thereby increasing the density and strength of the compacted mixture. The second theory presumes that the finer particles of filler which remain suspended in the asphaltic binder produce mastic, a denser, thicker, and tougher liquid than bitumen alone. Thus, filler can increase the film thickness, improve the cohesion of the binders, and increase the stiffness of the asphalt mixtures depending upon the type of filler and the type of asphalt used. However, an excess amount of filler can also lead to a greater mixture-stiffness and a loss of adhesive qualities of the binder [6].

Hydrated lime has gained considerable recognition as a useful additive (filler) for improving the performance of the asphalt pavements since the early 1900s. Metcalf conducted a survey on the use of hydrated lime as a filler in tar or bitumen road surfacing, concluding that hydrated lime modified asphalt mixtures reduced stripping [7]. Afterwards in numerous studies [6,8-16], hydrated lime was reported to improve the resistance against the moisture induced damage of HMA mixtures. By maintaining a good adhesion between the aggregate and the asphalt cement in the presence of water, hydrated lime worked successfully as an antistripping agent. Its ability to reduce viscosity building polar components in the asphalt binder enabled hydrated lime to show effect as an oxidation reducing agent. In addition,

hydrated lime can increase mixture stiffness by filling air voids in the mixture with its tiny particles, which makes it an effective mineral filler to resist rutting and improve toughness of the mixture.

The addition of hydrated lime in HMA mixtures can be a cost effective way to improve pavement performance against failure. In Nevada, long-term pavement performance data indicated that pavements using lime-treated mixtures showed better performance with fewer requirements for maintenance and rehabilitation compared to the pavements using untreated mixtures when environmental and traffic conditions were similar. The analysis of the impact of lime on pavement life indicated that lime treatment extended performance life of HMA pavements by an average of three years [17].

Hydrated lime can be considered as a multifunctional additive with potential benefits. Petersen et al. reported that hydrated lime treatment reduced asphalt age hardening, increased the high-temperature stiffness of unaged asphalts, reduced the stiffness in aged asphalts at high temperatures, and increased the asphalt tensile-elongation at low temperatures [18]. They also stated that the relative response to hydrated lime treatment varied as a function of asphalt cement source. A similar observation was reported by Lesueur and Little [19] in their study.

Hydrated lime was found to improve the fatigue life and aging properties of asphalt binders [20, 21]. However, the degree of effectiveness was dependant on the type of asphalt binder. In another study, Little and Peterson [22] reported that the inclusion of hydrated lime particles toughened the mastic and significantly impacted the rate and level of microcrack-induced damage, microdamage healing, and the plastic and viscoelastic flow in mastics across a wide range of temperatures, which made the mixture more resistant to fracture and crack propagation.

Mechanistic laboratory tests indicated that hydrated lime has the potential to improve permanent deformation characteristics of HMA mixtures. Bari and Witczak evaluated the dynamic modulus (E^*) of HMA mixtures with varying hydrated lime contents [23]. The researchers concluded that hydrated lime may also be used to improve the stiffness characteristics and performance of HMA mixtures in addition to serving as an anti-stripping agent and filler. Another study by Aschenbrener et al. [24] at the Colorado Department of Transportation, utilized the Hamburg Wheel Tracking Device to evaluate the performance of several HMA mixtures, and concluded that hydrated lime significantly reduced the rut depth for all mixtures.

Recently, Atud et al. evaluated the laboratory performance-based properties (moisture damage and rutting resistance) of lime modified asphalt mixtures in comparison to the polymer modified asphalt mixtures [25]. Both asphalt binder test (rheological properties, creep and recovery tests) and asphalt mixture test (ITS, resilient modulus, and LWT tests) results indicated that hydrated lime significantly improved both the moisture damage and rutting resistance of mixture, whereas the polymer improved the rutting resistance only.

LADOTD also previously evaluated the influence of hydrated lime as an antistrip additive both in slurry and dry applications. In that study, Paul [11] reported that hydrated lime incorporated in the slurry condition outperformed all other antistrip additives considered to resist moisture susceptibility problems, whereas hydrated lime incorporated in the dry condition provided no difference in performance between antistrip additives and no additives. In a later study, Mohammad et al. reported an improvement in the permanent deformation characteristics and fatigue endurance of the lime-modified HMA mixtures designed by the Marshall Mix design method [15]. The improvement was apparent particularly at higher testing temperatures.

This paper presents the findings of the evaluation of fundamental engineering properties of HMA mixtures containing hydrated lime to conventional mixtures designed to meet the Louisiana Superpave specifications.

OBJECTIVES

The primary objective of this study was to compare the fundamental engineering properties of HMA mixtures containing hydrated lime with the conventional mixtures designed to meet the Louisiana Superpave specifications. A secondary objective was to evaluate the influence of the method of adding hydrated lime on the mechanical properties of the resulting HMA mixtures. The third objective was to compare the laboratory performance of hydrated lime treated mixtures containing a lower “PG graded” asphalt binder with the conventional mixtures containing a relatively higher “PG graded” asphalt binder.

SCOPE

A Louisiana Superpave 19.0 mm Nominal Maximum Aggregate Size Level II (3-30 million ESALs) HMA mixture was designed and examined in this study. The test factorial included siliceous limestone aggregates and three asphalt binders, a neat PG 64-22 and two Styrene-Butadiene (SB) polymer modified binders meeting Louisiana specifications for PG 70-22M and PG 76-22M. Based on the same mixture design, three conventional and six hydrated lime treated HMA mixtures were developed. The conventional mixtures contained no hydrated lime and the three aforementioned asphalt binders, respectively. Lime treated mixtures were produced by incorporating hydrated lime into the HMA mixture in two ways: “slurry” or “paste” method when hydrated lime was mixed with the aggregate as slurry and “dry” or “no-paste” method when dry hydrated lime was blended with the asphalt binders. For each lime treatment method, three HMA mixtures were produced using the three identical asphalt cements (PG 64-22, PG 70-22M, and PG 76-22M) utilized in the three conventional mixtures.

Physical and rheological tests were performed on asphalt binders to characterize their conformance to Louisiana binder specifications [2]. In addition to mixture characterization tests, ITS, SCB, DCSE, Simple Performance (Dynamic Modulus, Flow Number, and Flow Time tests), and LWT tests were conducted to define the permanent deformation (stability) and fatigue life (durability) of HMA mixtures considered in this study.

METHODOLOGY

The experimental program included in this study investigated the potential benefits of hydrated lime to improve the permanent deformation and fatigue failure performance of HMA mixtures. A series of laboratory tests were performed on asphalt binders and HMA mixtures considered in this study.

Material Properties and Mixture Design

Aggregate Properties

Siliceous limestone commonly used in highway construction in Louisiana was evaluated in this study. A washed sieve analysis was performed on aggregates in accordance with AASHTO T 27 to determine as-received gradation from the source. Table 1 presents the test protocols, specifications, and corresponding properties of aggregate used in this study.

Table 1
Aggregate consensus properties

Property	Test Protocol	Specification	Conventional Mixtures	Lime Treated Mixtures
CAA, %	ASTM D 5821	95+, 2 face	100	100
FAA, %	AASHTO T 304	45+	46	47
F&E, %	ASTM D 4791	10-, 5:1 ratio	0	0
SE,%	AASHTO T 176	45+	62	65

*Note: CAA: Coarse Aggregate Angularity, FAA: Fine Aggregate Angularity
F&E: Flat and Elongated Particles, SE: Sand Equivalent*

Hydrated Lime

Hydrated lime is a naturally occurring mineral derived from limestone or chalk. In this study, hydrated lime was incorporated at a rate of 1.5 percent of the total aggregate weight into the HMA mixture in two ways: “slurry” or “paste” and “dry” or “no-paste.” In the paste method, hydrated lime was mixed with water in the ratio (by weight) of 1:3. Later, the hydrated lime slurry was mixed thoroughly with the dry aggregate blend. On the other hand, in the “no-paste” method, hydrated lime was blended with the asphalt cement and then the lime-modified binder was used to prepare the asphalt mixtures. Specific gravities (e.g., G_{sb} and G_{sa}) and the gradation of the hydrated lime that was used in this study are shown in Table 2.

Table 2
Aggregate gradation for hydrated lime

Sieve Size Metric (U.S.)	Percent Passing (%)
4.75 mm (No. 4)	100
2.36 mm (No. 8)	100
1.18 mm (No. 16)	100
0.6 mm (No. 30)	100
0.3 mm (No. 50)	100
0.150 mm (No. 100)	95
0.075 mm (No. 200)	85
G_{sb}	2.555
G_{sa}	2.621

Asphalt Binder Characterization

Two sets of asphalt cement binders were used in this study, while three binders were included in each set. The first set contained two SB elastomeric polymer modified asphalt cements meeting Louisiana specifications for PG 76-22M, PG 70-22M, and a neat PG 64-22 asphalt. The second set contained three binders formulated by the addition of 1.5 percent hydrated lime (by total aggregate weight) to PG 76-22M, PG 70-22M, and PG 64-22 binders respectively. A high-speed mixer (Figure 1) was used to blend the hydrated lime and binder at 320°F for 20 minutes. This mixing process was aimed to simulate hydrated lime injected into the drum mixer.



Figure 1
High-speed mixer

Table 3 presents current LADOTD specifications for the three binder types used in this study.

Table 3
LADOTD performance graded asphalt cement specification

Property	AASHTO Test Method	Specification		
		PG 76-22M	PG 70-22M	PG 64-22
Tests on Original Binder				
Rotational Viscosity @ 135°C, Pa.s	T 316	3.0-	3.0-	3.0-
Dynamic Shear, 10 rad/s, G*/Sin Delta, kPa	T 315	1.00+ @ 76°C	1.00+ @ 70°C	1.30+ @ 64°C
Force Ductility Ratio F2/F1 (4°C, 5 cm/min, F2 @ 30 cm elongation)	T 300	0.30+	N/A	N/A
Force Ductility, (4°C, 5 cm/min, 30 cm elongation, kg)	T 300	N/A	0.23+	N/A
Tests on RTFO Residue				
Dynamic Shear, 10 rad/s, G*/Sin Delta, kPa	T 315	2.20+ @ 76°C	2.20+ @ 70°C	2.20+ @ 64°C
Elastic Recovery, 25°C, 10 cm elongation, %	T 301	60+	40+	N/A
% Mass Loss	T 240	1.00-	1.00-	1.00-
Tests on PAV Residue				
Dynamic Shear, @ 25°C, 10 rad/s, G*Sin δ, kPa	T 315	5000-	5000-	5000-
Bending beam Creep Stiffness, S, Mpa	T 313	300-	300-	300-
Bending beam Creep Slope, m value	T 313	0.300+	0.300+	0.300+

Note: N/A: Not Applicable

Asphalt Mixture Design

The Job Mix Formula of all mixtures used in this study are summarized in Table 4. A Louisiana Superpave Level II design ($N_{\text{initial}} = 8-$, $N_{\text{design}} = 100-$, $N_{\text{final}} = 160$ -gyrations) was performed according to AASHTO T 312-04 and Section 502 of the “Louisiana Standard Specifications for Roads and Bridges” [2]. Also, the fine aggregate gradation was adjusted to account for the addition of the hydrated lime. Figure 2 represents graphically the aggregate

gradation used in this study. It can be noticed that mixtures containing hydrated lime had lower optimum asphalt cement content than the mixtures with no hydrated lime. The decrease might be attributed to the fact that the No. -270 (0.053mm) sieve size fraction of the hydrated lime acted as an extender which caused their reduction in the design binder content of the HMA mixture containing hydrated lime.

HMA Specimen Preparation

AASHTO T 312-04 procedure was followed to prepare the HMA specimens for this study. The specimen preparation was a two-step process. First, the HMA mixture was prepared and then adequate amount of mixture was compacted to the specified dimensions. Four sizes of specimens were fabricated for the fundamental engineering property tests included in this study. These include 101.6 mm in diameter by 63.5 mm high, 150 mm diameter by 170 mm high, 150mm by 57 mm high cylindrical specimens and 80 x 260 x 320 mm beam specimens. The cylindrical specimens were compacted with the Superpave Gyratory Compactor (SGC) while the beam samples were compacted using a Kneading Compactor.

The 101.6 mm by 63.5 mm high cylindrical specimens and 80 x 260 x 320 mm beams were employed in ITS and LWT tests, respectively. For the SCB test, semi-circular shaped specimens were prepared by slicing the 150 mm by 57 mm high cylindrical specimens along their central axes into two equal semi-circular samples. A vertical notch was then introduced along the symmetrical axis of each semi-circular specimen. Three nominal notch depths of 25.4, 31.8, and 38.0 mm were introduced using a special saw blade of 3.0 mm thickness, where each sample contained a single vertical notch along its symmetrical axis. Figure 3 represents the fabrication process of SCB specimens.

Table 4
Job mix formula

Mixture Designation	64CO	64LS	64LM	70CO	70LS	70LM	76CO	76LS	76LM	
Mix Type	19.0 mm Superpave									
Aggregate Blend	#67 LS	37%	38%	38%	37%	38%	38%	37%	38%	38%
	#78 LS	25%	25.5%	25.5%	25%	25.5%	25.5%	25%	25.5%	25.5%
	#11 LS	29%	21%	21%	29%	21%	21%	29%	21%	21%
	CS	9%	14%	14%	9%	14%	14%	9%	14%	14%
	HL	N/A	1.5%	N/A	N/A	1.5%	N/A	N/A	1.5%	N/A
Binder type	PG64-22	PG64-22	PG64-22+HL	PG70-22M	PG70-22M	PG76-16	PG76-22M	PG76-22M	PG76-22M	PG88-16
% G _{mm} at N _{ini}	87.0	87.0	87.0	87.0	87.0	87.0	87.0	87.0	87.0	87.0
% G _{mm} at N _{Max}	97.6	97.7	97.7	97.6	97.7	97.7	97.6	97.7	97.7	97.7
Binder content, %	4.0	3.6	3.6	4.0	3.6	3.6	4.0	3.6	3.6	3.6
Design air void, %	3.7	3.6	3.6	3.7	3.6	3.6	3.7	3.6	3.6	3.6
VMA, %	13	13	13	13	13	13	13	13	13	13
VFA, %	68	69	69	68	69	69	68	69	69	69
Metric (U. S.) Sieve	Blend Gradation									
37.5 mm (1½ in.)	100	100	100	100	100	100	100	100	100	100
25 mm (1 in.)	100	100	100	100	100	100	100	100	100	100
19 mm (¾ in.)	98	98	98	98	98	98	98	98	98	98
12.5 mm (½ in.)	77	76	76	77	76	76	77	76	76	76
9.5 mm (⅜ in.)	61	60	60	61	60	60	61	60	60	60
4.75 mm (No. 4)	41	40	40	41	40	40	41	40	40	40
2.36 mm (No. 8)	29	30	30	29	30	30	29	30	30	30
1.18 mm (No. 16)	21	23	23	21	23	23	21	23	23	23
0.6 mm (No. 30)	15	17	17	15	17	17	15	17	17	17
0.3 mm (No. 50)	8	9	9	8	9	9	8	9	9	9
0.075 mm (No. 200)	4.6	5.0	5.0	4.6	5.0	5.0	4.6	5.0	5.0	5.0

Note: N/A: Not Applicable, LS: Limestone, HL: Hydrated Lime, CS: Coarse Sand
64CO: Conventional HMA Mixture containing PG 64-22 and no HL.
64LS: HL treated HMA Mixture containing PG 64-22. HL was added in "slurry" or "paste" method.
64LM: HMA Mixture produced from HL treated PG 64-22. HL was mixed with the binder in "dry" or "no-paste" method.
70CO: Conventional HMA Mixture containing PG 70-22M and no HL.
70LS: HL treated HMA Mixture containing PG 70-22M. HL was added in "slurry" or "paste" method.
70LM: HMA Mixture produced from HL treated PG 70-22M. HL was mixed with the binder in "dry" or "no-paste" method.
76CO: Conventional HMA Mixture containing PG 76-22M and no HL.
76LS: HL treated HMA Mixture containing PG 76-22M. HL was added in "slurry" or "paste" method
76LM: HMA Mixture produced from HL treated PG 70-22M. HL was mixed with the binder in "dry" or "no-paste" method.

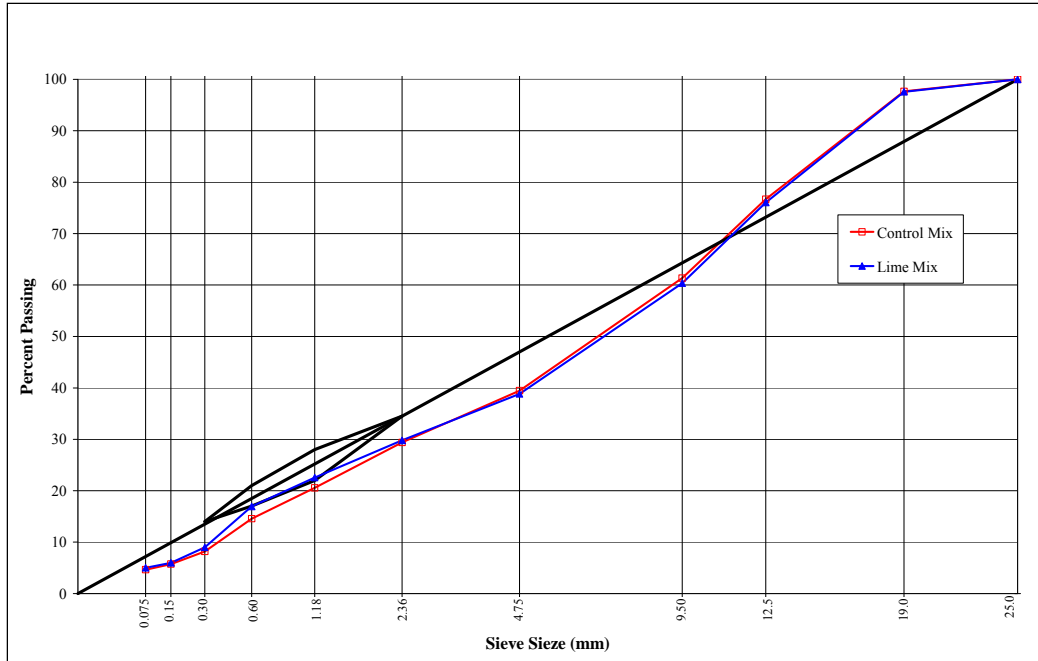


Figure 2
Aggregate gradation curves

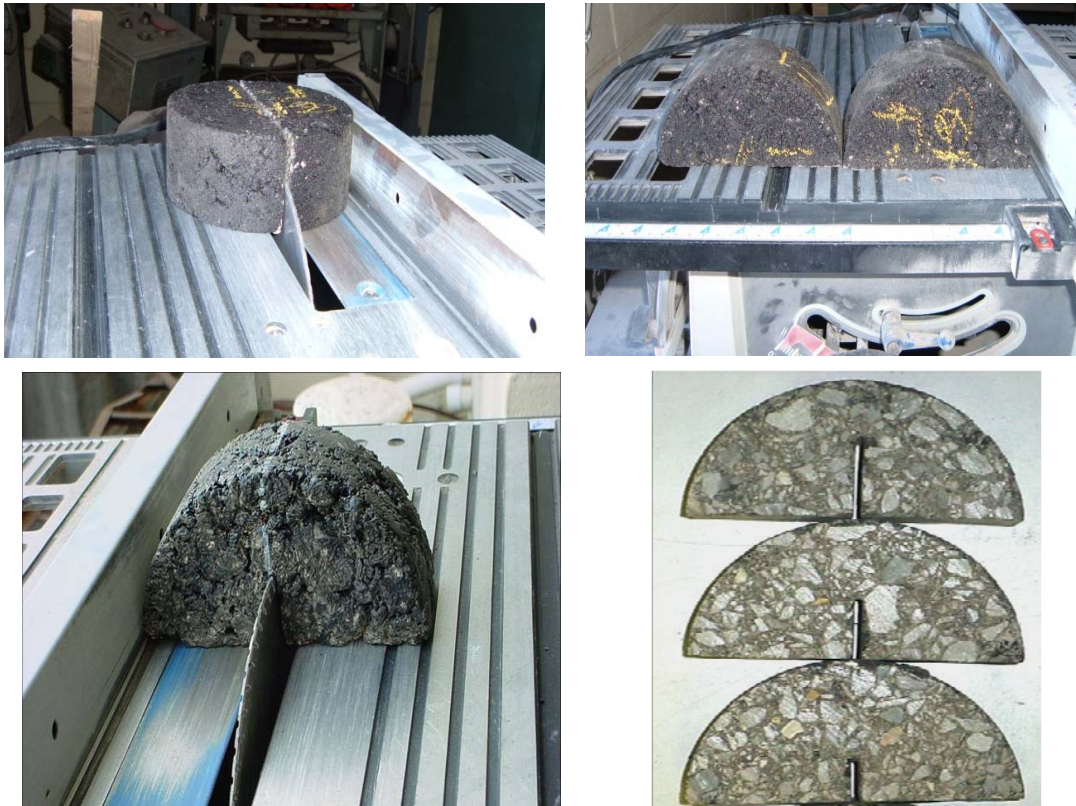


Figure 3
Sample fabrication for the SCB test

The cylindrical specimens for the Simple Performance Tests (i.e., Dynamic Modulus, Flow Number and Flow Time tests) were fabricated by coring and sawing 100 mm diameter by 150 mm high test specimens from the middle of 150 mm diameter by 170 mm high SGC compacted cylindrical specimens. The specimen preparation procedure described in the Appendix of NCHRP Report 465 and AASHTO TP-62 was followed to prepare Simple Performance Tests specimens [26]. As shown in Figure 4, a portable core drilling machine was used to core a 100 mm diameter specimen from the center of the 150 mm diameter cylindrical specimen (Figure 5). The height of the specimen was then trimmed to 150 mm using a grinding machine as shown in Figure 6. Specimens were grinded approximately equal from each end of the cored sample (Figure 7) to ensure the uniformity of the specimens.

The specimens for Dynamic Modulus test needed more fabrication works. Six metallic studs were fixed on one specimen surface so that three Linear Variable Displacement Transducers (LVDTs) could be mounted on the specimen to measure the axial deformation of the specimen. A vertical gauge length of 70 mm was maintained between two studs. Devcon Plastic Steel 5 Minute Epoxy Putty_(SF) 10240 was used as the adhesive while a pressure machine (Figure 8) was used to attach the studs by applying pressure for thirty minutes.



Figure 4
Coring operation



Figure 5
Cored sample and waste ring



Figure 6
Grinding operation



Figure 7
Grinded specimen and its ends

The SGC compacted 150 mm diameter by 57 mm high cylindrical specimens were employed in DCSE testing after necessary fabrication works. The height of the cylindrical specimens was trimmed down to 50 mm to create a smooth surface to attach the deflection-measuring studs properly. The grinding machine shown in Figure 6 was used to grind approximately 3.5 mm from each side of the specimen. Four gauge points were installed to hold two units of single integral, bi-axial extensometers Model 3910 from Epsilon Technology on each face of the specimen along the vertical and horizontal axis. The gauge points were installed in such a way that they allowed the deflection measurement of the sample over a gauge length of 3 in. A fixture plate as shown in Figure 9 was employed to fix the metallic studs (gauge points) on the specimen.

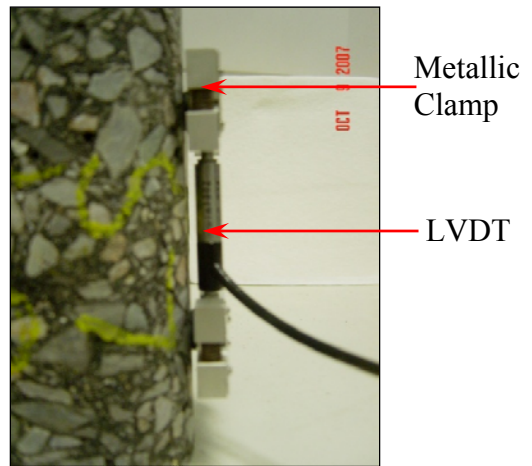


Figure 8
Fixation of Metallic Studs on E* Specimen

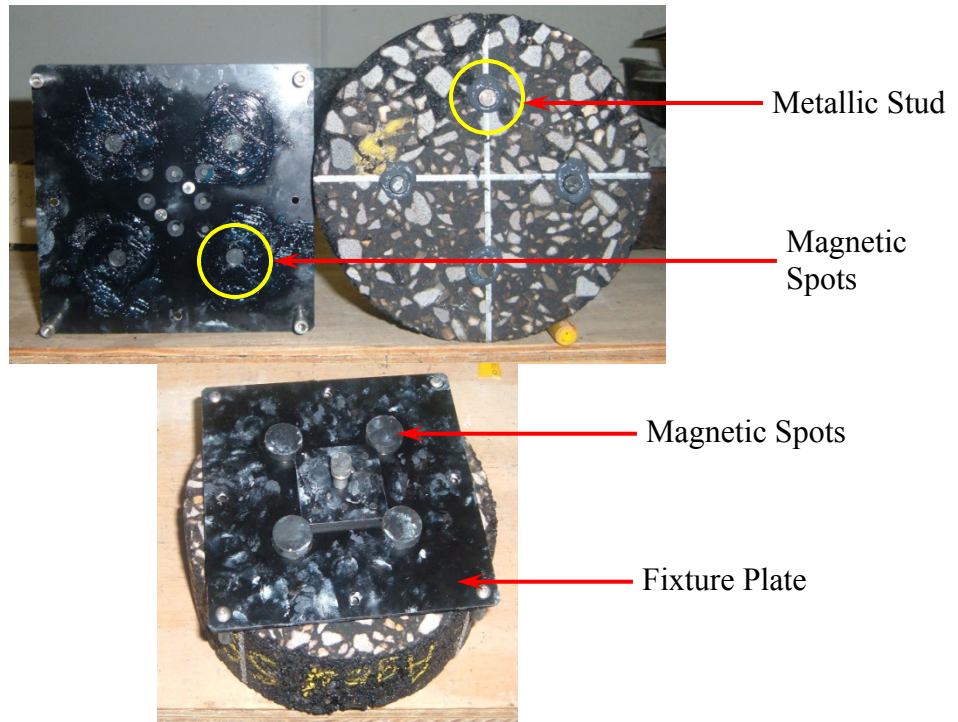


Figure 9
Instrumentation for DCSE test specimen

Triplicate specimens were prepared for each individual HMA mixture test included in this study. The only exception was for the LWT test where two specimens were tested. Therefore, a total of 288 specimens were required to complete this study. Table 5 presents the test factorial adopted in this study. The target air voids for all specimens characterized in this study was maintained as 7.0 ± 0.5 percent. Throughout this study, whenever aged specimens were employed, specimens were kept in a forced draft oven at 85°C for five days to ensure long term aging procedure described in AASHTO PP-02.

Table 5
Test factorial

Mixture Type	Asphalt Binder	Hydrated Lime	Laboratory Tests										
			ITS				SCB		DCSE	E*	FN	FT	LWT
			Unaged		Aged		Unaged	Aged					
			25°C	40°C	25°C	40°C							
64CO	PG 64-22	None	3	3	3	3	3	3	3	3	3	3	2
64LS		HL/paste	3	3	3	3	3	3	3	3	3	3	2
64LM		HL/no-paste	3	3	3	3	3	3	3	3	3	3	2
70CO	PG 70-22M	None	3	3	3	3	3	3	3	3	3	3	2
70LS		HL/paste	3	3	3	3	3	3	3	3	3	3	2
70LM		HL/no-paste	3	3	3	3	3	3	3	3	3	3	2
76CO	PG 76-22M	None	3	3	3	3	3	3	3	3	3	3	2
76LS		HL/paste	3	3	3	3	3	3	3	3	3	3	2
76LM		HL/no-paste	3	3	3	3	3	3	3	3	3	3	2

Note: The Number in each box indicates the number of specimens tested for that corresponding test.

Laboratory Tests for HMA Mixture Characterization

A suite of fundamental and simple material characterization tests were conducted to evaluate the laboratory performance of mixtures included in this study. During the service period, permanent deformation (rutting), fatigue (load-associated) cracking, and low temperature cracking are the three major distress conditions initiated by a variety of loading and environmental conditions that act on pavements. Although these three types of distress conditions are important and should not be overlooked, this research work focused only on the first two distress types (i.e. permanent deformation and fatigue cracking) considering the local climate of Louisiana. Table 6 summarizes the laboratory tests used in this study. A detailed description of each of these tests is described in Appendix A.

Table 6
HMA mixture performance test conditions

Laboratory Test	Performance Indication	Test Temperature	Test Protocol
ITS	Resistance to fatigue and thermal cracking	25°C/ 40°C	AASHTO T 322-03
SCB	Resistance to crack propagation	25°C	Mohammad et al.[27]
DCSE	Fracture resistance	10°C	Roque et al. [28]
Dynamic Modulus	Elastic properties of rutting analysis	Various Temperatures	AASHTO TP 62-03
Flow Number	Resistance to permanent deformation	54.4°C	NCHRP Report-513
Flow Time	Resistance to permanent deformation	54.4°C	NCHRP Report-513
LWT, Hamburg	Moisture sensitivity and permanent deformation	50°C	AASHTO T 324-04

DISCUSSION OF RESULTS

The individual test results of the asphalt binders and mixtures are presented in Tables B1-B25 of the Appendix B. For the discussion and presentation purposes, the abbreviated names of the HMA mixtures (i.e. 64CO, 64LS, etc.) as listed in Table 4 are used.

Statistical Analysis Methods and Approaches

Statistical analyses of laboratory experimental data were performed with the Statistical Analysis System (SAS) system for Windows Version 9 (SAS Institute Inc., Cary, NC). The General Linear Models (GLM) procedure was used for the Analysis of Variance (ANOVA) analysis. ANOVA typically refers to partitioning the difference in a variable's value into the difference between and within several groups of observations. The Least Significant Difference (LSD) test was used to separate significant means where differences were declared significant at the alpha level of 0.05. In other words, if they are termed significantly different, 95 percent of the time these groups are compared there will be a difference among them. LSD performs a pair-wise t-test, which is equivalent to Fisher's least significant difference test. Fisher's least significant difference test aims to determine whether the difference found between two groups is due to the group or a random chance.

The means and statistical rankings of the laboratory test results were reported for every single mixture included in this study. Generally, the letter A was assigned to the highest mean value followed by letters in an appropriate order (i.e., B/C/D). However, mixture properties, such as rut depth, fatigue parameter, etc, where a lower value indicated a better performance, the rankings were done in the reverse order. More specifically, the lowest value was assigned to the highest ranking "A" and so on. Therefore, in this report, a mixture with a ranking "A" always indicates a superior mix and the successive letters follow a descending order of performances. A double (or more) letter designation, such as A/B (or A/B/C), indicates the difference in the means was not clear-cut, and the mean was close to either group in that analysis.

In this study, the main purpose of the statistical analyses was to determine if the addition of hydrated lime brought any significant change in the mechanical properties of lime-treated mixtures. First of all, the nine mixtures considered in this study were divided into three individual mixture groups (i.e. three mixtures per group) according to the type of asphalt binder utilized to prepare those mixtures. For example, 64CO, 64LS, and 64LM mixtures were grouped together and named 64 HMA mixture group. Similarly, 70CO, 70LS, and 70LM mixtures formed the 70 HMA mixture group, and the 76 HMA mixture group consisted of 76CO, 76LS, and 76LM mixtures. Among a particular HMA mixture group, the

three individual mixtures were compared with each other, and a statistical ranking of experimental results within that HMA mixture group (i.e., 64 HMA/ 70 HMA/ 76 HMA mixture group) was established.

The next task was to compare hydrated lime treated mixtures containing lower “high temperature PG graded” asphalt binder with the conventional mixture containing relatively higher “high temperature PG graded” asphalt. For example, 70LM and 70LS mixtures were compared with the mixture 76CO to examine if the mechanical properties of hydrated lime-treated 70LM and 70LS mixtures were as good as mixture 76CO. In addition, the three conventional mixtures (i.e., 64CO, 70CO, and 76CO) were compared to one another to determine the effect of untreated asphalt binders on the HMA mixtures’ laboratory performance.

In this study, both linear and non-linear regression analysis techniques were utilized to establish a relationship between different mechanical properties of HMA mixtures. The reliability of a regression model is statistically evaluated based on the goodness of fit parameters: correlation coefficient (R^2), standard error of estimate (Se), and standard error ratio (Se/Sy).

The goodness of fit for a linear model is measured by R^2 computed from the sum of squares of the distances of the points from the best-fit curve provided by the regression process. Mathematically, coefficient of correlation is expressed as:

$$R^2 = 1 - \frac{SSE}{SST} \quad (6)$$

where,

$$\text{Sum of squares due to error, } SSE = \sum_{i=1}^n (y_i - \hat{y})^2$$

$$\text{Total sum of squares, } SST = \sum_{i=1}^n (y_i - \bar{y})^2$$

The value of R^2 is a unit-less fraction between 0.0 and 1.0. A higher value indicates that the model fits the data better. The value of R^2 equal to 1.0 means a perfect linear relationship exists between the dependent and independent variables, while R^2 equal to 0.0 indicates that the independent variables do not have any impact on its dependent counterpart.

However, for non-linear regression analysis, R^2 is not always reliable as a parameter to measure the goodness of fit for linear regression analysis. In that case, another parameter called standard error ratio, calculated by S_e/S_y , is used to determine the goodness of fit of a

model. Unlike R^2 , a lower value (closer to 0.0) for standard error ratio indicates a better fit model and vice versa.

Asphalt Binder Test Results

Table 7 presents the corresponding physical and rheological test results for binders considered in this study in comparison to the LADOTD Performance Graded (PG) asphalt binder specifications. It was observed that the rotational viscosity measured at 135°C for all binders passed the specified value of 3.0 Pa.s (maximum allowable value at 135°C) with an exception for the hydrated lime-treated PG 76-22M. Binder PG 76-22M contained higher percentage of SB polymer, and therefore, the addition of hydrated lime possibly increased its stiffness and reduced the viscosity of binder. Table 7 also shows that the addition of hydrated lime made the binders stiffer and significantly increased the rutting factor “ $G^*/\text{Sin}\delta$,” values for every asphalt binder considered in this study. In fact, the stiffening that results from addition of hydrated lime increased the high temperature performance grade (PG) rating of asphalt cement at least by one full grade. Alternatively, a decrease in low temperature properties of one grade, from -22°C to -16°C was observed when the binders contained hydrated lime. At intermediate temperature (25°C), the fatigue factor, $G^*\text{Sin}\delta$ value for lime-treated PG 70-22M binder exceeded the LADOTD’s PG binder specification limit of 5000 kPa (Table 7). However, the fatigue factor values of all other binders were within the limit of PG binder specification. Overall, it can be concluded that the addition of hydrated lime to PG 76-22M, PG 70-22M, and PG 64-22 asphalt binders changed their rheological properties and transformed them into PG 88-16, PG 76-16, and PG 70-16 binders respectively.

Figure 10 is a graphical representation of the binder master curves constructed by using RHEA software, by Abutech Inc. of Doyleson, PA, while Figure 11 presents the complex shear modulus (G^*) isotherms for PG 76-22M, PG 70-22M, and hydrated lime-treated PG 70-22M (i.e., PG 76-16) binders in a log-log scale. The binders’ complex shear modulus (G^*) and phase angle (δ) values were measured at four temperatures (4, 25, 37.8, and 54.4°C) and 13 frequencies (0.01, 0.02, 0.05, 0.1, 0.2, 0.5, 1, 2, 3, 4, 5, 10, and 25Hz) using the TA Instruments Model AR 2000 rheometer. Due to equipment limitations, the PG 64-22, lime-treated PG 64-22, and lime-treated PG 76-22M could not be included in the binders’ complex shear modulus testing program performed in this study. The detailed dataset of the complex shear modulus tests is reported in the Appendix.

Table 7
LADOTD performance graded asphalt cement specification and test results

Property	Binder Tested						Specification
	PG 76-22M	PG 76-22M + HL	PG 70-22M	PG 70-22M + HL	PG 64-22	PG 64-22 + HL	
Tests on Original Binder							
Rotational Viscosity @ 135°C, Pa.s	1.7	5.0*	0.9	3.0	0.5	1.2	3.0-
Dynamic Shear, 10 rad/s, G*/Sin Delta, kPa							
@ 88°C	–	2.50	–	–	–	–	1.00+@76°C for PG 76-22M
@ 82°C	1.29	3.50	–	0.87	–	–	1.00+@70°C for PG 70-22M
@ 76°C	1.82	5.13	–	2.35	–	–	1.30+@64°C for PG 64-22
@ 70°C	–	–	1.64	4.34	0.88	1.98	
@ 64°C	–	–	–	–	1.92	4.02	
Force Ductility Ratio (F2/F1, 4°C, 5 cm/min, F2 @ 30 cm elongation)	0.49	N/A	N/A	N/A	N/A	N/A	0.30+ for PG 76-22M
Force Ductility, (4°C, 5 cm/min, 30 cm elongation, kg)	N/A	N/A	0.31	N/A	N/A	N/A	0.23+ for PG 70-22M
Tests on RTFO Residue							
Dynamic Shear, 10 rad/s, G*/Sin Delta, kPa							
@ 88°C	–	3.09	–	–	–	–	2.20+@76°C for PG 76-22M
@ 82°C	1.67	4.90	–	1.81	–	–	2.20+@70°C for PG 70-22 M
@ 76°C	2.48	7.29	1.65	3.50	–	–	2.20+@64°C for PG 64-22
@ 70°C	–	–	3.14	4.34	1.61	3.33	
@ 64°C	–	–	–	–	3.25	5.45	
Elastic Recovery, 25°C, 10 cm elongation, %	70	47.5*	65	42.5	N/A	N/A	60+ for PG 76-22M 40+ for PG 70-22M
% Mass Loss	0.08	0.12	0.04	0.13	0.025	0.035	1.00-
Tests on PAV Residue							
Dynamic Shear, @ 25°C, 10 rad/s, G*Sin δ, kPa	2297	4523	4615	6870*	2774	4948	5000-
Bending beam Creep Stiffness, S, Mpa							
@ -12°C	162	348*	196	496*	234	428*	300-
@ -6°C	–	153	–	253	–	173	
Bending beam Creep Slope, m value							
@ -12°C	0.327	0.295*	0.317	0.269*	0.312	0.286*	0.300+
@ -6°C	–	0.362	–	0.350	–	0.351	
PG Grading Based on Test Results	PG76-22	PG88-16	PG70-22	PG76-16	PG64-22	PG70-16	

Note: N/A: Not Applicable, HL: Hydrated Lime, *: Exceeded the specification limit

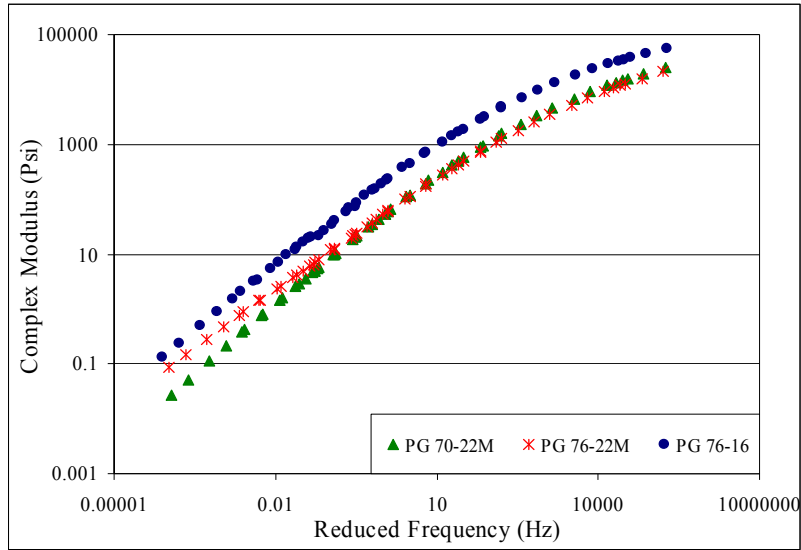


Figure 10
Master curves for asphalt binders

As expected, both master curves and isotherms (Figures 10 and 11) show that the addition of hydrated lime to PG 70-22M resulted in a stiffer binder (PG76-16) than the untreated binders (i.e., PG 70-22M and PG 76-22M) at every temperature and frequency. This indicates that the binder PG 76-16 should show better rut resistant at high temperature, whereas its low temperature thermal cracking potential may increase at the same time. Furthermore, binder PG 76-22M possessed greater G^* values at high temperatures (37.8°C and 54.4°C) and smaller G^* values at low temperatures (4°C and 25°C) when compared to binder PG 70-22M, Figure 17. These results indicate that the PG 76-22M binder showed more elasticity at lower temperature and higher stiffness at higher temperature. The quantity of SB polymer is more in PG 76-22M than that of PG 70-22M, which is the reason why PG 76-22M showed better high temperatures stiffness and low temperature elasticity.

Figure 12 describes the characterization of phase angles for PG 70-22M, PG 76-22M, and PG 76-16 (i.e., PG 70-22M + HL) asphalt binders for various temperatures and test frequencies. It was apparent that the phase angle values of all binders increased with an increase in temperature and a decrease in frequency at low (4°C) and intermediate (25°C) temperature region. At higher temperatures (37.8°C and 54.4°C), the phase angle isotherms showed that there was very little change in phase angle values with the change in loading frequencies. However, the rise in phase angles with the increase in temperatures indicated that the binders became more viscous with the increase in temperature. Also as expected, it was noticed that the addition of hydrated lime to PG 70-22M (PG 76-16) stiffened the binder and consequently, reduced the phase angle values at all frequencies and temperatures when compared to its conventional counterpart (PG 70-22M).

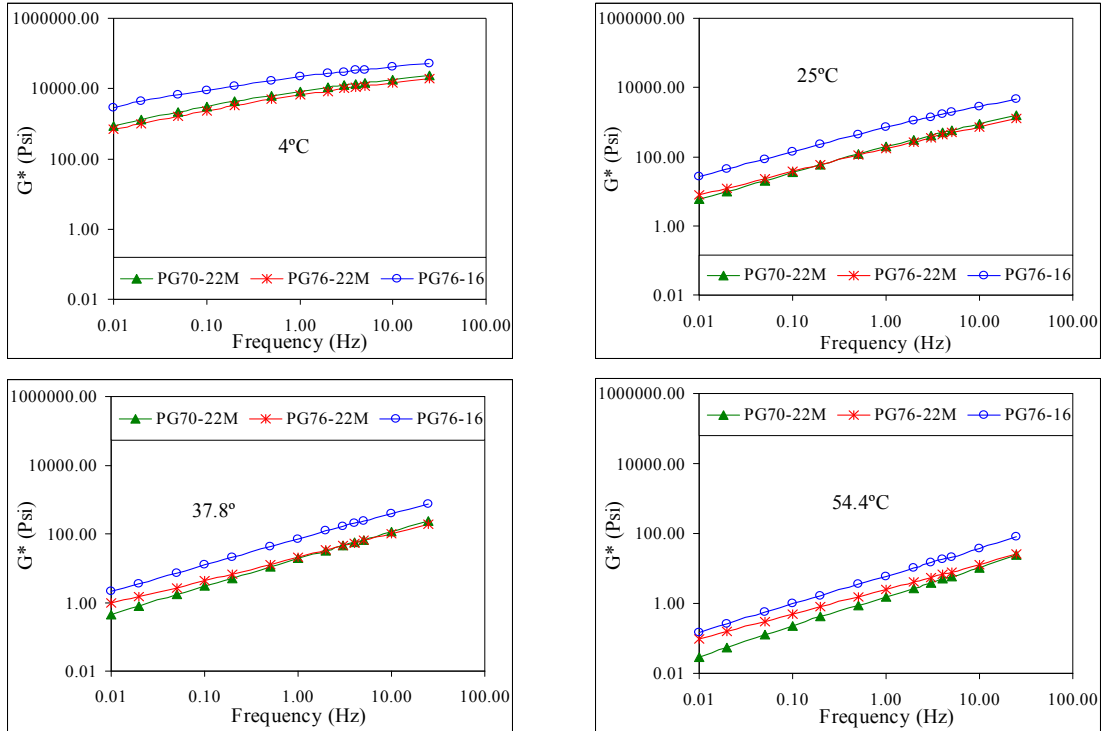


Figure 11
Binder shear modulus isotherms

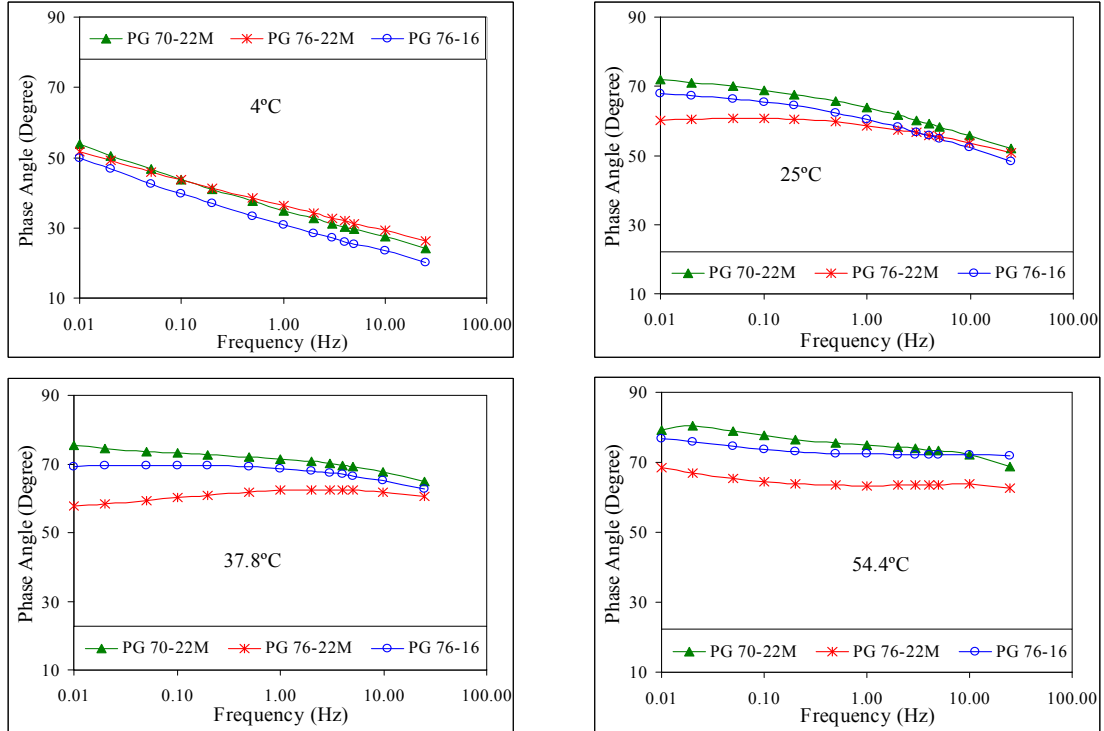


Figure 12
Binder phase angle isotherms

Laboratory Characterization of Mixtures

Indirect Tensile Strength (ITS) Test Results

Figures 13 through 18 present the mean indirect tensile (IT) strength, IT strain, and TI results for both unaged and aged mixtures at 25°C and 40°C respectively. Higher IT strength, strain, and TI values are desirable as they correspond to a strong and durable mixture. In contrast, the lower the TI value, the lesser the amount of energy absorbed by the mixture under tensile strain which eventually increases the chances of developing fatigue cracks.

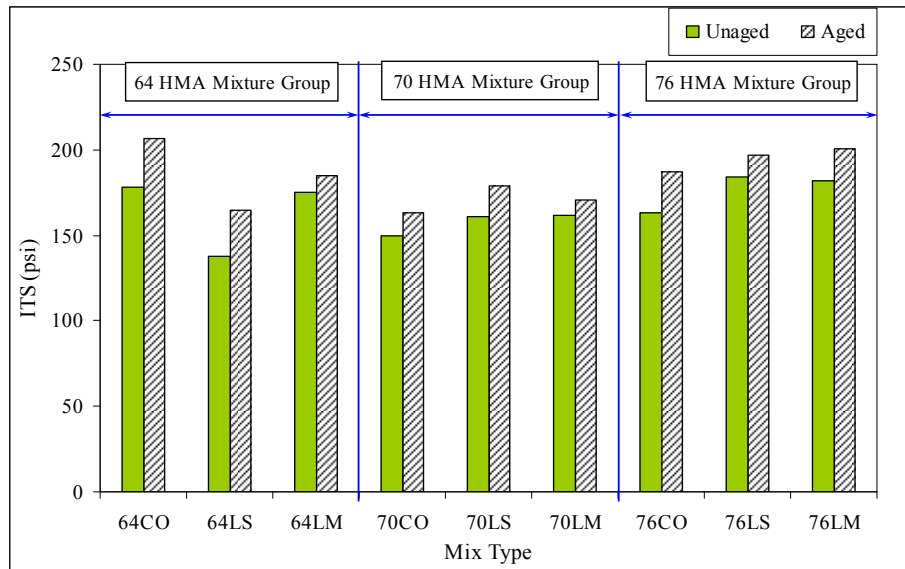


Figure 13
ITS strength results at 25°C

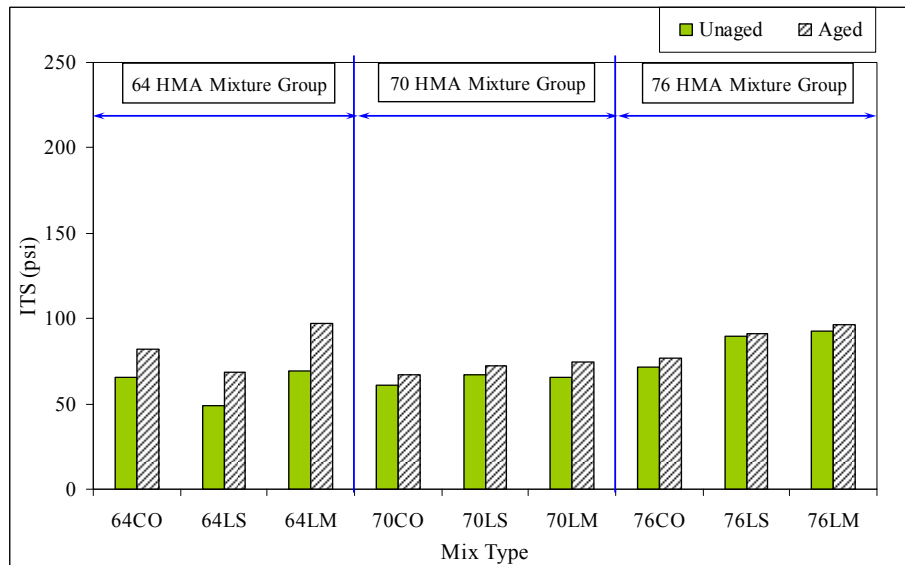


Figure 14
ITS strength results at 40°C

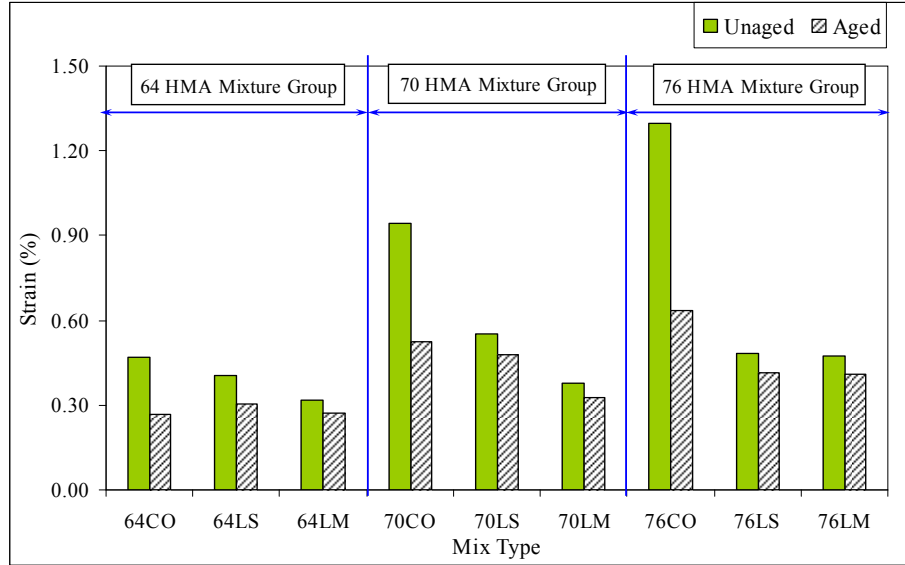


Figure 15
ITS results strain at 25°C

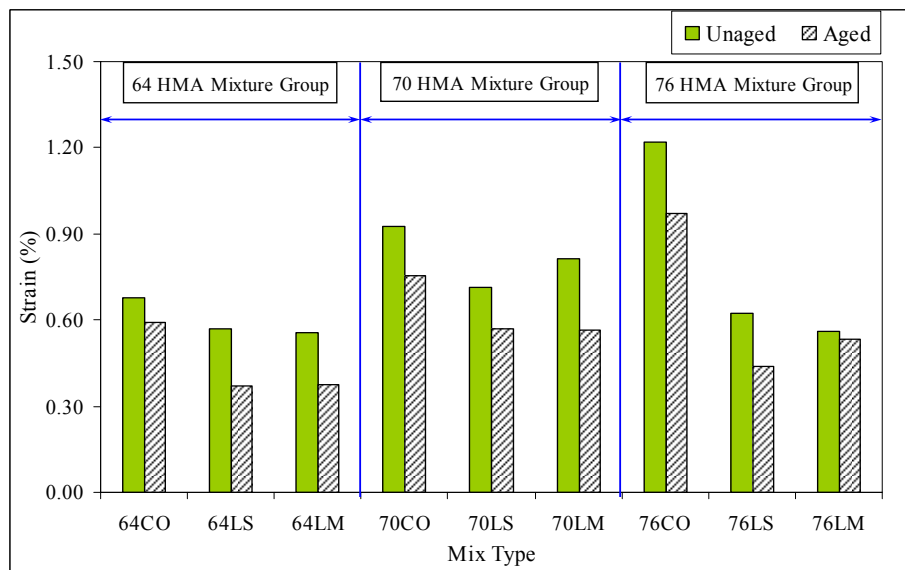


Figure 16
ITS strain results at 40°C

In general, the addition of hydrated lime improved the IT strength of all mixtures (except 64LS). Similarly, a reduction in strain and TI was observed from the addition of hydrated lime. The binder test results showed that the presence of hydrated lime reduced the low temperature elasticity of all binders. This may be the reason for the reduction in strain and TI values for the lime-treated mixtures considered in this study. It is noted that the TI values for all the mixtures evaluated were greater than 0.60 (a minimum value observed for fatigue resistant mixtures).

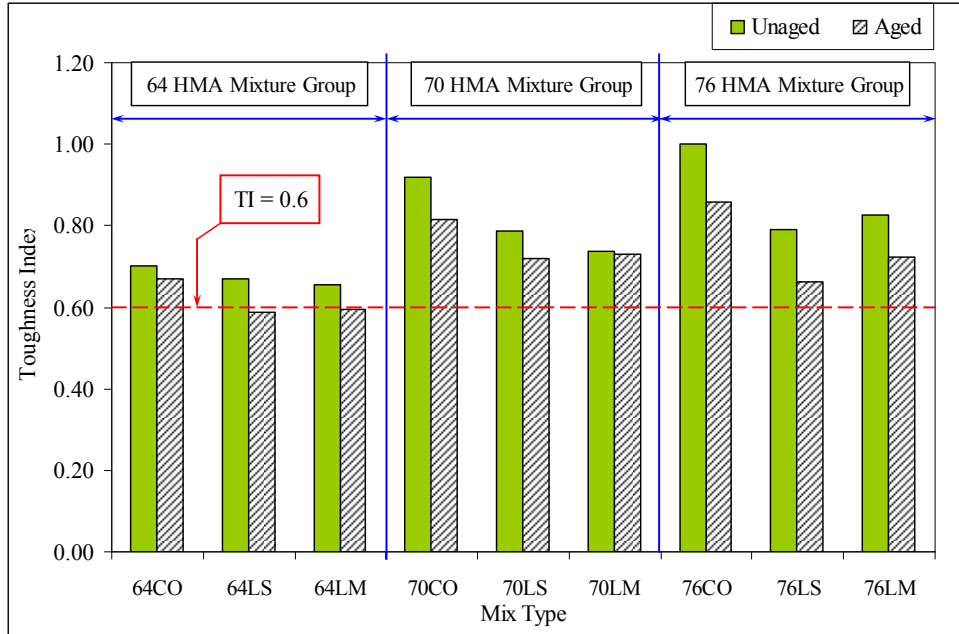


Figure 17
TI results at 25°C

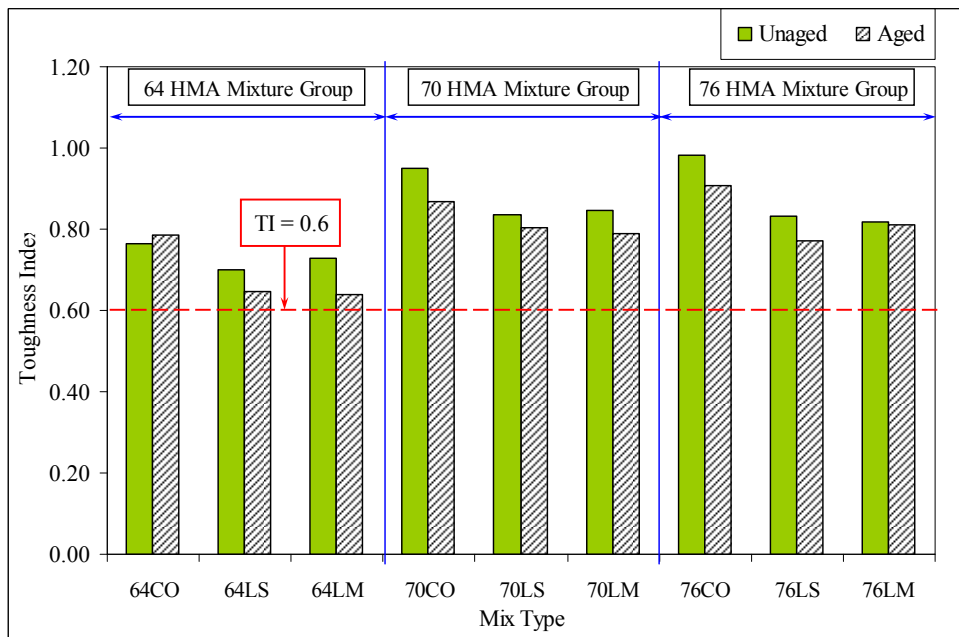


Figure 18
TI results at 40°C

Tables 8 and 9 present the statistically analyzed ITS data for each individual HMA mixture group (i.e. 64 HMA/70 HMA/76 HMA mixture group, etc.). For 64 HMA mixture group, the addition of hydrate lime in paste method significantly reduced the IT strength of mixture 64LS in every case (i.e., temperature and aging conditions). No-paste method (i.e. 64LM)

did not make any significant difference in IT strength when the mixture was unaged, whereas for the aged mixture, significant improvement was noticed only at 40°C. In the 70 HMA mixture group, the 70LS and 70LM mixtures did not show any considerable difference in IT strength at any temperature and aging condition except for the aged 70LS mixture at 25°C, where a substantial improvement was identified. In general, the 76LS and 76LM mixtures showed significant improvement in terms of IT strength at both temperatures and aging conditions compared to their conventional counterpart in the 76 HMA mixture group, except the 76LS and 76 LM of aged condition.

Unlike ITS results, strain and TI results for the 76LS and 76LM mixtures showed reduction at every temperature and aging condition when compared to the 76CO mixture. However, the strain and TI results for the 64 HMA and 70 HMA mixture groups did not follow the same reduction pattern as the 76 HMA mixture group. For the 64 HMA mixture group, the TI of mixtures the 64LS and 64LM were significantly lower at both 25°C and 40°C for aged mixtures. However, except for aged condition at 40°C, no significant reduction in strain was noted for those mixtures (64LS and 64LM). For the 70 HMA mixture group, both aged and unaged, the 70LS and 70LM mixtures obtained lower strain and TI values at 25°C when compared to their conventional counterpart (70CO). However, at 40°C the addition of hydrated lime in either form did not influence the strain and TI properties of the 70LS and 70LM mixture. This analysis indicated that the degree of effectiveness of hydrated lime on a HMA mixture was dependent upon the type of asphalt binder the mixture contained [22]. Also, the tensile strengths of hydrated lime-treated HMA mixtures obtained higher statistical rankings at 40°C than that of 25°C. This indicates the effect of hydrated lime on the tensile strength properties of HMA mixtures more pronounced at higher temperatures.

The ITS test results were further analyzed to statistically compare the indirect tensile properties of hydrated lime-treated mixtures containing lower “high temperature PG graded” asphalt binder with the conventional mixture containing relatively higher “high temperature PG graded” asphalt. In general, the 70LS and 70LM mixture possessed similar IT strengths as the 76CO mixture at both testing temperatures (25°C and 40°C). The only exception was for the 76CO aged mixture at 25°C when it outperformed both the aged 70LS and 70LM mixture. On the other hand, the 64LM mixture always showed greater ITS than the 70CO mixture. This indicated that a hydrated lime-treated mixture containing lower “high temperature PG graded” binder was effective to replace a mixture containing higher “high temperature PG graded” binder and no hydrated lime when a greater tensile strength was desired.

Table 8
ITS test results at 25°C

Analytical Grouping	Property	ITS (psi)				IT Strain (%)				Toughness Index			
	Aging Criterion	Unaged		Aged		Unaged		Aged		Unaged		Aged	
	Mixture Type	Mean	Rank	Mean	Rank	Mean	Rank	Mean	Rank	Mean	Rank	Mean	Rank
64 HMA Group	64CO	178	A	207	A	0.47	A	0.26	A	0.70	A	0.67	A
	64LS	138	B	165	C	0.41	A	0.30	A	0.67	A	0.59	B
	64LM	175	A	185	B	0.32	B	0.27	A	0.66	A	0.59	B
70 HMA Group	70CO	150	A	163	B	0.94	A	0.53	A	0.92	A	0.82	A
	70LS	161	A	179	A	0.55	B	0.48	A	0.79	B	0.72	B
	70LM	161	A	170	A/B	0.38	C	0.33	B	0.74	B	0.73	B
76 HMA Group	76CO	163	B	187	A	1.30	A	0.63	A	1.00	A	0.86	A
	76LS	184	A	197	A	0.48	B	0.41	B	0.79	B	0.66	B
	76LM	182	A	201	A	0.48	B	0.41	B	0.83	B	0.72	B
64LS and 64LM versus 70CO	64LS	138	B	165	B	0.41	B	0.30	B	0.67	B	0.59	B
	64LM	175	A	185	A	0.32	B	0.27	B	0.66	B	0.59	B
	70CO	150	B	163	B	0.94	A	0.53	A	0.92	A	0.82	A
70LS and 70LM versus 76CO	70LS	161	A	179	B	0.55	B	0.48	A/B	0.79	B	0.72	B
	70LM	161	A	170	C	0.38	C	0.33	B	0.74	B	0.73	B
	76CO	163	A	187	A	1.30	A	0.63	A	1.00	A	0.86	A
Con. Group	64CO	178	A	207	A	0.47	C	0.26	B	0.70	C	0.67	B
	70CO	150	C	163	C	0.94	B	0.53	A	0.92	B	0.82	A
	76CO	163	B	187	B	1.30	A	0.63	A	1.00	A	0.86	A

*Note: Rank: Statistical Ranking (Rows with the same letter indicate no significant difference)
Con. Group: Conventional HMA Mixture Group*

Table 9
ITS test results at 40°C

Analytical Grouping	Property	ITS (psi)				IT Strain (%)				Toughness Index			
	Aging Criterion	Unaged		Aged		Unaged		Aged		Unaged		Aged	
	Mixture Type	Mean	Rank	Mean	Rank	Mean	Rank	Mean	Rank	Mean	Rank	Mean	Rank
64 HMA Group	64CO	65	A	82	B	0.68	A	0.59	A	0.76	A	0.78	A
	64LS	49	B	68	C	0.57	A	0.37	B	0.70	A	0.65	B
	64LM	69	A	97	A	0.56	A	0.38	B	0.73	A	0.64	B
70 HMA Group	70CO	61	A	67	A	0.93	A	0.75	A	0.95	A	0.87	A
	70LS	67	A	72	A	0.71	A	0.57	B	0.84	A	0.80	A
	70LM	65	A	75	A	0.82	A	0.57	B	0.84	A	0.79	A
76 HMA Group	76CO	72	B	77	B	1.22	A	0.97	A	0.98	A	0.91	A
	76LS	89	A	91	A	0.62	B	0.44	B	0.83	B	0.77	B
	76LM	93	A	97	A	0.56	B	0.54	B	0.82	B	0.81	B
64LS and 64LM versus 70CO	64LS	49	B	68	B	0.57	B	0.37	B	0.70	B	0.65	B
	64LM	69	A	97	A	0.56	B	0.38	B	0.73	B	0.64	B
	70CO	61	A	67	B	0.93	A	0.75	A	0.95	A	0.87	A
70LS and 70LM versus 76CO	70LS	67	A	72	A	0.71	B	0.57	B	0.84	B	0.80	B
	70LM	65	A	75	A	0.82	B	0.57	B	0.84	B	0.79	B
	76CO	72	A	77	A	1.22	A	0.97	A	0.98	A	0.91	A
Con. Group	64CO	65	A/B	82	A	0.68	B	0.59	B	0.76	B	0.78	B
	70CO	61	B	67	B	0.93	A/B	0.75	B	0.95	A	0.87	A
	76CO	72	A	77	A	1.22	A	0.97	A	0.98	A	0.91	A

*Note: Rank: Statistical Ranking (Rows with the same letter indicate no significant difference)
Con. Group: Conventional HMA Mixture Group*

The comparison between conventional mixtures indicates that both the aged and unaged 64CO mixtures showed higher tensile strength than mixtures 70CO and 76CO at 25°C, as shown in Table 8. However, testing at 40°C, the 76CO mixture obtained similar statistical rankings as the 64CO mixture as shown in Table 9. The tensile strength for the 70CO mixture was always lower than that of the two other conventional mixtures (64CO and 76CO). On the other hand, IT strain and TI results showed that the conventional mixtures

containing polymer-modified asphalt binders (i.e., PG 70-22M and PG 76-22M) possessed higher IT strain and TI values than that of mixture 64CO which did not contain SB polymer modified binder regardless of testing temperatures and aging conditions.

Aging Index from TI. The extent of age hardening of HMA mixtures can be quantified by a term called aging index, considering the change in TI value of a mixture before and after the aging process. In this study, the aging index of a mixture was calculated by dividing the TI value of aged mixture by the TI value of the unaged one and presented in Figure 19. It is apparent that generally the addition of hydrated lime did not affect the aging mechanism of mixtures as both conventional and lime-treated mixtures in each mixture group obtained similar aging index values. However, the addition of lime in no-paste method substantially improved the age hardening attribute of the 70LM mixture as it obtained considerably higher aging index than that of the 70CO mixture.

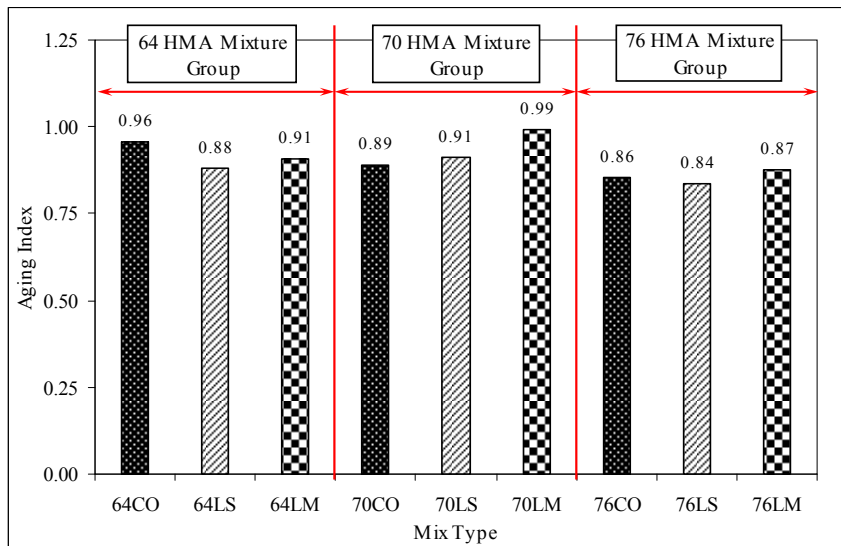


Figure 19
Aging index – from TI result

Semi-Circular Bend (SCB) Test Results

Figure 20 is the graphical representation of the computed critical fracture resistance (J_c) values for mixtures evaluated in this study. It appears; the aging process increases the stiffness of binders, and therefore, reducing the fracture resistance of HMA mixtures. The addition of hydrated lime did not show any substantial decrease on the J_c values for the mixtures contained in 64 HMA mixture group. In the 70 HMA and 76 HMA mixture groups, hydrated lime treated mixtures achieved lower J_c values when compared to their conventional counterparts respectively. Since the parameter J_c represents the fracture resistance of a

material, the higher the value of J_c the better fracture resistance the material possesses. Numerous previous studies [27], reported that a mixture achieving a J_c value greater than 0.65 KJ/m^2 is expected to exhibit good fracture resistance. On this regard, mixtures 70LS, 70LM, 76LS, and 76LM showed satisfactory laboratory performances against fracture resistance even though there was a reduction in J_c values after the addition of hydrated lime.

When the 64LS and 64LM mixtures are compared with the 70CO, both 64LS and 64LM mixtures, they were found to be more susceptible to crack propagation regardless of aging condition. On the other hand, mixtures 70LS, 70LM, and 76CO were found to possess a J_c value greater than the minimum required value of 0.65 KJ/m^2 . Therefore, it can be stated that hydrated lime-treated mixtures containing PG 70-22M asphalt showed acceptable fracture resistance when compared to the conventional mixtures containing PG 76-22M asphalt.

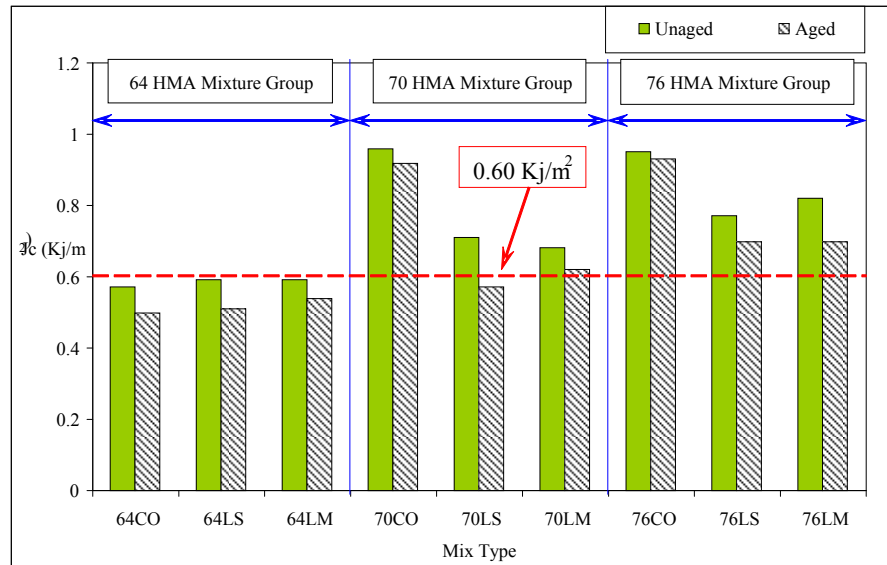


Figure 20
SCB test results

A comparison of fracture resistance between three conventional mixtures (i.e., 64CO, 70CO, 76CO) indicated that the presence of SB polymer in asphalt binder improved the elastic property of HMA mixtures, which improved the fracture resistance of mixtures 70CO and 76CO in comparison to mixture 64CO. However, both conventional mixtures containing polymer modified binders (70CO and 76CO) showed almost similar fracture resistance properties determined from the SCB test.

Figure 21 presents the aging index of mixtures as a measure of determining the affect of aging on the fracture resistance property of mixtures considered in this study. The aging indices were calculated by dividing J_c values of aged mixture by values of unaged ones.

Therefore, the more the fracture resistance values of a mixture would reduce by aging process, the lower the resulting aging index of the mixture would be. It was observed that all three mixtures in the 64 HMA group (i.e., 64CO, 64LS, and 64LM) obtained almost identical aging index values, which indicated that the addition of hydrated lime did not have any significant effect on the aging of the mixtures in that group.

In the 70 HMA mixture group, mixture 70CO and 70LM obtained almost similar aging index values, whereas the aging index value for the 70LS mixture was significantly lower than the other two mixtures in that group. On the other hand, hydrated lime treatment reduced the fracture resistance of aged mixtures in the 76 HMA group regardless of the method of adding hydrated lime. In general, it was observed that the effect of hydrated lime treatment on the age-hardening of HMA mixtures was related to the type of binder contained by the mixture. At this point, it is beyond the scope of this study to investigate further to explain the behavior of asphalt-lime clearly. It is also apparent from Figure 21 that mixtures 70CO and 76CO obtained higher aging index values when compared to 64CO indicating that the mixtures contained polymer-modified PG 70-22M and PG 76-22M binders performed better against age hardening than the mixture contained neat PG 64-22.

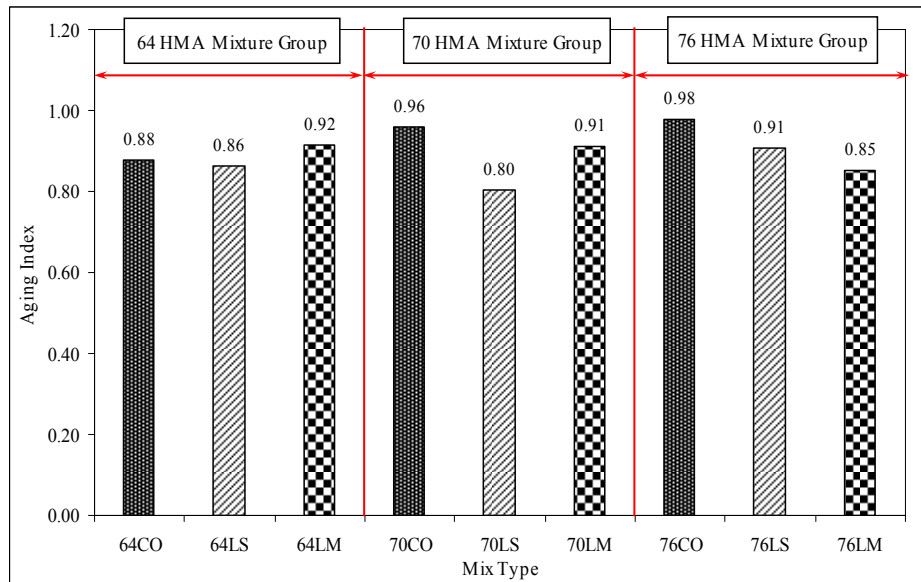


Figure 21
Aging indices computed from SCB test

Dissipated Creep Strain Energy (DCSE) Test Results

Dissipated creep strain energy is the limiting energy that a mixture can stand before it fractures. Rouque et al. reported that a DCSE value of 0.75 KJ/m^3 was the value to differentiate cracked and uncracked pavements [30]. Pavements having a DCSE value

greater than 0.75 KJ/m³ did not crack and vice versa. Therefore, mixtures having lower DCSE values are considered more vulnerable to cracking than the mixtures having higher DCSE values when both mixtures are exposed to similar loading and environmental conditions.

A summary of test results obtained from DCSE tests is shown in Table 10 while the entire DCSE test dataset is reported in Tables B5-B6 of the Appendix. It is noted that all the mixtures evaluated in this study exhibited good laboratory performance measured by this test as none of those had DCSE value lower than 0.75 KJ/m³ (Figure 28).

Table 10
Summary of the DCSE test results

Mix Type	Resilient Modulus (Gpa)	Failure Strain (Microstrain)	ITS (Mpa)	Initial Strain (Microstrain)	Elastic Energy (KJ/m ³)	Fracture Energy (KJ/m ³)	DCSE (KJ/m ³)
64CO	12.3	1287	2.19	1108	0.20	1.42	1.22
64LS	14.5	1990	3.13	1772	0.34	3.11	2.77
64LM	17.2	1261	2.92	1090	0.25	1.85	1.60
70CO	12.8	2272	2.42	2081	0.23	2.75	2.52
70LS	14.7	1630	2.68	1429	0.27	2.18	1.91
70LM	16.4	1560	2.46	1409	0.19	1.90	1.71
76CO	10.5	3826	2.35	3587	0.28	4.48	4.20
76LS	11.2	2098	2.51	1870	0.29	2.57	2.28
76LM	11.2	2951	2.19	2752	0.22	3.24	3.02

Figure 22 also indicates that mixtures 70LS, 70LM, 76LS, and 76LM obtained lower DCSE values when compared to the conventional mixtures (70CO/76CO) of the respective HMA mixture groups. Alternatively, both mixtures 64LS and 64LM showed improvement against fatigue cracking when compared to the mixture 64CO (Figure 23). Thus, in general, hydrated lime treatment decreased the DCSE values for mixtures containing PG 70-22M and PG 76-22M binders, but a dissimilar trend was observed for mixtures containing PG 64-22 binders.

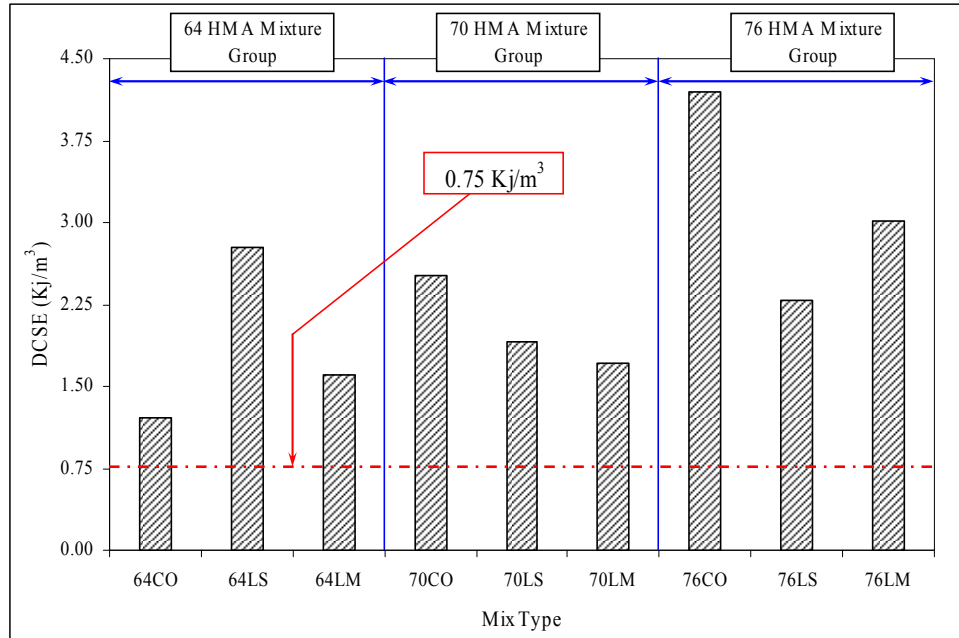


Figure 22
DCSE test results for all mixtures

Tables 11 through 13 show an in depth statistical analysis on DCSE test results for the 64 HMA, 70 HMA, and 76 HMA mixture groups, respectively. The results reported in Table 11 indicate that hydrated lime did show significant improvement when added in the paste method to a mixture containing PG 64-22 binder (64LS). Results reported in Table 12 show that the mixtures 70LS and 70LM had similar ranking indicating that the method of adding lime to the mixture did not affect the DCSE values. Similar observations were noted for the 76LS and 76LM mixtures in Table 13.

Table 11
DCSE test results for 64 HMA mixture group

Mix Type	Sample ID	Air Void	DCSE (KJ/m ³)	Mean DCSE	St. Dev	%CV	Rank
64 CO	C5	6.9	1.377	1.22	0.2	18.4	B
	C9	7.0	1.060				
64 LS	LS2	7.0	2.504	2.77	0.4	13.6	A
	LS4	7.2	3.037				
64 LM	LM9	6.5	1.228	1.60	0.3	20.1	B
	LM11	6.6	1.789				
	LM12	7.2	1.784				

Note: Rank: Statistical Ranking (Rows with the same letter indicate no significant difference)
St. Dev: Standard Deviation, %CV: Coefficient of Variance (%)

Table 12
DCSE test results for 70 HMA mixture group

Mix Type	Sample ID	Air Void	DCSE (KJ/m ³)	Mean DCSE	St. Dev	%CV	Rank
70 CO	C3	7.6	2.212	2.52	0.4	14.2	A
	C4	6.6	2.441				
	C11	7.4	2.912				
70 LS	LS3	6.4	2.106	1.91	0.2	9.6	B
	LS5	6.9	1.742				
	LS6	6.4	1.895				
70 LM	LM13	6.8	1.614	1.71	0.1	5.6	B
	LM14	7.4	1.709				
	LM15	6.4	1.805				

*Note: Rank: Statistical Ranking (Rows with the same letter indicate no significant difference)
St. Dev: Standard Deviation, %CV: Coefficient of Variance (%)*

The addition of hydrated lime in slurry method to a mixture containing PG 64-22 binder (i.e., 64LS) improved the fatigue-cracking resistance to obtain an equal statistical ranking to mixture 70CO (Table 14). But when lime was added in dry method, the mixture (64LM) showed reduced performance to the 64LS and 70CO mixtures. The comparison between lime-treated mixtures containing PG 70-22M and conventional mixture containing PG 76-22M displays that the 76CO mixture had a higher DCSE value than both the 70LS and 70LM mixtures (Table 15). When the three conventional mixtures were compared, a better resistance to crack generation was observed when the mixture contained higher PG graded polymer modified asphalt binder (Table 16). It is worth noting that these results followed similar trend that reported for TI values calculated from ITS test results.

Table 13
DCSE test results for 76 HMA mixture group

Mix Type	Sample ID	Air Void	DCSE (KJ/m ³)	Mean DCSE	St. Dev	%CV	Rank
76 CO	C12	7.0	4.337	4.20	0.5	12.7	A
	C13	7.2	4.654				
	C14	6.8	3.612				
76 LS	LS12	7.1	1.742	2.28	0.5	20.6	B
	LS13	7.0	2.571				
	LS14	6.7	2.542				
76 LM	LM2	6.9	3.526	3.02	0.7	22.9	B
	LM3	7.6	2.234				
	LM15	7.1	3.300				

*Note: Rank: Statistical Ranking (Rows with the same letter indicate no significant difference)
St. Dev: Standard Deviation, %CV: Coefficient of Variance (%)*

Table 14
Comparison of DCSE results between mixtures 64LS, 64LM, and 70CO

Mix Type	Sample ID	Air Void	DCSE (KJ/m ³)	Mean DCSE	St. Dev	%CV	Rank
64 LS	LS2	7.0	2.504	2.77	0.4	13.6	A
	LS4	7.2	3.037				
64 LM	LM9	6.5	1.228	1.60	0.3	20.1	B
	LM11	6.6	1.789				
	LM12	7.2	1.784				
70 CO	C3	7.6	2.212	2.52	0.4	14.2	A
	C4	6.6	2.441				
	C11	7.4	2.912				

*Note: Rank: Statistical Ranking (Rows with the same letter indicate no significant difference)
St. Dev: Standard Deviation, %CV: Coefficient of Variance (%)*

Table 15
Comparison of DCSE results between mixtures 70LS, 70LM, and 76CO

Mix Type	Sample ID	Air Void	DCSE (KJ/m ³)	Mean DCSE	St. Dev	%CV	Rank
70 LS	LS3	6.4	2.106	1.91	0.2	9.6	B
	LS5	6.9	1.742				
	LS6	6.4	1.895				
70 LM	LM13	6.8	1.614	1.71	0.1	5.6	B
	LM14	7.4	1.709				
	LM15	6.4	1.805				
76 CO	C12	7.0	4.337	4.20	0.5	12.7	A
	C13	7.2	4.654				
	C14	6.8	3.612				

*Note: Rank: Statistical Ranking (Rows with the same letter indicate no significant difference)
St. Dev: Standard Deviation, %CV: Coefficient of Variance (%)*

Table 16
Comparison of DCSE results for conventional mixture group

Mix Type	Sample ID	Air Void	DCSE (KJ/m ³)	Mean DCSE	St. Dev	%CV	Rank
64 CO	C5	6.9	1.377	1.22	0.2	18.4	C
	C9	7.0	1.060				
70 CO	C3	7.6	2.212	2.52	0.4	14.2	B
	C4	6.6	2.441				
	C11	7.4	2.912				
76 CO	C12	7.0	4.337	4.20	0.5	12.7	A
	C13	7.2	4.654				
	C14	6.8	3.612				

Dynamic Modulus (E^*) Test Results

Figures 23 and 24 show the dynamic modulus isotherms for all mixtures at different temperatures and frequencies. In general, the E^* values for all mixtures increased with an increase in frequency and a decrease in temperature. At low temperatures (-10°C to 4.4°C) the E^* isotherms maintained the pattern of inclined straight-line, which indicated that the mixture behavior was in the linear viscoelastic region and predominately affected by the binders at those temperatures. However, at intermediate and high temperatures (25 , 37.8 , and 54.4°C), the E^* isotherms gained a concave shape (Figure 30), which represents the non-linear behavior in HMA mixtures under compression.

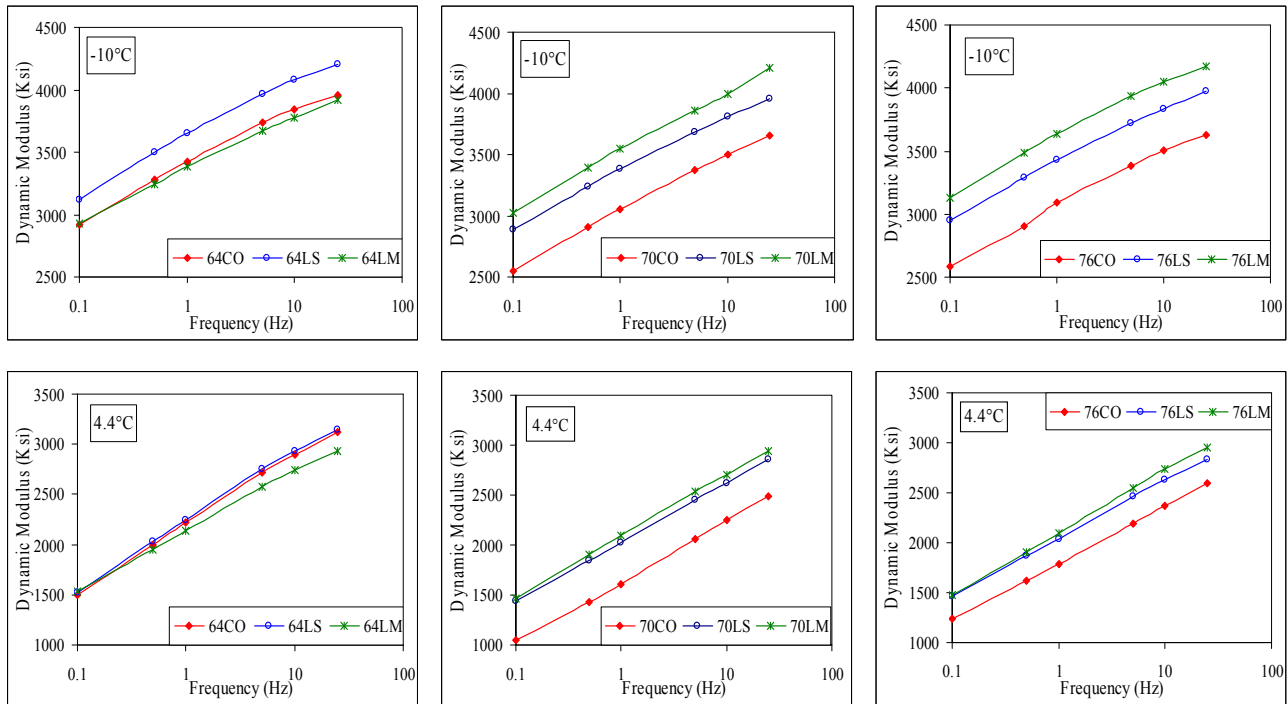


Figure 23
Dynamic modulus isotherms at low temperatures

The variation of the phase angles with respect to the Dynamic Modulus is shown in Figure 25 for the six frequencies and five temperatures for each mixture tested in this study. The figure shows that the phase angle increased with increasing frequency, reached a peak, and then decreased. This response is different from the asphalt binder in that the phase angle for an asphalt binder generally decreases with increasing frequency. At high frequency (low temperature), the asphalt binder primarily affects the phase angle of asphalt mixtures (i.e., binder viscoelastic follows similar trend) whereas, at low frequency (high temperature), it is predominantly affected by the aggregate. Therefore, the phase angle for asphalt mixtures

decreases with decreasing frequency or increasing temperature because of the aggregate influence.

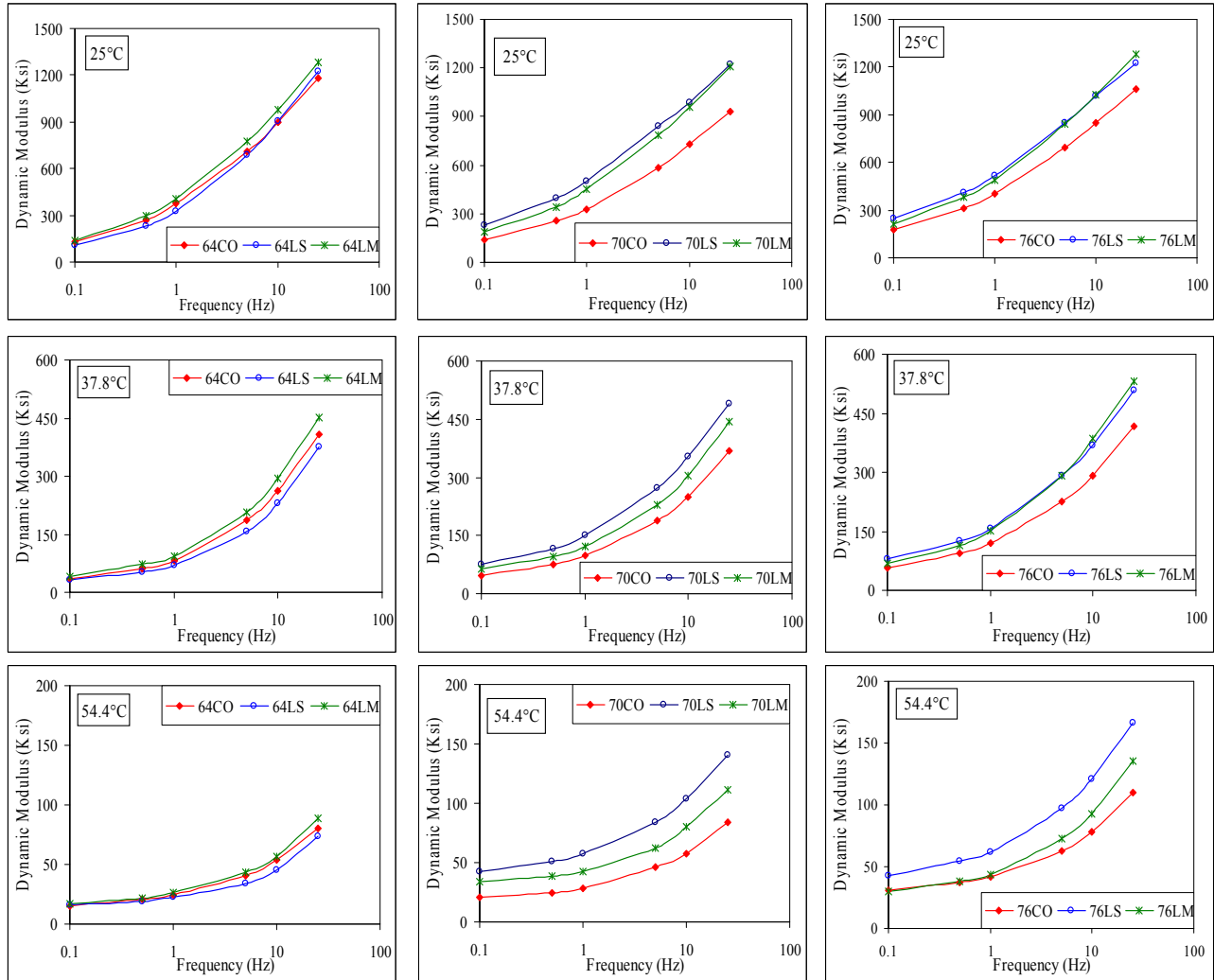


Figure 24
Dynamic modulus isotherms at intermediate and high temperatures

Figures 26 and 27 further describe the behavior of phase angles for all mixtures from low to high temperatures at various test frequencies. The phase angles of all mixtures increased with an increase in temperature and a decrease in frequency at the low temperature (-10°C to 4.4°C) region. At 25°C, the phase angle had a slight increase with an increase in frequency, reached a peak at about 0.5 Hz, and then decreased as the frequency further increased. Similar trend was observed at 37.7°C, but in that case, mixtures reached a peak phase angle value at about 1 Hz. However, at 54.4°C the phase angle values increased with an increase in frequency (opposite to low temperature performances). This observation implied that at high frequency and low temperature, the phase angle of HMA mixtures was primarily affected by the binder itself. Hence, the phase angle of the asphalt binder and the asphalt mixture

follows a similar trend. On the other hand, at low frequency and high temperature, asphalt binder is less viscous, more energy is dissipated in visco-plasticity, and the phase angle of the mixture was predominantly affected by the aggregate structure. Therefore, the phase angle for asphalt mixtures decreased with increasing temperature or decreasing frequency.

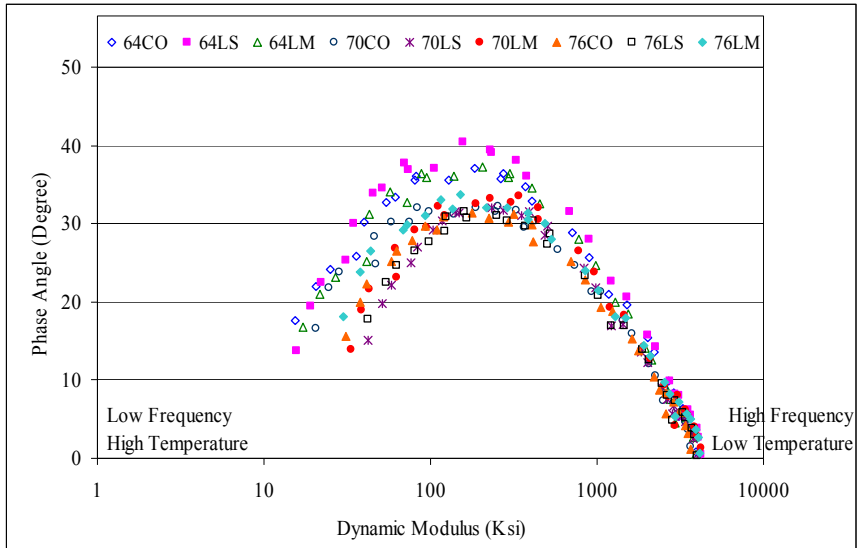


Figure 25
Variation of phase angles with dynamic modulus

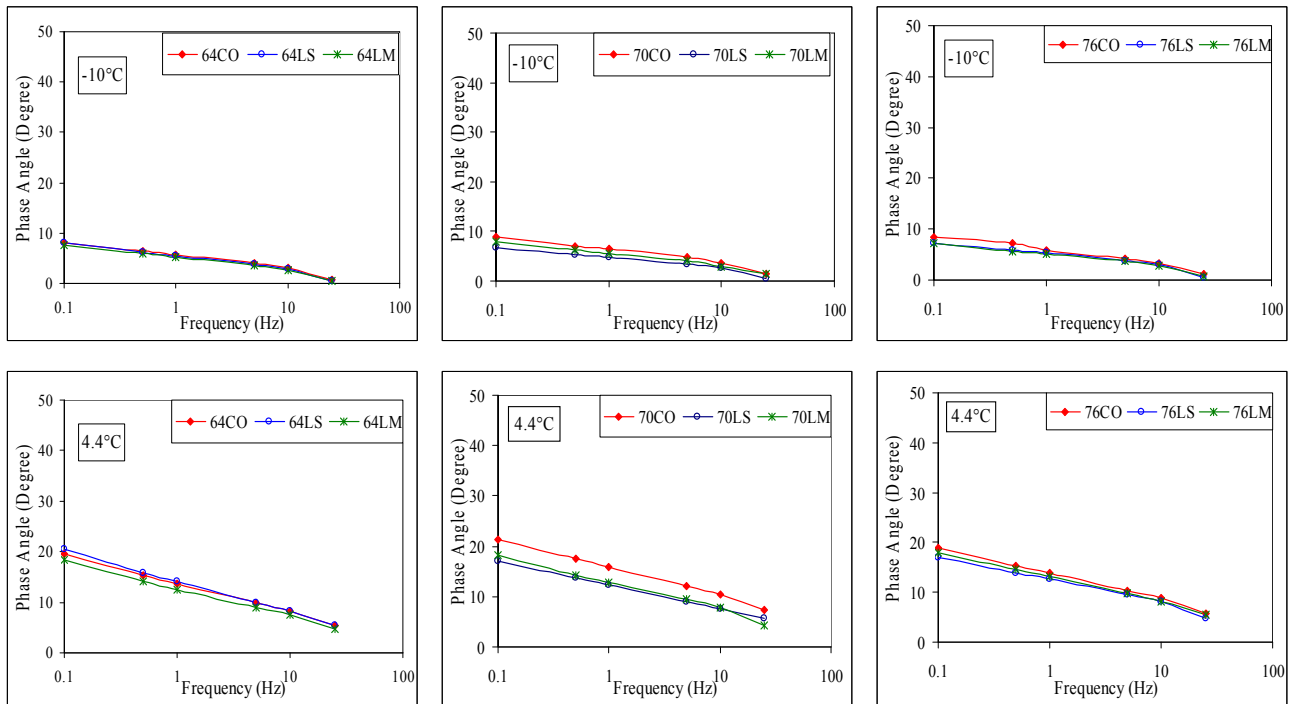


Figure 26
Phase angle isotherms at low temperatures

It was also observed from Figures 23 and 26 that at lower temperatures (-10°C to 4.4°C), the addition of hydrated lime either by paste or no paste method increased the dynamic modulus value and reduced the phase angle value for all mixtures except mixture 64LM when compared to their conventional counterparts. Figure 24 shows that at higher temperatures (25°C to 54.4 °C), the addition of hydrated lime generally increased the dynamic modulus values of all lime-treated mixtures in the 70 HMA and 76 HMA mixture groups comparing to their conventional counterparts. However, for the 64 HMA group, mixture exhibited higher E^* values only when lime was added in “no-paste” (64LM) method.

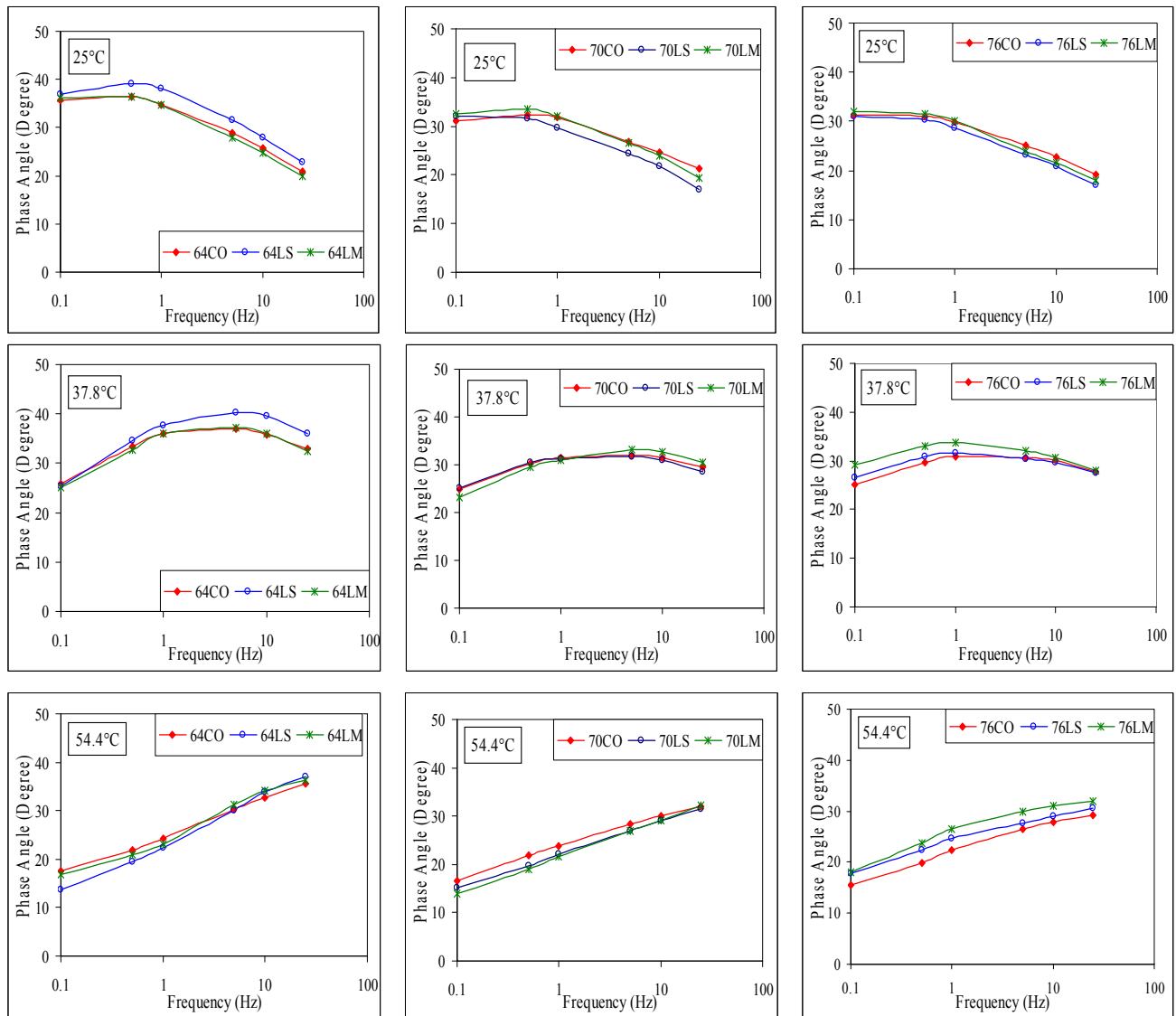


Figure 27
Phase angle isotherms at intermediate and high temperatures

Figure 28 presents a comparison between mixtures 70CO, 64LS, and 64LM on the basis of dynamic modulus computed at 5 Hz and various temperatures. To facilitate this comparison, the E^* values for the 70CO mixture at different temperatures were normalized as the unit value (i.e. $E^* = 1$). The values reported for mixtures 64LS and 64LM were the corresponding E^* ratios of those mixtures with respect to E^* of mixture 70CO at different temperatures. Thus, when a mixture (64LS or 64LM) is reported to have a E^* ratio greater than 1.0, it indicates that the mixture achieved a greater stiffness than that of mixture 70CO. Alternatively, a E^* ratio smaller than 1.0 indicates a mixture with lesser stiffness. It appears from Figure 34 that at lower and intermediate temperatures (from -10°C to 25°C), mixtures 64LS and 64LM showed greater stiffness than mixture 70CO, whereas, at higher temperature (37°C and 54.4°C), the stiffness of the 64LS and 64LM mixtures dropped below that of mixture 70CO. This indicates that the 64LS and 64LM mixtures are more susceptible to fatigue (at low temperatures) and rutting (at high temperature) when compared to mixture 70CO.

On the other hand, Figure 29 shows that mixtures 70LS and 70LM obtained E^* ratios greater than 1.0 at every temperature. This indicates that both 70LS and 70LM mixtures showed better high temperature permanent deformation resistance than that of mixture 76CO. However, this improvement was more substantial when lime was added in slurry method (i.e., 70LS).

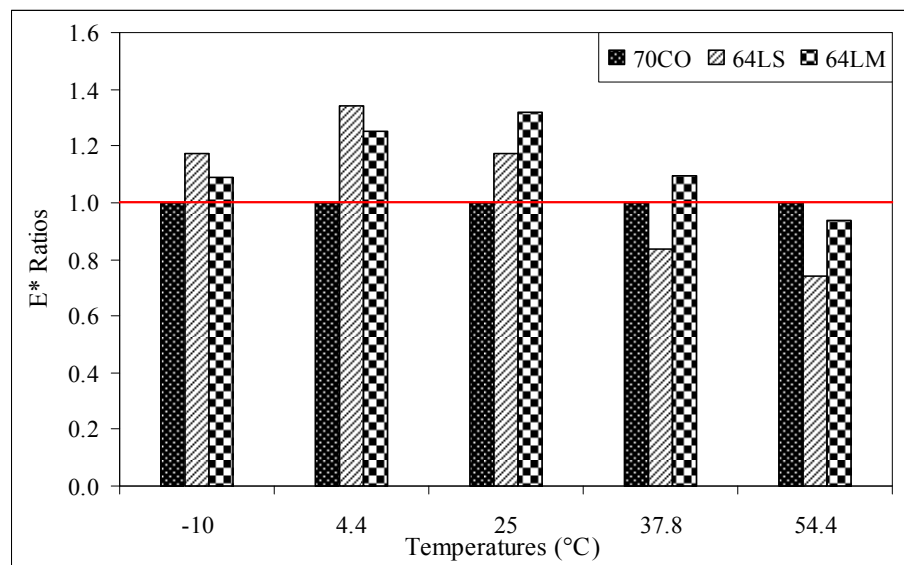


Figure 28
Comparison of E^* results between 70CO, 64LS, and 64LM mixtures

A similar comparison of E^* results between three conventional mixtures is shown in Figure 30. The results indicate that at lower temperatures (from -10°C to 25°C), the E^* ratios for

mixtures 70CO and 76CO were lower than that of the 64CO mixture, whereas, at higher temperatures (from 37.8°C to 54.4°C), the E^* ratios for mixtures 70CO and 76CO followed an opposite trend. Therefore, mixtures containing polymer-modified binders showed better elasticity at lower temperatures and higher stiffness at higher temperatures, which is desirable. However, among mixtures containing polymer-modified binders (70CO and 76CO), mixture 76CO showed better performance at higher temperatures, whereas mixture 70CO had a slight edge at lower temperatures.

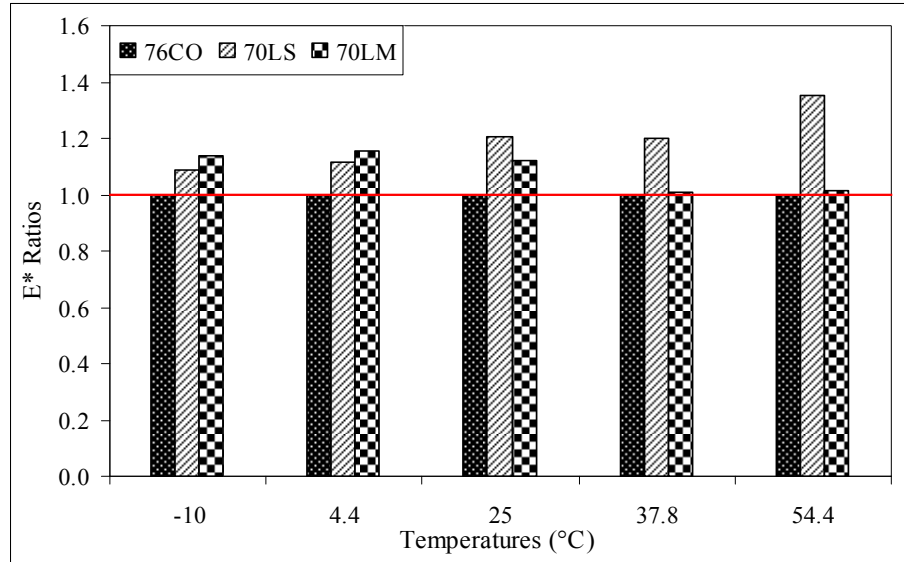


Figure 29
Comparison of E^* results between 76CO, 70LS, and 70LM mixtures

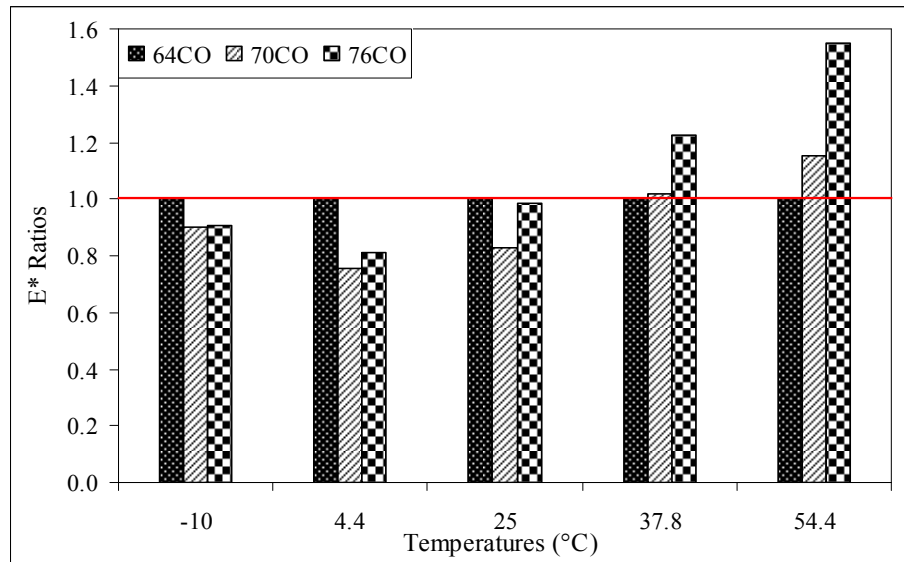


Figure 30
Comparison of E^* results between conventional mixtures

Evaluation of Rutting and Fatigue Resistance from Dynamic Modulus Tests.

The rutting factor, a parameter to measure rutting characteristics of asphalt mixtures, is defined as $E^*/\sin\phi$ (where, ϕ indicates the phase angle) at a particular frequency and temperature. In this study, the $E^*/\sin\phi$ value at a loading frequency of 5 Hz and a testing temperature of 54.4°C was selected as the rutting factor [26]. A higher E^* value and a lower phase angle value represents a mixture to be stiffer and more rut-resistant. Therefore, the higher the rutting factor value, the better the mixture would perform against rutting.

Figure 31 presents that the addition of hydrated lime increased the rutting factor values for all lime-treated mixtures in 70 HMA and 76 HMA groups. However, the improvement was more significant when lime was added in the slurry method. On the other hand, for 64 HMA group, only 64LM showed slight improvement in rutting factor than its conventional counterpart (64CO). Hence, it can be concluded that the addition of hydrated lime improved the rut resistance characteristics of all HMA mixtures except for mixture 64LS.

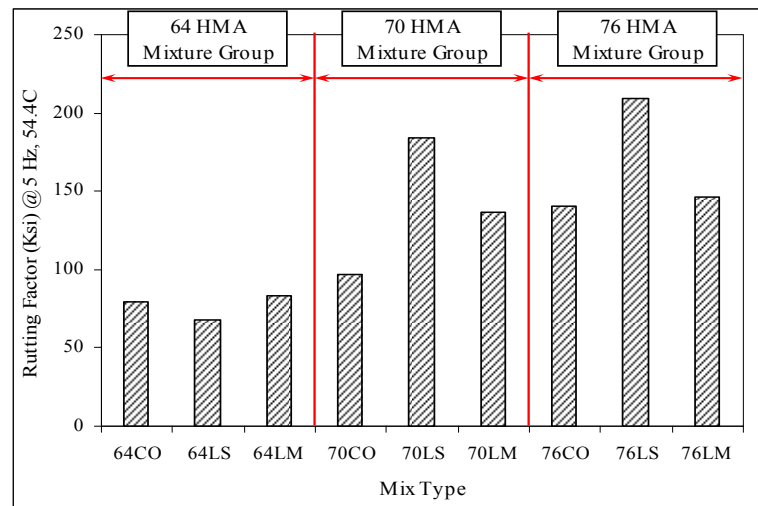


Figure 31
Rutting factor at 5 Hz and 54.4°C

A fatigue cracking parameter named, fatigue factor, defined by $E^*\sin\phi$ at a loading frequency of 5 Hz and a testing temperature of 25°C was considered as the mixtures' fatigue factor in this study [26]. Low E^* and phase angle values at low or intermediate temperature (here, 25°C) are desired for fatigue resistant mixtures. Figure 32 showed that the addition of hydrated lime increased the fatigue factor values for all lime-treated mixtures included in this study when compared to corresponding conventional mixtures of the same HMA mixture group.

Table 17 summarizes results from statistical analyses performed on dynamic modulus test results for different HMA mixture groups to statistically rank the mixtures contained within each HMA mixture group. In general, the addition of hydrated lime improved the rut resistance of mixtures (except 64LS) in comparison to the conventional mixture of the same HMA mixture group no matter how lime was added to the mixture. However, in 70 HMA and 76 HMA mixture groups, the rut resistance was more pronounced when lime was added in slurry method. No substantial difference in mixtures' fatigue performance was observed when hydrated lime was added in either way (paste or no-paste) to mixtures containing PG 64-22 binder. It is noted that the addition of hydrated lime increased the fatigue factor of mixtures containing both PG 70-22M and PG 76-22M asphalts. This type of mixture is ideally suited for a base course or binder course layer in a perpetual pavement structure where a stiff and durable mixture is desired.

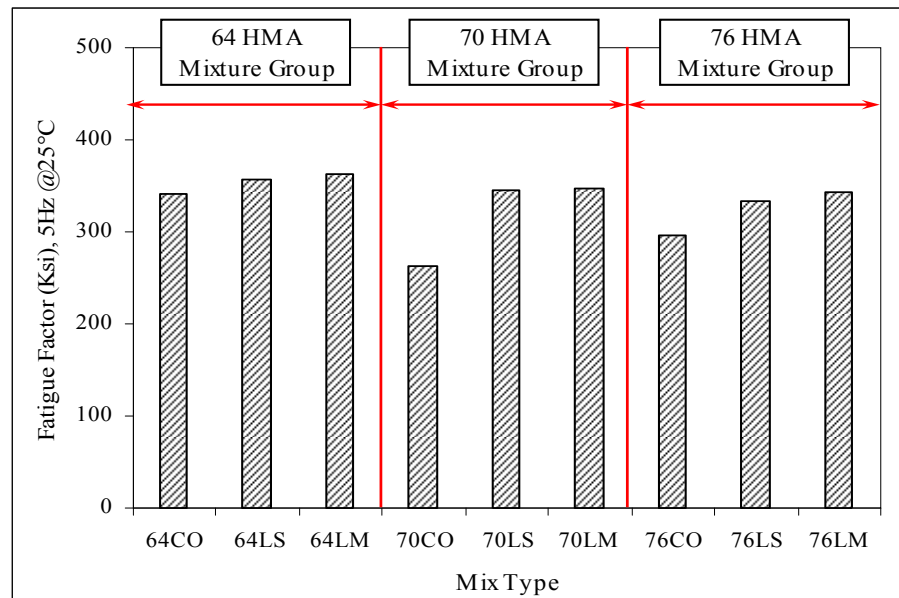


Figure 32
Fatigue factor at 5 Hz and 25°C

When mixtures 70LS and 70LM were compared to 76CO mixture, it was observed that mixture 70LM exhibited similar rutting performance as mixture 76CO, whereas, mixture 70LS showed better rutting resistance than 76CO. However, mixture 76CO had higher fatigue factor than both 70LS and 70LM. The comparison among the conventional mixtures reported in Table 17 indicates that the 76CO was the best performer against both fatigue and rutting.

Table 17
Statistical analyses on dynamic modulus test data

Analytical Grouping	Mixture Type	E* (Ksi) @ 5Hz and 54.4°C		Rutting Factor E*/Sinφ@ 5Hz and 54.4°C		Fatigue Factor E*Sinφ@ 5Hz and 25°C	
		Mean	Ranking	Mean	Ranking	Mean	Ranking
64 HMA Group	64CO	40	A/B	79.6	A/B	340.5	A
	64LS	34	B	68.1	B	357.1	A
	64LM	43	A	83.2	A	363.2	A
70 HMA Group	70CO	46	C	96.7	C	262.9	A
	70LS	84	A	184.1	A	345.5	B
	70LM	62	B	136.6	B	347.4	B
76 HMA Group	76CO	62	B	141.0	B	296.5	A
	76LS	97	A	209.0	A	333.1	A/B
	76LM	73	B	146.2	B	342.3	B
64LS and 64LM vs. 70CO	64LS	34	B	68.1	B	357.1	B
	64LM	43	A	83.2	A/B	363.2	B
	70CO	46	A	96.7	A	262.9	A
70LS and 70LM vs. 76CO	70LS	84	A	184.1	A	345.5	B
	70LM	62	B	136.6	B	347.4	B
	76CO	62	B	141.0	B	296.5	A
Conventional Group	64CO	40	B	79.6	B	340.5	B
	70CO	46	B	96.7	B	262.9	A
	76CO	62	A	141.0	A	296.5	A/B

Note: Ranking: Statistical Ranking (Rows with the same letter indicate no significant difference)

Flow Number Test Results

Figure 33 presents the flow number results where each vertical bar represents the average flow number value of the three specimens per mixture. As flow number indicates the starting point of tertiary flow, the higher the flow number, the better the mixture against rutting. Note that, when a specimen did not show any tertiary flow during the entire loading cycle (i.e., 10,000 cycles), the flow number value of that specimen was reported as 10,000 cycles.

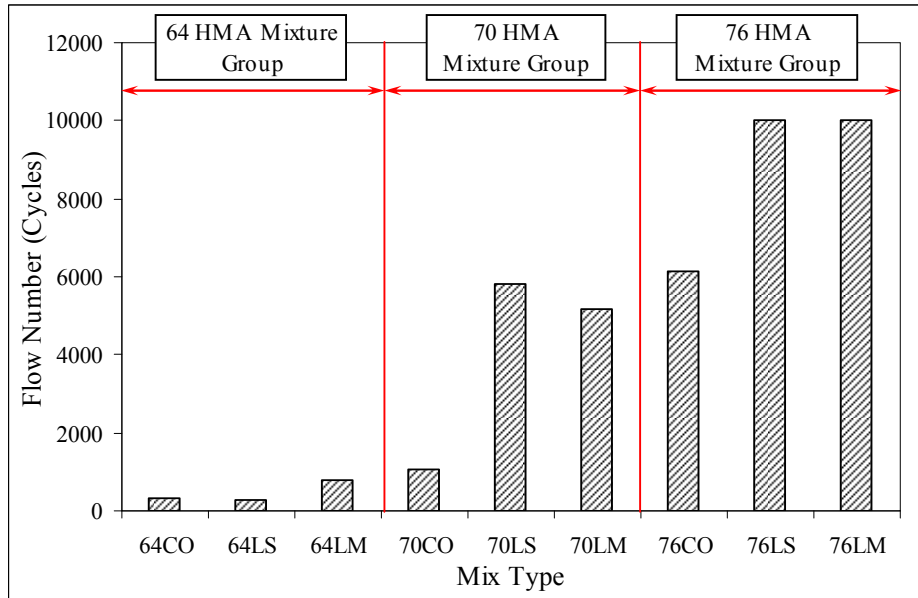


Figure 33
Flow number test results for all mixtures

Tables 18 through 20 present statistically analyzed flow number test results for 64 HMA, 70 HMA, and 76 HMA mixture groups, respectively. The statistical rankings indicate that the addition of hydrated lime significantly improved the rutting resistance of mixtures containing PG 70-22M and PG 76-22M binder regardless of how lime was added. For 64 HMA group, mixture 64LS did not show considerable improvement, whereas the improvement on 64LM mixture was significant.

Table 18
Flow number test results for 64 HMA mixture group

Mix Type	Sample ID	Air Void	Flow Number (Cycles)	Mean Flow Number	St. Dev	%CV	Rank
64CO	1	7.0	304	324	58.6	18.1	B
	2	7.4	390				
	14	7.5	278				
64LS	5	7.1	239	268	39.3	14.6	B
	8	7.6	253				
	9	6.6	313				
64LM	6	7.1	730	797	158.5	19.9	A
	7	6.5	683				
	10	6.4	978				

Table 19
Flow number test results for 70 HMA mixture group

Mix Type	Sample ID	Air Void	Flow Number (Cycles)	Mean Flow Number	St. Dev	%CV	Rank
70CO	12	7.0	1190	1068	144.2	13.5	B
	13	7.1	909				
	14	7.0	1106				
70LS	4	6.4	6101	5811	648.6	11.2	A
	8	6.7	5068				
	9	6.7	6264				
70LM	1	7.3	6121	5160	917.2	17.8	A
	2	6.8	5064				
	12	7.3	4294				

*Note: Rank: Statistical Ranking (Rows with the same letter indicate no significant difference)
St. Dev: Standard Deviation, %CV: Coefficient of Variance (%)*

Table 20
Flow number test results for 76 HMA mixture group

Mix Type	Sample ID	Air Void	Flow Number (Cycles)	Mean Flow Number	St. Dev	%CV	Rank
76CO	1	7.3	5493	6132	851.0	13.9	B
	8	6.7	5805				
	11	7.2	7098				
76LS	6	7.0	10000	10000	N/A	N/A	A
	11	6.4	10000				
	14	6.6	10000				
76LM	1	6.9	10000	10000	N/A	N/A	A
	2	6.5	10000				
	6	7.4	10000				

*Note: Rank: Statistical Ranking (Rows with the same letter indicate no significant difference)
St. Dev: Standard Deviation, %CV: Coefficient of Variance (%), N/A: Not Applicable*

Tables 21 and 22 show the comparison of flow numbers between hydrated lime treated mixtures containing lower “high temperature PG graded” asphalt binder and the conventional mixture containing relatively higher “high temperature PG graded” asphalt. . It appears that both 64LS and 64LM exhibited lower flow numbers when compared to 70CO. However, the

addition of hydrated lime substantially improved the rut resistance of 70LS and 70LM mixtures as they obtained a similar statistical ranking to mixture 76CO (Table 22).

Table 21
Comparison of flow number between 64LS, 64LM, and 70CO mixtures

Mix Type	Sample ID	Air Void	Flow Number (Cycles)	Mean Flow Number	St. Dev	%CV	Ranking
64LS	5	7.1	239	268	39.3	14.6	C
	8	7.6	253				
	9	6.6	313				
64LM	6	7.1	730	797	158.5	19.9	B
	7	6.5	683				
	10	6.4	978				
70CO	12	7.0	1190	1068	144.2	13.5	A
	13	7.1	909				
	14	7.0	1106				

*Note: Ranking: Statistical Ranking (Rows with the same letter indicate no significant difference)
St. Dev: Standard Deviation, %CV: Coefficient of Variance (%)*

Table 22
Comparison of flow number between 70LS, 70LM, and 76CO mixtures

Mix Type	Sample ID	Air Void	Flow Number (Cycles)	Mean Flow Number	St. Dev	%CV	Rank
70LS	4	6.4	6101	5811	648.6	11.2	A
	8	6.7	5068				
	9	6.7	6264				
70LM	1	7.3	6121	5160	917.2	17.8	A
	2	6.8	5064				
	12	7.3	4294				
76CO	1	7.3	5493	6132	851.0	13.9	A
	8	6.7	5805				
	11	7.2	7098				

*Note: Rank: Statistical Ranking (Rows with the same letter indicate no significant difference)
St. Dev: Standard Deviation, %CV: Coefficient of Variance (%)*

Table 23 presents the comparison of flow number test results among the three conventional mixtures. It is noted that the influence of polymer in 76CO and 70CO mixtures improved the

permanent deformation characteristic of HMA mixtures and the improvement was more substantial with an increase in binder's polymer content.

Table 23
Comparison of flow number between conventional mixtures

Mix Type	Sample ID	Air Void	Flow Number (Cycles)	Mean Flow Number	St. Dev	%CV	Rank
64CO	1	7.0	304	324	58.6	18.1	C
	2	7.4	390				
	14	7.5	278				
70CO	12	7.0	1190	1068	144.2	13.5	B
	13	7.1	909				
	14	7.0	1106				
76CO	1	7.3	5493	6132	851.0	13.9	A
	8	6.7	5805				
	11	7.2	7098				

*Note: Rank: Statistical Ranking (Rows with the same letter indicate no significant difference)
St. Dev: Standard Deviation, %CV: Coefficient of Variance (%)*

Flow Time Test Results

The results for flow time tests are presented in Figure 34, where each vertical bar represents the average flow time value of three specimens for each mixture type. Similar to flow number test, when a specimen did not show tertiary flow during the entire loading period (i.e., 10,000 sec), the flow time value of that specimen was reported as 10,000 seconds. A greater flow time value is indicative of a mixture having better rutting resistance and stability compared to a mixture with a smaller flow time value, when the applied stress and the temperature are the same. In general, the addition of hydrated lime substantially increased the flow time value for all lime-treated mixtures except 64LM, however, all three mixtures in 64 HMA group achieved very small flow time values comparing to the other mixtures evaluated in this study.

Tables 24 through 26 present the results from the statistical analyses performed on the flow time test results for mixtures contained in the 64 HMA, 70 HMA, and 76 HMA mixture groups respectively. In the 64 HMA mixture group, 64LM did not show any difference whereas, 64LS showed significant improvement when compared to 64CO (Table 24). However, Tables 25 and 26 showed that all lime-treated mixtures in 70 HMA and 76 HMA mixture groups gained significantly higher rankings than their conventional counterparts

(70CO and 76CO respectively). Furthermore, the method of adding hydrated lime did not show any influence on the permanent deformation of the mixtures.

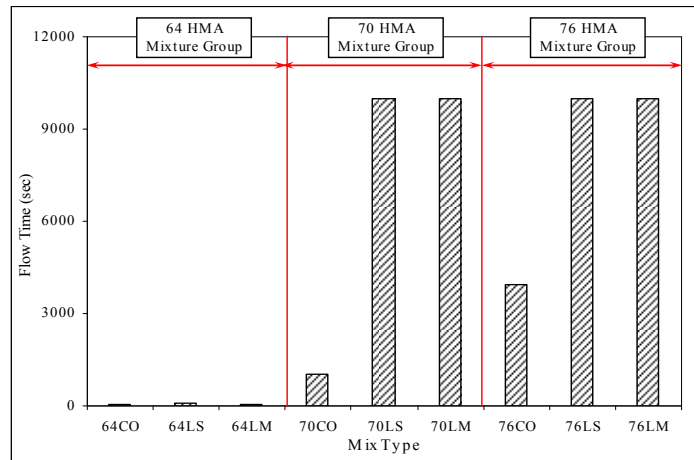


Figure 34
Flow time test results for all mixtures

Table 24
Flow time test results for 64 HMA mixture group

Mix Type	Sample ID	Air Void	Flow Time (Sec)	Mean Flow Time	St. Dev	%CV	Ranking
64 CO	9	7.1	42	38	5.7	14.9	B
	11	7.2	34				
64 LS	13	7.3	90	96	7.8	8.1	A
	14	7.3	101				
64 LM	2	7.5	38	37	1.4	3.8	B
	9	7.1	36				

Note: Ranking: Statistical Ranking (Rows with the same letter indicate no significant difference)
St. Dev: Standard Deviation, %CV: Coefficient of Variance (%)

Table 25
Flow time test results for 70 HMA mixture group

Mix Type	Sample ID	Air Void	Flow Time (Sec)	Mean Flow Time	St. Dev	%CV	Ranking
70 CO	15	6.7	861	1008	207.9	20.6	B
	17	6.5	1155				
70 LS	3	7.2	10000	10000	N/A	N/A	A
	7	6.8	10000				
70 LM	3	6.8	10000	10000	N/A	N/A	A
	8	6.4	10000				

Note: Ranking: Statistical Ranking (Rows with the same letter indicate no significant difference)
St. Dev: Standard Deviation, %CV: Coefficient of Variance (%), N/A: Not Applicable

Table 26
Flow time test results for 76 HMA mixture group

Mix Type	Sample ID	Air Void	Flow Time (Sec)	Mean Flow Time	St. Dev	%CV	Ranking
76 CO	13	7.3	4172	3926	347.9	8.9	B
	15	7.5	3680				
76 LS	12	7.5	10000	10000	N/A	N/A	A
	13	6.7	10000				
76 LM	7	7.4	10000	10000	N/A	N/A	A
	8	6.8	10000				

*Note: Ranking: Statistical Ranking (Rows with the same letter indicate no significant difference)
St. Dev: Standard Deviation, %CV: Coefficient of Variance (%), N/A: Not Applicable*

The comparison of flow time values between mixtures 64LS, 64LM, and 70CO is presented in Table 27, while Table 28 shows the comparison of flow time between mixtures 70LS, 70LM, and 76CO. The flow number values for mixtures 64LS and 64LM were extremely lower than that of mixture 70CO. However, hydrated lime treatment significantly increased the flow time values of mixtures containing PG 70-22M asphalt binder as both mixtures 70LS and 70LM obtained a better statistical ranking than mixture 76CO (Table 28).

Table 29 presents the comparison of flow time test results among the three conventional mixtures. Similar to flow number test results, mixture 76CO exhibited the highest statistical ranking followed by mixtures 70CO and 64CO, respectively. This indicates that the addition of polymer to the neat binder improved the permanent deformation characteristic of HMA mixtures.

Table 27
Comparison of flow time between mixtures 64LS, 64LM, and 70CO

Mix Type	Sample ID	Air Void	Flow Time (Sec)	Mean Flow Time	St. Dev	%CV	Ranking
64LS	13	7.3	90	96	7.8	8.1	B
	14	7.3	101				
64LM	2	7.5	38	37	1.4	3.8	B
	9	7.1	36				
70CO	15	6.7	861	1008	207.9	20.6	A
	17	6.5	1155				

*Note: Ranking: Statistical Ranking (Rows with the same letter indicate no significant difference)
St. Dev: Standard Deviation, %CV: Coefficient of Variance (%)*

Table 28
Comparison of flow time between mixtures 70LS, 70LM, and 76CO

Mix Type	Sample ID	Air Void	Flow Time (Sec)	Mean Flow Time	St. Dev	%CV	Ranking
70LS	3	7.2	10000	10000	N/A	N/A	A
	7	6.8	10000				
70LM	3	6.8	10000	10000	N/A	N/A	A
	8	6.4	10000				
76CO	13	7.3	4172	3926	347.9	8.9	B
	15	7.5	3680				

*Note: Ranking: Statistical Ranking (Rows with the same letter indicate no significant difference)
St. Dev: Standard Deviation, %CV: Coefficient of Variance (%), N/A: Not Applicable*

Table 29
Comparison of flow time between conventional HMA mixture groups

Mix Type	Sample ID	Air Void	Flow Time (Sec)	Mean Flow Time	St. Dev	%CV	Ranking
64 CO	9	7.1	42	38	5.7	14.9	C
	11	7.2	34				
70CO	15	6.7	861	1008	207.9	20.6	B
	17	6.5	1155				
76CO	13	7.3	4172	3926	347.9	8.9	A
	15	7.5	3680				

*Note: Ranking: Statistical Ranking (Rows with the same letter indicate no significant difference)
St. Dev: Standard Deviation, %CV: Coefficient of Variance (%)*

Loaded Wheel Tracking (LWT) Test Results

Figure 35 compares the mean rut depth of mixtures recorded from the LWT test at 20,000 passes. Mixtures are considered to pass the LWT test if the rut depth of the specimen remains less than 6.0 mm after 20,000 passes. It is noted from Figure 41 that all three mixtures of 64 HMA group were susceptible to rutting (rut depths greater than 6.0 mm). However, the other six mixtures performed very well and passed the minimum rut depth requirement of 6.0 mm. The continuous rut profile reported in Figure 36 indicates that there was no sign of stripping for any of the mixtures.

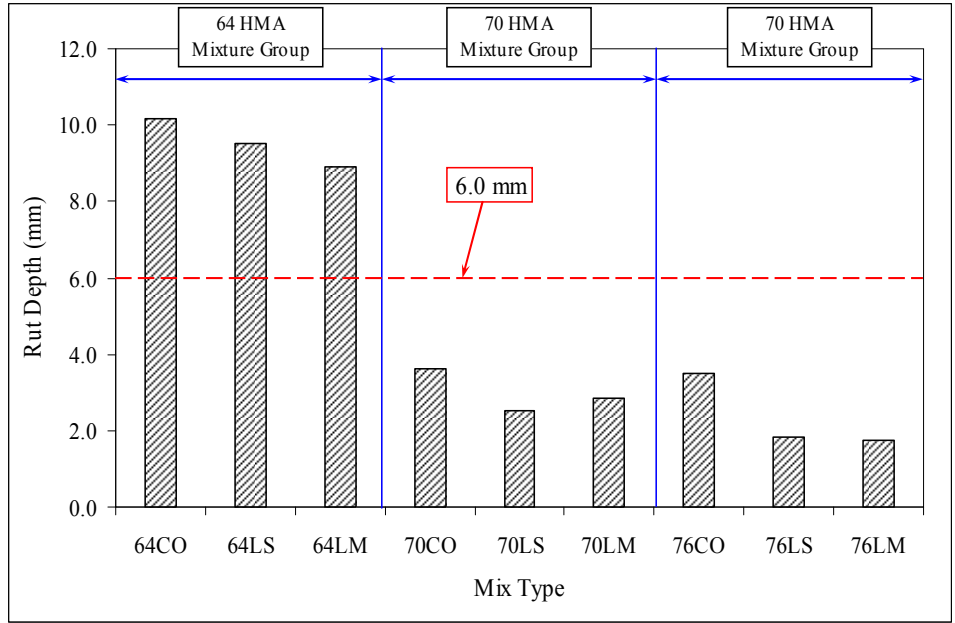


Figure 35
LWT test results – rut depth

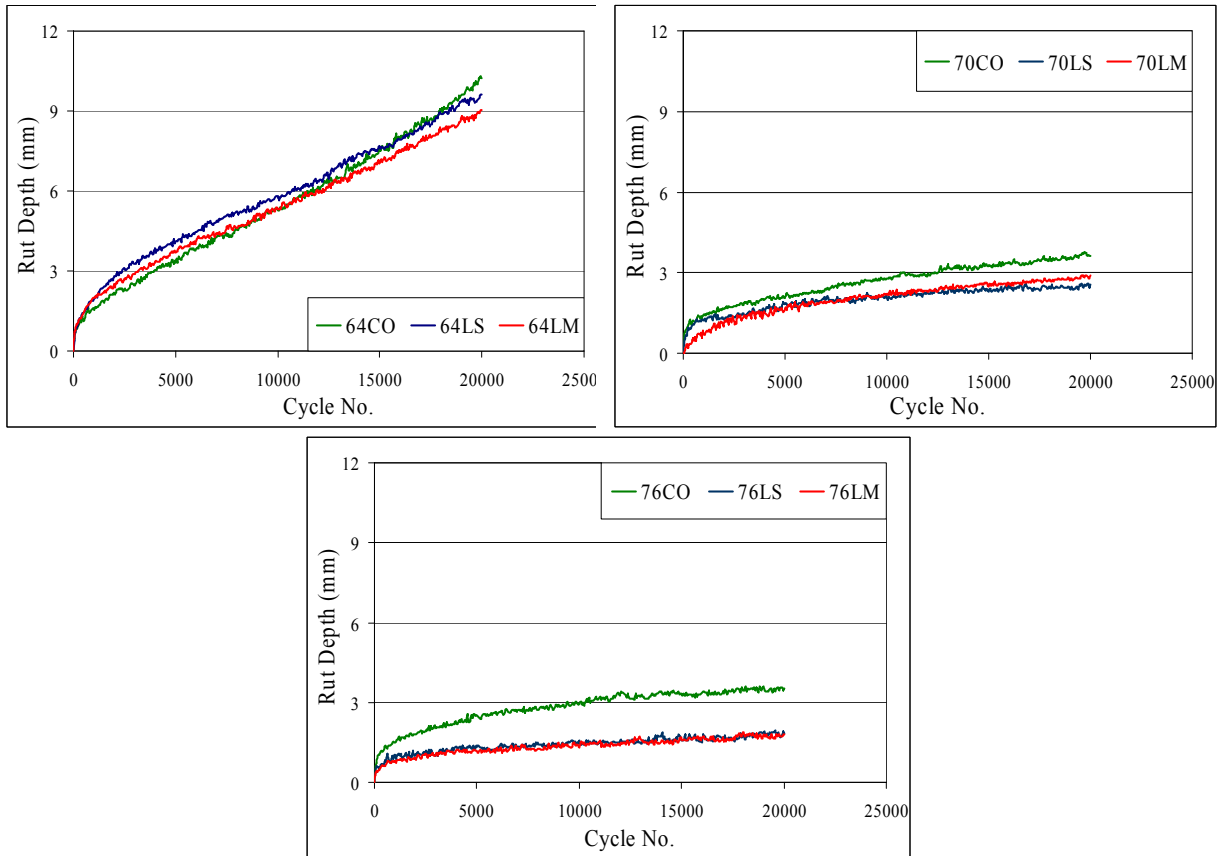


Figure 36
LWT test results – rut profile

As shown in Table 30, the addition of hydrated lime to the mixtures containing PG 64-22 asphalt binder did not show improvement to resist rutting, as measured by the LWT test, no matter how lime was incorporated. Moreover, all three mixtures in 64 HMA mixture group exceeded the maximum acceptable rut depth of 6.0 mm at 20,000 passes.

Table 30
LWT results for 64 HMA mixture group

Mix Type	Sample ID	Air Void	Rut Depth (mm)	Mean Rut Depth	St Dev.	%CV	Ranking
64 CO	1	7.1	9.1	10.2	1.5	14.9	A
	2	7.1	11.3				
64 LS	1	7.2	8.8	9.5	1.0	10.6	A
	2	6.7	10.2				
64 LM	1	6.8	7.5	9.0	2.0	22.9	A
	2	7.2	10.4				

*Note: Ranking: Statistical Ranking (Rows with the same letter indicate no significant difference)
St. Dev: Standard Deviation, %CV: Coefficient of Variance (%)*

The statistical analyses presented in Tables 31 and 32 indicate that all hydrated lime-treated HMA mixtures containing PG 70-22M and PG 76-22M binders showed improved rut resistance than their conventional counterparts (70CO and 76CO) respectively. Moreover, the method of lime application did not make any significant difference on LWT test performance. It is worth noting that all mixtures in 70 HMA and 76 HMA mixture groups performed very well in this test and passed the maximum rut depth requirement of 6.0 mm.

Table 31
LWT results for 70 HMA mixture group

Mix Type	Sample ID	Air Void	Rut Depth (mm)	Mean Rut Depth	St. Dev.	%CV	Ranking
70 CO	1	7.4	3.4	3.7	0.4	9.8	B
	2	7.6	3.9				
70 LS	1	6.6	2.4	2.6	0.2	9.6	A
	2	6.4	2.7				
70 LM	1	7.3	2.7	2.9	0.2	7.7	A/B
	2	7.6	3.0				

*Note: Ranking: Statistical Ranking (Rows with the same letter indicate no significant difference)
St. Dev: Standard Deviation, %CV: Coefficient of Variance (%)*

Table 32
LWT results for 76 HMA mixture group

Mix Type	Sample ID	Air Void	Rut Depth (mm)	Mean Rut Depth	St. Dev.	%CV	Ranking
76 CO	1	7.0	3.4	3.5	0.2	4.8	B
	2	7.6	3.6				
76 LS	1	6.5	1.6	1.9	0.4	21.0	A
	2	6.6	2.1				
76 LM	1	6.7	1.8	1.8	0.1	5.4	A
	2	7.3	1.7				

*Note: Ranking: Statistical Ranking (Rows with the same letter indicate no significant difference)
St. Dev: Standard Deviation, %CV: Coefficient of Variance (%)*

The comparison between 64LS, 64LM, and 70CO mixtures has been summarized in Table 33, while Table 34 shows the comparison between mixtures 70LS, 70LM, and 76CO. It is clear that the addition of hydrated lime to 64LM and 64LS did not improve the rut resistance in comparison to mixture 70CO. On the other hand, hydrated lime significantly improved the rutting performance for 70LS and 70LM mixtures, and consequently, they outperformed 76CO mixture.

Table 33
Comparisons of LWT results between 64LS, 64LM, and 70CO mixtures

Mix Type	Sample ID	Air Void	Rut Depth (mm)	Mean Rut Depth	St. Dev.	%CV	Ranking
64 LS	1	7.2	8.8	9.5	1.0	10.6	B
	2	6.7	10.2				
64 LM	1	6.8	7.5	9.0	2.0	22.9	B
	2	7.2	10.4				
70 CO	1	7.4	3.4	3.7	0.4	9.8	A
	2	7.6	3.9				

*Note: Ranking: Statistical Ranking (Rows with the same letter indicate no significant difference)
St. Dev: Standard Deviation, %CV: Coefficient of Variance (%)*

The comparison of LWT test results between the three conventional mixtures presented in Table 35 indicated that the mixtures contained SB modified binders (70CO and 76CO) showed excellent rut resistance. However, no significant difference was observed between the rut resistance of mixture 70CO and 76CO.

Table 34
Comparisons of LWT results between 70LS, 70LM, and 76CO mixtures

Mix Type	Sample ID	Air Void	Rut Depth (mm)	Mean Rut Depth	St. Dev.	%CV	Ranking
70 LS	1	6.6	2.4	2.6	0.2	9.6	A
	2	6.4	2.7				
70 LM	1	7.3	2.7	2.9	0.2	7.7	A/B
	2	7.6	3.0				
76 CO	1	7.0	3.4	3.5	0.2	4.8	B
	2	7.6	3.6				

*Note: Ranking: Statistical Ranking (Rows with the same letter indicate no significant difference)
 St. Dev: Standard Deviation, %CV: Coefficient of Variance (%)*

Table 35
Comparisons of LWT results between conventional HMA mixture groups

Mix Type	Sample ID	Air Void	Rut Depth (mm)	Mean Rut Depth	St. Dev.	%CV	Ranking
64 CO	1	7.1	9.1	10.2	1.5	14.9	B
	2	7.1	11.3				
70 CO	1	7.4	3.4	3.7	0.4	9.8	A
	2	7.6	3.9				
76 CO	1	7.0	3.4	3.5	0.2	4.8	A
	2	7.6	3.6				

*Note: Ranking: Statistical Ranking (Rows with the same letter indicate no significant difference)
 St. Dev: Standard Deviation, %CV: Coefficient of Variance (%)*

Correlation between Test Results

This section presents the correlation among the results of different laboratory tests performed in this study. The regression procedure of statistical analysis was applied to determine the level of relationship. Both linear and non-linear regression analyses were employed, and correlation coefficients were computed to measure the goodness of fit.

Correlation between Binder and Mixture Properties

Figure 37 presents the correlations between binder and mixture stiffness for PG 70-22M, PG 76-22M, and PG 76-16 (i.e., hydrated lime-treated PG 70-22M) binders and their corresponding HMA mixtures (i.e., 70CO, 76CO, and 70LM). It was observed that there was

a strong relationship between the binder's complex modulus and the mixture's dynamic modulus, $R^2 = 0.99$. The relationship was expressed by the following:

$$E^* = AG^{*B} \tag{8}$$

where,

E^* = mixture dynamic modulus,

G^* = binder complex modulus, and

A and B = constants

It is noted that the constant B, which represents the slope of the E^* vs. G^* plot, was independent of the binder used as the values remained constant.

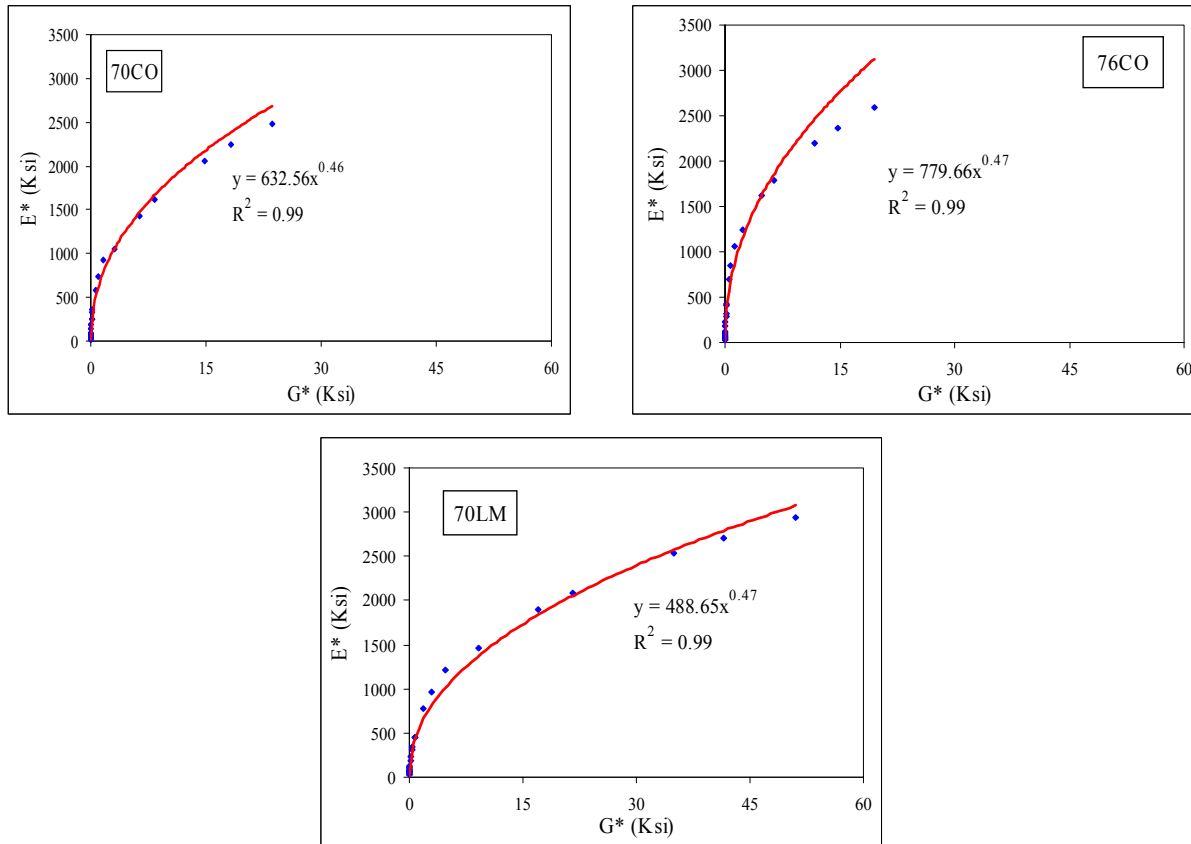


Figure 37
Correlation – binder and mixture stiffness

Figure 38 shows the relationship between binder and mixture rut factor, expressed by $G^*/\text{Sin}\delta$ and $E^*/\text{Sin}\phi$, respectively, at 5 Hz and 54.4°C. A strong linear relationship was observed between these two rutting parameters regardless of the type of binder utilized. It is

also apparent that the addition of hydrated lime to the binder did not affect the relationship between binder and mixture properties reported in Figures 37 and 38.

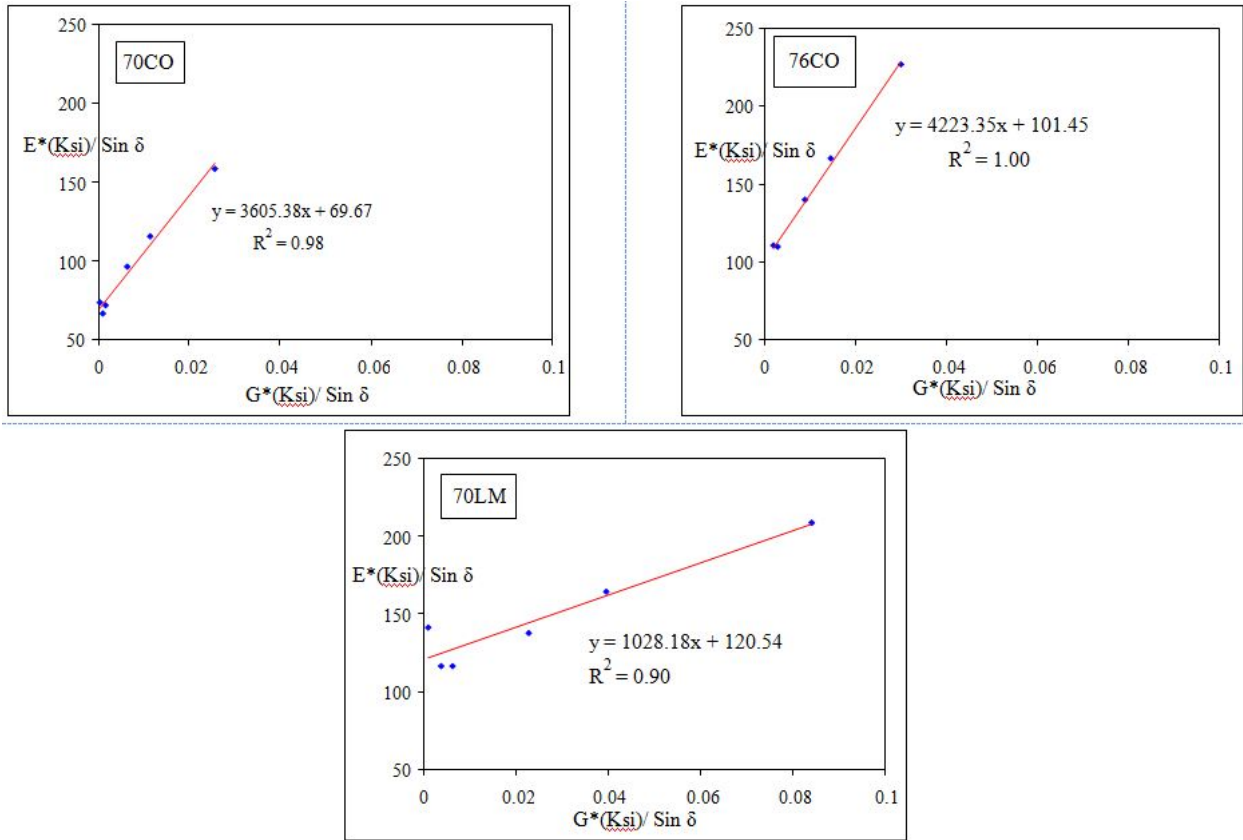


Figure 38
Correlation – binder and mixture rut factor at 5 Hz and 54.4°C

Correlation between Fatigue Related Properties of HMA Mixtures

Figure 39 presents the correlation between ITS (TI) and SCB (J_c) test results for both unaged and aged mixtures. A better correlation was observed for the unaged mixtures ($R^2 = 0.93$) than the aged ones ($R^2 = 0.75$).

Figures 40 through 43 present correlations among various fatigue parameters for the mixtures included in this study. Each figure contains three individual linear correlations, one for each mixture group (64 HMA, 70 HMA, and 76 HMA). Figures 46 and 47 show that the linear correlations between DCSE and TI and DCSE and J_c are poor ($R^2 = 0.48$) for the 64 HMA mixture group. However, very good correlations were observed between DCSE and TI and DCSE and J_c for mixtures contained in 70 HMA and 76 HMA mixture groups (R^2 values are 0.89, 0.99, 0.98, and 0.99, respectively). Likewise, 70 HMA and 76 HMA mixture groups showed very good relationship ($R^2 = 0.98$ and 0.88 respectively) between fatigue factor (E^*

Sin ϕ at 5Hz and 25°C) and J_c values (Figure 49) whereas, a poor relationship was observed between these two parameters for 64 HMA group. Considering fatigue factor and TI values excellent correlations ($R^2 = 1.0, 0.94,$ and 0.87) were observed for all mixtures included in this study (Figure 43).

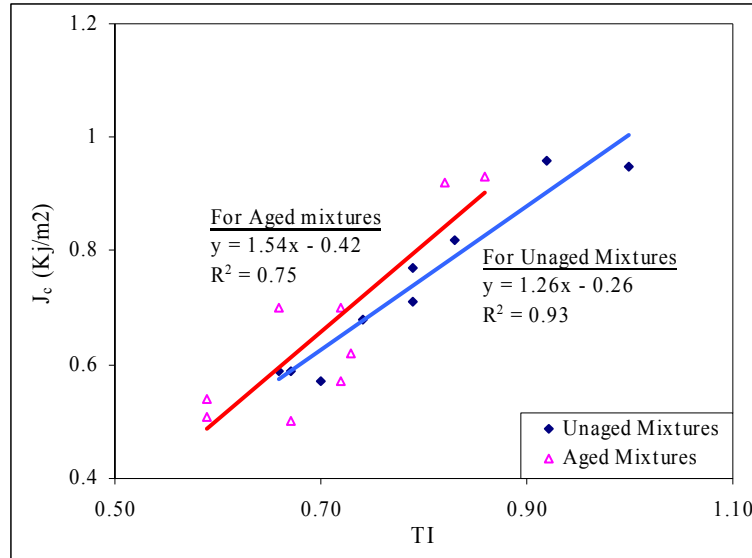


Figure 39
Correlation – TI and J_c

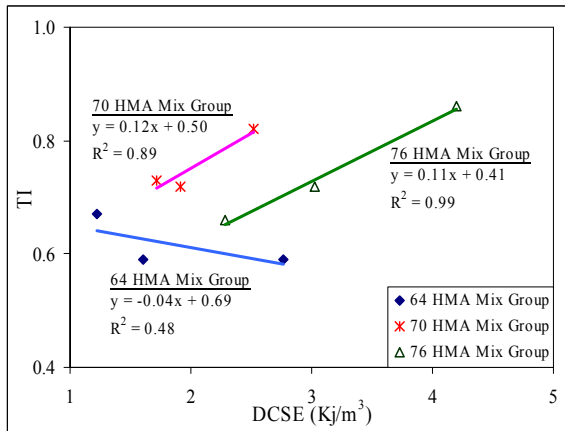


Figure 40
Correlation – DCSE and TI

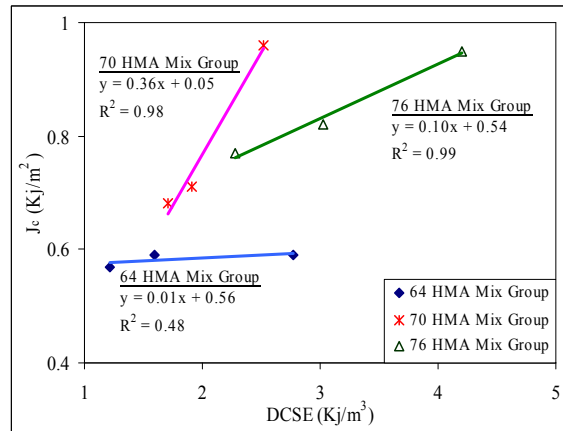


Figure 41
Correlation – DCSE and J_c

Overall, the correlations between fatigue parameters were very good for the mixtures containing polymer modified PG 70-22M and PG 76-22M binders. However, for mixtures containing PG 64-22 binder, the relationship was not so good. This possibly relates to the reaction between hydrated lime and polymer modified asphalt binders (PG 70-22M and PG 76-22M). A different chemical reaction between hydrated lime and the virgin binder (PG 64-22) might have caused the difference in the trend in mixture-parameters.

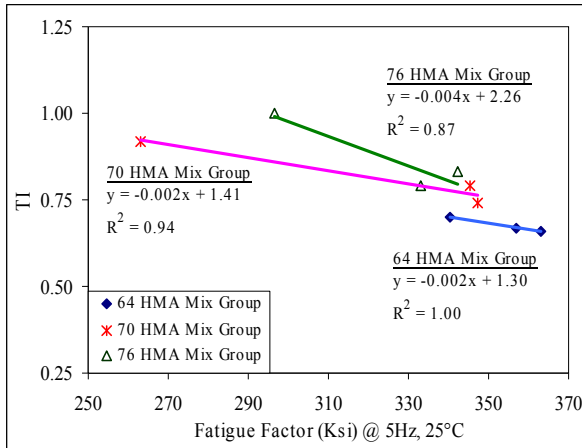


Figure 42
Correlation – fatigue factor and TI

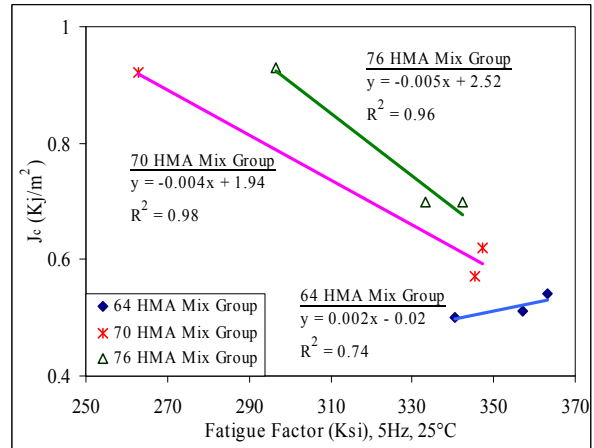


Figure 43
Correlation – fatigue factor and J_c

Correlation between Permanent Deformation Properties of HMA Mixtures

Power models were utilized to correlate the rut depth data obtained from LWT tests with the permanent deformation characterization data obtained from other laboratory tests [26]. The permanent deformation observed in the LWT tests was related to the viscoelastic properties of HMA mixtures, which are most commonly expressed in terms of power functions when the mechanistic analysis of these mixtures is performed [34]. The goodness of fit for a power model cannot be measured by the R^2 value only because it is a nonlinear model. Instead, a parameter called standard error ratio, S_e/S_y (in which S_e is the standard error of estimate, and S_y is the standard deviation of the variable), is applied along with R^2 , coefficient of determination. Table 36 presents the criteria to evaluate the goodness of fit for statistical analysis [26].

Table 36
Criteria for goodness of fit statistical parameters

Criteria	R^2	S_e/S_y
Excellent	≥ 0.90	≤ 0.35
Good	0.70 – 0.89	0.36 – 0.55
Fair	0.40 – 0.69	0.56 – 0.75
Poor	0.20 – 0.39	0.76 – 0.89
Very Poor	≤ 0.19	≥ 0.90

Figures 44 through 47 present the best fit power curves that correlate LWT rut depth to flow number, flow time, dynamic modulus (at 5 Hz and 54.4°C), and rut factor ($E^*/\text{Sin}\phi$ at 5Hz and 54.4°C), respectively. A summary of the goodness of fit and rating of these correlations are presented in Table 37. It indicates that flow time data showed excellent correlation with the LWT rut depth. Notably, flow number, dynamic modulus and rutting parameter values also showed good relationships with rut depth values.

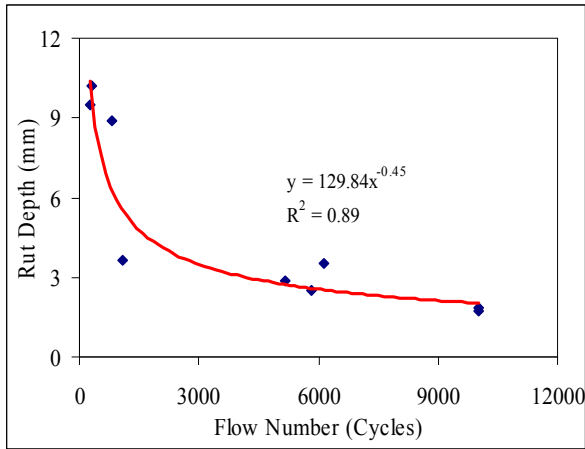


Figure 44
Correlation – flow number and rut depth

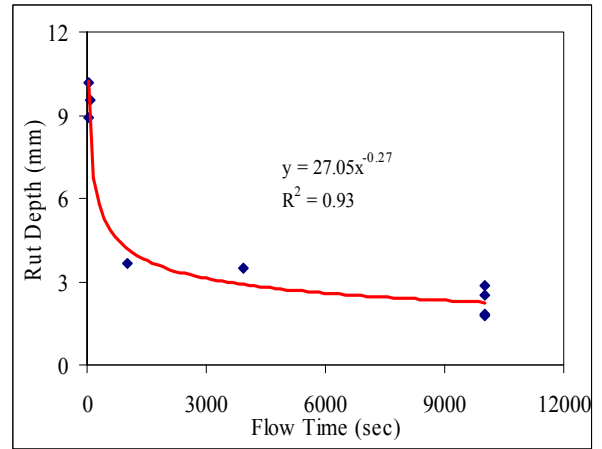


Figure 45
Correlation – flow time and rut depth

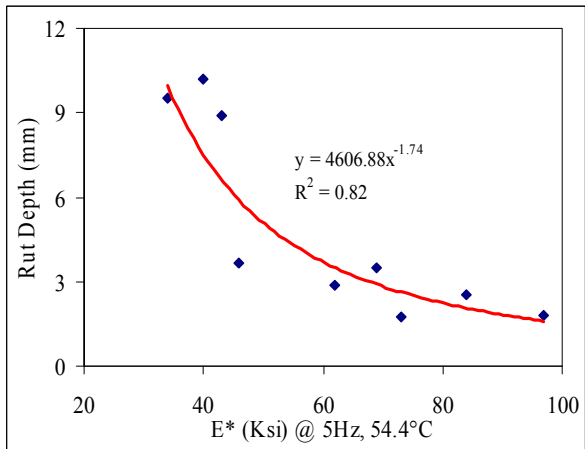


Figure 46
Correlation – E* and rut depth

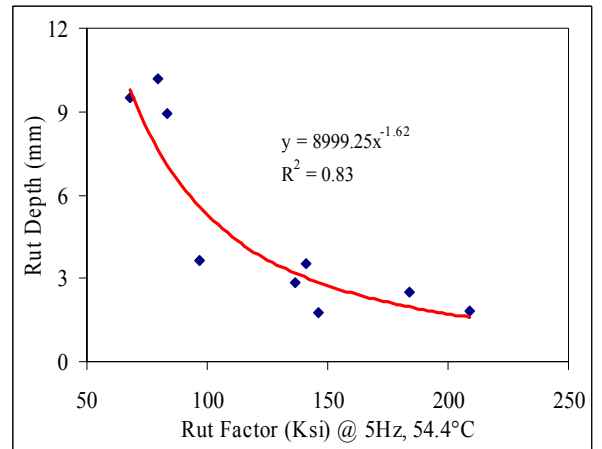


Figure 47
Correlation – rut factor and rut depth

Table 37
Statistical measure of goodness of fit

Test Parameter	Model Type	Statistical Measure				Rating
		Se	Sy	Se/Sy	R ²	
Flow Number	Power	1.34	3.50	0.38	0.89	Good
Flow Time	Power	0.91	3.50	0.26	0.93	Excellent
E* @ 5Hz, 54.4°C	Power	1.67	3.50	0.48	0.82	Good
Rut Factor	Power	1.52	3.50	0.44	0.83	Good

CONCLUSIONS

This study compared the fundamental engineering properties of HMA mixtures containing hydrated lime with the conventional mixtures designed to meet the Louisiana Superpave specifications. The influence of the method of adding hydrated lime on the mechanical properties of the resulting HMA mixtures was also evaluated. Based on the results of this study, the following conclusions are drawn:

- In general, the addition of hydrated lime to mixtures containing PG 64-22 binder showed improvement in rut resistance whereas; the improvement is not very significant in case of fatigue endurance. For the mixtures containing SB polymer modified asphalt binders (PG 70-22M and 76-22M), the addition of hydrated lime improved the rut resistance but there was a decrease in the measured fatigue properties. However, it is noted that despite this decrease, these mixtures met the minimum required values for fracture resistance mixtures.
- No substantial difference in mixtures' fatigue or rutting laboratory performance was observed when hydrated lime was added either in paste or no-paste method to mixtures containing PG 64-22 binder. However, the paste method resulted in mixtures that performed better in rutting than the no-paste method when PG 70-22M or PG 76-22M was used, whereas, the fatigue resistance for both methods were similar.
- Lime-treated mixtures containing PG 70-22M asphalt binder outperformed the conventional mixture with PG 76-22M binder when permanent deformation characteristics were considered. A decrease in the measured fatigue properties was noticed. However, it is noted that despite this decrease, these mixtures did meet the minimum required values for fracture resistance mixtures. On the other hand, lime treated mixtures containing PG 64-22 binder showed decreased fatigue and rut resistance in comparison to the conventional mixture with PG 70-22M binder.
- The addition of hydrated lime both in paste or no-paste form improved the IT strength of all HMA mixtures (except for 64LS) at 25°C and 40°C regardless of the mixtures' aging criteria. However, the addition of hydrated lime in either form decreased the strain and TI of mixtures in most of the cases. It is noted that despite of this decrease, the TI values for the mixtures evaluated were greater than 0.60, a minimum value observed for fatigue resistant mixtures.
- In general, mixtures 70LS and 70LM possessed similar IT strengths as mixture 76CO at both testing temperatures (25°C and 40°C). Also, IT strain and TI results showed that conventional mixtures containing polymer-modified asphalt binders (PG 70-22M and PG

76-22M) possessed higher IT strain and TI values than mixture 64CO, which did not contain a polymer modified-asphalt (i.e., PG 64-22).

- Mixtures 70LS, 70LM, 76LS, and 76LM showed satisfactory performances against fracture resistance as measured by the J_c values. These values were higher than the minimum required value of 0.60 KJ/m^3 .
- Dynamic Modulus tests used to evaluate the visco-elastic response of HMA mixtures indicate that the E^* values for all mixtures increased with an increase in frequency and a decrease in temperature. In addition, at lower temperatures (10°C and 4.4°C) the E^* isotherms show that the HMA mixtures are in the visco-elastic range and are primarily affected by the asphalt cement. As the temperatures increase the isotherms shape changes to a nonlinear one which is indicative of the mechanical response caused by the aggregate structure of the HMA mixture overwhelming the viscous influence of the asphalt cement binder.
- In general, the addition of hydrated lime improved the permanent deformation resistance of all mixtures (except 64LM) evaluated in this study as measured by flow number and flow time tests.
- LWT test results indicated that mixtures containing hydrated lime exhibited better rutting resistance as compared to the conventional mixtures containing the same asphalt binder. The method of adding hydrated lime (paste or no-paste) did not show any considerable difference in LWT measured rut depths. No signs of stripping were observed for any of the mixtures evaluated. Notably, all three mixtures prepared with PG 64-22 asphalt had rut depths greater than 6.0 mm.
- The results indicated that the presence of SB polymer in asphalt binder improved the elastic property of HMA mixtures and, as a result, this improved the fracture resistance of mixtures 70CO and 76CO in comparison to mixture 64CO. However, both conventional mixtures (70CO and 76CO) containing SB polymer modified binders showed similar fracture resistance properties as determined from the SCB test results.
- Mixtures 70CO and 76CO exhibited higher aging index values when compared to 64CO indicating that the polymer modified PG 70-22M and PG 76-22M binders performed better against age hardening than that of the neat PG 64-22 asphalt.

RECOMMENDATIONS

The outcome of this study clearly indicates that the introduction of hydrated lime improved the permanent deformation resistance of HMA mixtures. Therefore, based on the results of this study, specifications were developed and added to LADOTD standard specifications for the HMA mixture and asphalt cement binder to allow the use of the hydrated lime in HMA mixtures. The use of hydrated lime in Louisiana's Superpave mixes should provide for a longer life expectancy of the completed roadway structure.

Specifically, it is recommended that the Louisiana specification for asphalt mixture section 502 be amended to state, "when adding hydrated lime in accordance with standard specifications 503.05 to mixtures containing PG 70-22M, the binder may be substituted for mixtures containing PG 76-22M." The new proposed specifications due for release in late 2013 will require additional LWT testing requirements.

It is further recommended that this specification be promulgated at first regionally to those production facilities that are capable of the addition of hydrated lime to allow for the validation of the laboratory test results obtained from this study.

REFERENCES

1. LADOTD. "Louisiana Standard Specifications for Roads and Bridges." State of Louisiana Department of Transportation and Development, Baton Rouge, Louisiana, 2000.
2. LADOTD. "Louisiana Standard Specifications for Roads and Bridges." State of Louisiana Department of Transportation and Development, Baton Rouge, Louisiana, 2006.
3. Christensen, Jr., D.W. and Bonaquist, R.F. "Volumetric Requirements for Superpave Mix Design." *National Cooperative Highway Research Program (NCHRP) Report 567*, TRB, National Research Council, Washington, D.C., 2006, p.3.
4. AASHTO. "Standard Specification for Mineral Filler for Bituminous Paving Mixtures." AASHTO Designation: M 17-07, *American Association of State Highways and Transportation Officials*, Washington, D.C., 2007.
5. Puzinauskas, V.P. 1969. "Filler in Asphalt Mixtures." Asphalt Institute Research Report 69-2, The Asphalt Institute, Lexington, Kentucky.
6. Cooley, L.A.; Stroup-Gardiner, M.; and Brown, E.R. "Characterization of Asphalt-Filler Mortars with Superpave Binder Tests." *Journal of the Association of Asphalt Paving Technologists*, Vol. 67, 1998, pp. 42-65.
7. Metcalf, J.B., "A Survey of the Use of Hydrated Lime as a Filler in Tar or Bitumen Road Surfacing." Chalk Lime & Allied Industries Research Association, Hertz, Australia, 1959.
8. Kennedy, T.W.; Roberts, F.L.; and Lee, K.W. "Evaluation of Moisture Susceptibility of Asphalt Mixtures Using the Texas Freeze-Thaw Pedestal Test." *Journal of the Association of Asphalt Paving Technologists*, Vol. 51, 1982, pp. 327-341.
9. Kennedy, T. and Ping, W.V. "An Evaluation of Effectiveness of Antistripping Additives in Protecting Asphalt Mixtures from Moisture Damage." *Journal of the Association of Asphalt Paving Technologists*, Vol. 60, 1991, pp. 230-263.
10. Pickering, K.; Sebaaly, P.E.; Stroup-Gardiner, M.; and Epps, J.A. "Evaluation of New Generation of Antistripping Additives." *Transportation Research Record: Journal of the Transportation Research Board*, No. 1342, TRB, National Research Council, Washington, D.C., 1992, pp. 26-34.

11. Paul, H.R., "Compatibility of Aggregate, Asphalt Cement and Antistrip Materials." Louisiana Transportation Research Center, Report No. FHWA/LA-95-292, 1995.
12. McCann, M. and Sebaaly, P.E. "Evaluation of Moisture Sensitivity and Performance of Lime in Hot Mix Asphalt: Resilient Modulus, Tensile Strength, and Simple Shear Tests." *Transportation Research Record: Journal of the Transportation Research Board*, No. 1832, TRB, National Research Council, Washington, D.C., 2003, pp. 9-16.
13. Huang, S., Petersen, J.C., Robertson, R.E. and Branthaver J.F. "Effect of Hydrated Lime on Long-Term Oxidative Aging Characteristics of Asphalt." *Transportation Research Record: Journal of the Transportation Research Board*, No. 1810, TRB, National Research Council, Washington, D.C., 2002, pp.17-25.
14. Khattak, M.J. and Kyatham, V. "Visco-Elastic Behavior of Asphalt Matrix & HMA under Moisture Damage Condition." *Transportation Research Board 87th Annual Meeting CD-ROM*, Washington, D.C., 2008.
15. Mohammad, L.N.; Abadie, C.; Gokmen, R. and Puppala, A.J. "Mechanistic Evaluation of Hydrated Lime in Hot-Mix Asphalt mixtures." *Transportation Research Record: Journal of the Transportation Research Board*, No. 1723, 2000, pp. 26-36.
16. Miro R.; Martinez A.; Perez F.; and Bianchetto, H. "Effect of Filler on the Aging Potential of Asphalt Mixtures." *Transportation Research Record: Journal of the Transportation Research Board*, No. 1901, TRB, National Research Council, Washington, D.C., 2005, pp. 10-17.
17. Sebaaly, P.E.; Hitti, E. and Weitzel, D. "Effectiveness of Lime in Hot Mix Asphalt Pavements." *Transportation Research Record: Journal of the Transportation Research Board*, No. 1832, TRB, National Research Council, Washington, D.C., 2003, pp. 34-41.
18. Petersen, J.C.; Plancher, H. and Harnsberger, P.M. "Lime Treatment of Asphalt to Reduce Age Hardening and Improve Flow Properties." *Journal of the Association of Asphalt Paving Technologists*, Volume 56, 1987, pp. 633-653.
19. Lesueur, D. and Little, D.N. "Effect of Hydrated Lime on Rheology, Fracture, and Aging of Bitumen." *Transportation Research Record: Journal of the Transportation Research Board*, No. 1661, TRB, National Research Council, Washington, D.C., 1999, pp. 93-105.
20. Huang, S.; Petersen, J.C.; Robertson, R.E. and Branthaver J.F. "Effect of Hydrated Lime on Long-Term Oxidative Aging Characteristics of Asphalt." *Transportation Research*

Record: Journal of the Transportation Research Board, No. 1810, TRB, National Research Council, Washington, D.C., 2002, pp. 17-25

21. Kim, Y-R.; Little, D.N. and Song, I. “Effect of Mineral Fillers on Fatigue Resistance and Fundamental Material Characteristics: Mechanistic Evaluation.” *Transportation Research Record: Journal of the Transportation Research Board*, No. 1832, TRB, National Research Council, Washington, D.C., 2003, pp. 1-8.
22. Little, D.N. and Petersen, J.C. “Unique Effects of Hydrated Lime Filler on the Performance-Related Properties of Asphalt Cements: Physical and Chemical Interactions Revisited.” *Journal of Materials in Civil Engineering*, Volume 17, No. 2, 2005, pp. 207-218.
23. Bari, J. and Witzcak, M. W. “Evaluation of the Effect of Lime Modification on Dynamic Modulus Stiffness of Hot-Mix Asphalt Use with the New Mechanistic-Empirical Pavement Design Guide.” *Transportation Research Record: Journal of the Transportation Research Board*, No. 1929, TRB, National Research Council, Washington, D.C., 2005, pp. 10-19.
24. Aschenbrener, T. and Far, N. “Influence of Compaction Temperature and Antistripping Treatment on the Results from the Hamburg Wheel-Tracking Device.” Colorado Department of Transportation, Report No. CDOT-DTD-R-94-9, 1994.
25. Atud, T.J.; Kanitpong, K.; and Martono, W. “Laboratory Evaluation of Hydrated Lime Application Process in Asphalt Mixture for Moisture Damage and Rutting Resistance.” *Transportation Research Board 86th Annual Meeting CD-ROM*, Paper No. 1508, Washington, D.C, 2007.
26. Witzcak, M.W.; Kaloush, K.; Pellinen, T.; El-Basyouny, M.; and Quintus, H.V. “Simple Performance Test for Superpave Mix Design.” *National Cooperative Highway Research Program (NCHRP) Report 465*, TRB, National Research Council, Washington, D.C., 2002.
27. Mohammad, L.N.; Wu, Z.; and Aglan, M.A. “Characterization of Fracture and Fatigue Resistance on Recycled Polymer-Modified Asphalt pavements.” *Proceedings, 5th International Conference*, Limoges, France, 2004, pp. 375-382.
28. Roque, R; Birgisson, B.; Zhang, Z.; Sangpetngam, B. and Grant, T. “Implementation of SHRPP Indirect Tension Tester to Mitigate Cracking in Asphalt Pavements and Overlays.” Final Report Submitted to Florida Department of Transportation, University of Florida, Gainesville, 2002.

29. Witczak, M.W. "Laboratory Determination of resilient Modulus for Flexible Pavement Design." Research Results Digest, *National Cooperative Highway Research Program (NCHRP) Report 1-28A*, TRB, National Research Council, No. 285, Washington, D.C., 2004.
30. Roque, R.; Birgisson, B.; Drakos, C.; and Dietrich, B. "Development and Field Evaluation of Energy-Based Criteria for Top-down Cracking Performance of Hot Mix Asphalt." *Journal of the Association of Asphalt Paving Technologists*, Vol.73, 2004, pp. 229-260.
31. Bonaquist, R.F.; Christensen, D.W. and Stump III, W. "Simple Performance Tester for Superpave Mix Design: First Article Development and Evaluation." *National Cooperative Highway Research Program (NCHRP) Report 513*, TRB, National Research Council, Washington, D.C., 2003.
32. Mull, M.A.; Stuart, K.; and Yehia, A. "Fracture Resistance Characterization of Chemically Modified Crumb Rubber Asphalt Pavement." *Journal of Materials Science*, Vol. 37, 2002, pp. 557-566.
33. Mull, M.A.; Othman, A.; and Mohammad, L. "Fatigue Crack Growth Analysis of Hot-Mix Asphalt Employing the Semi-Circular Notched Bend Specimen." *Transportation Research Board 85th Annual Meeting CD-ROM*, Washington, D.C., 2006.
34. Bhasin, A.; Button, J.W.; and Chowdhury, A., "Evaluation of Selected Laboratory Procedures and Development of Databases for HMA." Texas Department of Transportation Research and Technology Implementation Office, Report No.0-4203-3, College Station, Texas, 2005.

APPENDIX A

Descriptions of Test Procedures

Indirect Tensile Strength (ITS) Test

The ITS and strain tests were conducted according to the AASHTO T 322-03 procedure. Both unaged and aged specimens were tested at 25°C and 40°C. A 101.6 mm (4 in.) diameter by 63.5 mm (2.5 in.) high cylindrical specimen was loaded to failure at a deformation rate of 50.8 mm/min (2 in./min.) using a MTS 810 machine.

The load and deformations were recorded continuously with the help of two LVDT pairs. The ITS and strain tests were computed as follows:

$$ITS = \frac{2P}{\pi DT} \quad (1)$$

$$\varepsilon_p = 0.52H_t \quad (2)$$

where,

P = the peak load (lb),

D = specimen diameter (in.),

T = specimen thickness (in.),

H_t = horizontal deformation at peak load (in.), and

ε_p = strain corresponding to the peak stress.

Toughness Index (TI), a parameter that describes the toughening characteristics of the mixture in the post-peak stress region, was also computed from this test results (Figure 48).

A dimensionless indirect tensile toughness index is defined as follows:

$$TI = \frac{(A_\varepsilon - A_p)}{(\varepsilon - \varepsilon_p)} \quad (3)$$

where,

TI = Toughness Index,

A_ε = Area under the normalized stress-strain curve up to strain ε ,

A_p = Area under the normalized stress-strain curve up to strain ε_p ,

ε = Strain (here, 3%) at the point of interest, and

ε_p = Strain corresponding to the peak stress.

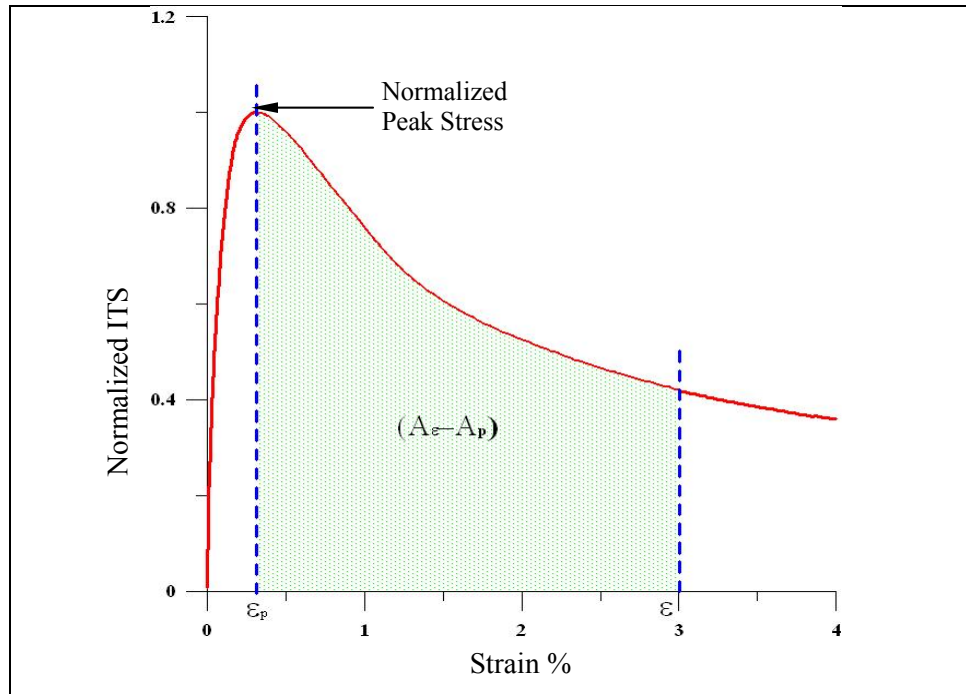


Figure 48
Computation of TI

Toughness Index compares the elastic performance of a specimen with a perfectly elastic reference material, where the TI remains a constant of 1.0. On the other hand, for an ideal brittle material with no post-peak load carrying capacity, TI equals zero.

Semi-Circular Bend (SCB) Test

This test was conducted according to the test procedure adopted by Mohammad et al. [27]. Triplicate specimens were experimented for each notch depth, and the test was performed at 25°C on both unaged and aged specimens. To determine the critical value of J-integral (J_c), semi-circular specimens with at least two different notch depths were needed to be tested. In this study, three notch depths of 25.4 mm, 31.8 mm, and 38.0 mm were selected based on an a/r_d ratio (the notch depth to the radius of the specimen, Figure 49) of between 0.5 and 0.75. However, application of three notch depths increased the accuracy of the calculated J_c values. Figure 49 shows specimen dimensions and a three-point bend load configuration used in the test.

Applying a constant cross-head deformation rate of 0.5 mm/min, the specimens were loaded monotonically on an MTS machine till fracture failure occurred. The load and deformation were recorded continuously and the critical value of J_c was determined using the following equation:

$$J_c = -\left(\frac{1}{b}\right) \frac{dU}{da} \quad (4)$$

where, b is sample thickness, a is the notch depth, and U is the strain energy to failure.

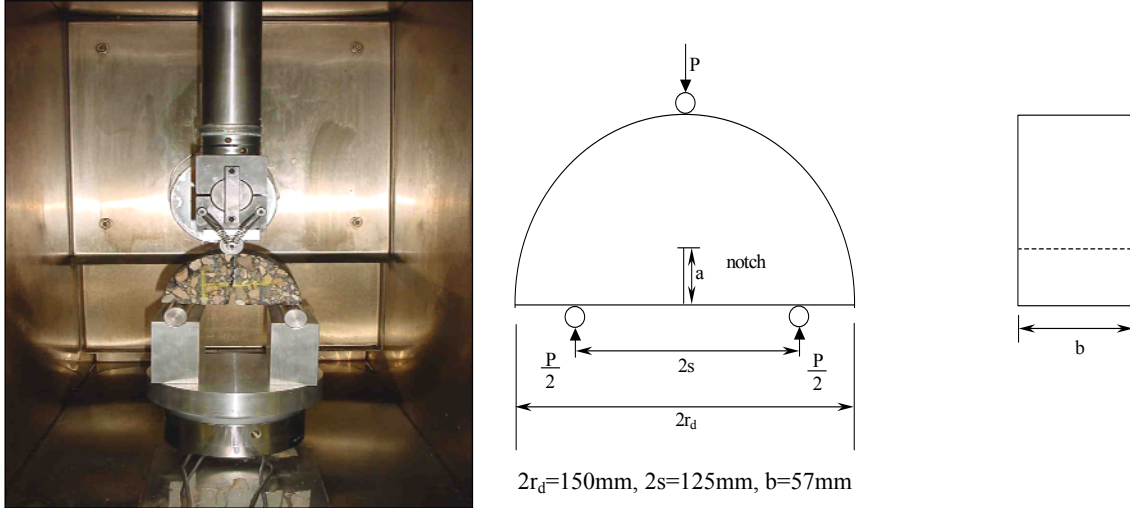


Figure 49
SCB test setup and specimen configuration

In Figure 50, a typical load-deformation plot obtained in a semi-circular bend test is presented. In order to obtain the critical value of fracture resistance J_c , the area under the loading portion of the load deflection curves up to the peak load is measured for each notch depth. This area represents the strain energy to failure, U . The average values of U (calculated from triplicate specimens) were then plotted against the different notch depths to compute a slope of a regression line, which is the value of (dU/da) in equation 4. The critical value of fracture resistance, J_c , was then computed by dividing the dU/da value by the specimen width, b .

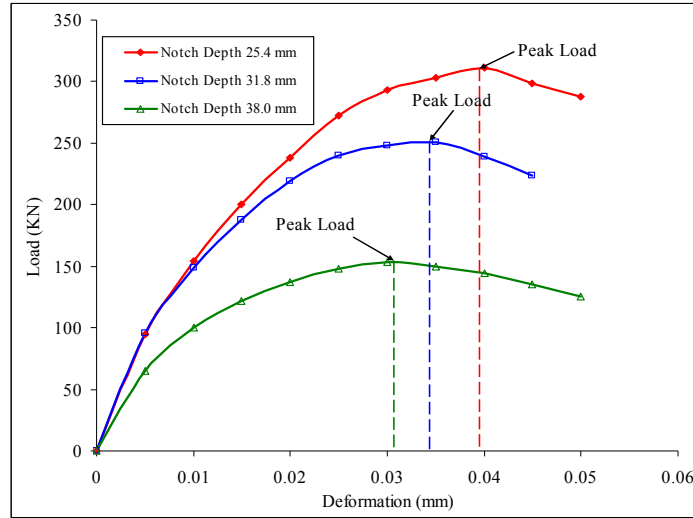


Figure 50
Typical load deformation curves from a SCB test

Dissipated Creep Strain Energy (DCSE) Test

The evaluation of DCSE of a HMA mixture involves two individual laboratory tests to be performed on the same specimen. Those tests are the indirect resilient modulus (M_R) test and the ITS test. The M_R test was conducted according to NCHRP Research Result Digest 285 [29], while the ITS test was performed in accordance with AASHTO T 322-03. Triplicate specimens 150 mm in diameter and 50 mm thick were tested at 10°C.

A four-cycle haversine load was applied along the diametrical plane of the specimen with 0.1 second loading and 0.4 second rest period in each loading cycle. The magnitude of the applied load was such that the resulting deformation was as close as possible to 100 microstrains. Two M_R test was conducted on the same specimen by rotating it to 90 degrees. The average value of those two test results was considered the final M_R of that specimen. Once the M_R test was complete, the ITS test was performed on the same specimen.

The DCSE calculation procedure executed in this study was introduced by Roque et al. [28, 30]. As shown in Figure 51, DCSE is defined as the Fracture Energy (FE) minus the Elastic Energy (EE). The FE is the area under the stress-strain curve up to the point where the specimen begins to fracture. In Figure 51, the area within the curve OA and x-axis (area OAB) represents the FE. On the other hand, the EE is the energy resulting from the elastic deformation. Therefore, M_R calculated from Resilient Modulus test is selected as the slope of the line AC, and the area of triangle ABC can be taken as the EE. The failure strain (ϵ_f), peak tensile strength (S_t), and FE are determined from the IT strength test.

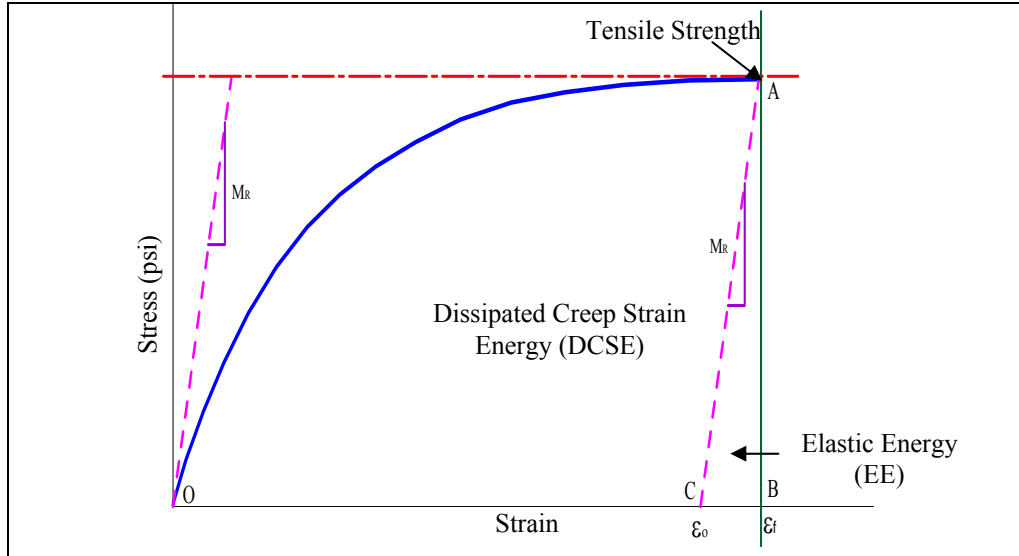


Figure 51
DCSE calculation procedure

A rather clear picture of DCSE calculation is described below:

$$M_r = \frac{S_t}{\varepsilon_f - \varepsilon_0}$$

$$\text{Therefore, } \varepsilon_0 = \frac{(M_r \times \varepsilon_f - S_t)}{M_r}$$

$$\text{Again, } EE = \frac{1}{2} \times S_t \times (\varepsilon_f - \varepsilon_0)$$

$$DCSE = FE - EE$$

$$\text{Thus, } DCSE = FE - \frac{1}{2} \times S_t \times (\varepsilon_f - \varepsilon_0) \quad (5)$$

Dynamic Modulus |E*| Test

The dynamic modulus test was conducted on unconfined cylindrical test specimens (100 mm diameter by 150 mm in height) in accordance with AASHTO Standard TP 62-03 and NCHRP Report 513 [31]. The stress-to-strain relationship under a continuous sinusoidal loading for linear viscoelastic materials is defined by a complex number called the “complex modulus” (E^*). The absolute value of the complex modulus, $|E^*|$, is defined as the dynamic modulus. Mathematically, dynamic modulus is defined as the maximum (peak) dynamic stress (σ_0) divided by the peak recoverable strain (ε_0):

$$|E^*| = \frac{\sigma_0}{\varepsilon_0}$$

A sinusoidal compressive stress was applied to test specimens at -10, 4, 25, 37.8 and 54.4°C with loading frequencies of 0.1, 0.5, 1.0, 5, 10, 25 Hz at each temperature to achieve a targeted vertical strain level of 100 microns. An increasing order of temperature (starting with the lowest temperature and proceeding to the highest one) was maintained throughout the whole test. Testing at a particular temperature began with the highest frequency of loading and proceeded to the lowest one.

Flow Number Test

The flow number test was conducted according to Annex B of NCHRP Report 513 [31] at a constant single temperature of 54.4°C and a stress level of 207 kPa (30 psi). A repeated dynamic load for 10,000 repetitions with a loading cycle of 1.0 second in duration, consisting of 0.1 second haversine load, followed by 0.9 second rest period was applied to determine the permanent deformation characteristics of paving materials.

The “Flow Number,” by definition is the starting point, or cycle number, at which tertiary flow occurs. To calculate flow number, first the rate of change (derivative) of the permanent axial strain with respect to the number of load cycles was determined. The derivatives were then smoothed, and the number of cycles corresponding to the lowest point of the running average against number of loading cycle graph, shown in Figure 52, was the calculated flow number of that specimen. If there was no lowest point, then the total number of loading cycles allowed (here 10,000) in the entire test was considered as the flow number of that mixture.

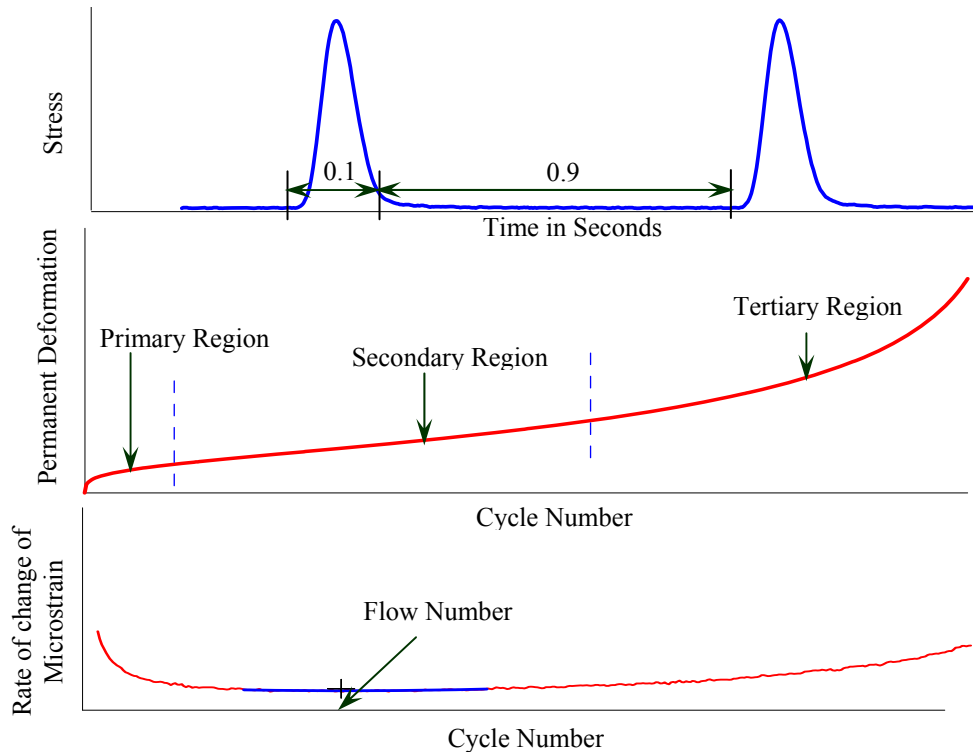


Figure 52
Typical permanent deformation curve and flow number computation

Flow Time Test

This test was conducted in accordance with the method described in Annex A of NCHRP Report 513 [31]. A constant axial compressive stress of 69 kPa (10 psi) was applied on an unconfined cylindrical specimen of 100 mm in diameter and 150 mm in height at a single constant temperature of 54.4°C.

The flow time is the time corresponding to the minimum rate of change in axial strain during the creep test. Similar to the flow number test, the time corresponding to the lowest rate of change of axial strain was calculated and reported as the flow time of a mixture (Figure 53). If there was no lowest point on the running average graph, the duration (i.e., time length) of the entire test was considered as the flow time of that mixture.

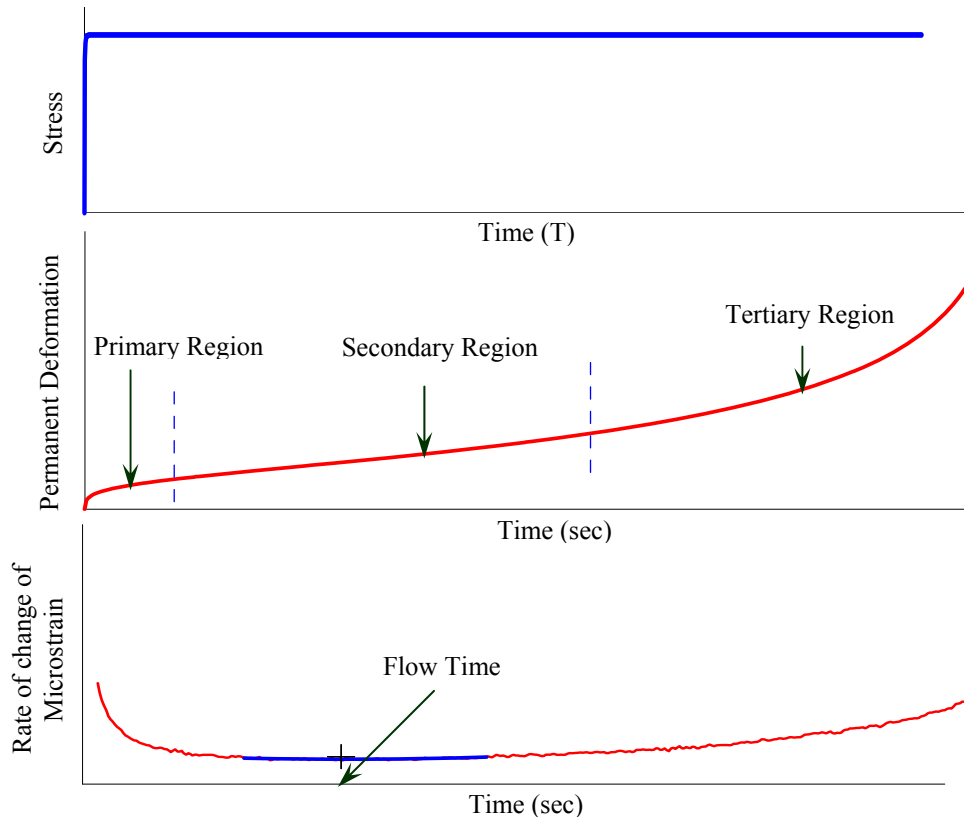


Figure 53
Typical permanent deformation curve and computation of flow time

Loaded Wheel Tracking (LWT) Test

This test was conducted according to AASHTO T 324-04 procedure to determine the rutting characteristics of HMA mixtures. The Hamburg type LWT device used in this study can test two slabs (320 mm x 260 mm x 80 mm) at a time using two reciprocating solid-steel wheels of 203.5 mm (8 in.) in diameter and 47 mm (1.85 in.) in width. The specimens, compacted by a kneading compactor were conditioned at 50°C for 90 minutes prior to the start of the test. A fixed load of 703 N (158 lb) with a rolling speed of 1.1 km/h (0.68 mi/h) at the rate of 50 passes/min was implied. Each wheel rolled 230 mm (9.1 in.) before reversing the direction. The steel wheel rolled repeatedly across the surface of the specimen that was submerged under hot water (50°C) throughout the duration of the test. The test continued for 20,000 cycles or until 20 mm deformation occurs, whichever reached first.

APPENDIX B

Individual Test Results of Binders

Table B1
Shear modulus and phase angles for asphalt binders at 4°C and 25°C

Temperature	Frequency (Hz)	Binder Properties					
		PG 70-22M		PG 70-22M + HL		PG 76-22M	
		G* (Psi)	Phase Angle (degree)	G* (Psi)	Phase Angle (degree)	G* (Psi)	Phase Angle (degree)
4°C	0.01	884.26	53.78	2949.24	49.81	683.61	51.64
	0.02	1347.28	50.61	4271.94	46.64	1026.32	49.11
	0.05	2198.69	46.69	6672.23	42.61	1671.50	45.96
	0.10	3119.65	43.76	9110.95	39.64	2358.96	43.62
	0.20	4274.11	41.04	12044.23	36.90	3248.01	41.40
	0.50	6356.06	37.53	17070.34	33.32	4871.65	38.38
	1.00	8394.49	34.98	21602.61	30.77	6456.85	36.22
	2.00	10870.92	32.55	26816.53	28.39	8385.79	34.11
	3.00	12439.45	31.25	30188.54	27.06	9845.54	32.80
	4.00	13760.70	30.24	32842.64	26.06	10881.07	31.95
	5.00	14799.13	29.51	34851.34	25.36	11752.72	31.27
	10.00	18317.62	27.32	41566.35	23.42	14799.85	29.23
	25.00	23589.56	24.15	51015.23	20.18	19499.64	26.23
25°C	0.01	5.69	71.95	26.02	67.80	7.73	60.12
	0.02	9.87	71.15	43.73	67.33	12.38	60.45
	0.05	20.28	70.01	86.06	66.45	23.09	60.74
	0.10	34.74	68.95	142.30	65.53	36.97	60.71
	0.20	58.98	67.69	232.49	64.34	59.22	60.47
	0.50	116.90	65.62	439.81	62.25	109.89	59.67
	1.00	192.75	63.73	698.98	60.31	173.39	58.68
	2.00	313.42	61.60	1094.63	58.14	272.59	57.45
	3.00	412.84	60.22	1410.30	56.73	353.59	56.55
	4.00	500.58	59.20	1681.22	55.72	425.31	55.85
	5.00	580.28	58.39	1915.16	54.90	484.12	55.34
	10.00	900.51	55.77	2866.57	52.23	743.65	53.45
	25.00	1563.45	52.08	4733.14	48.33	1264.32	50.70

Table B2
Shear modulus and phase angles for asphalt binders at 37.8°C and 54.4°C

Temperature	Frequency (Hz)	Binder Properties					
		PG 70-22M		PG 70-22M + HL		PG 76-22M	
		G* (Psi)	Phase Angle (degree)	G* (Psi)	Phase Angle (degree)	G* (Psi)	Phase Angle (degree)
37.8°C	0.01	0.45	75.47	2.14	69.16	0.94	57.80
	0.02	0.79	74.54	3.60	69.42	1.47	58.33
	0.05	1.68	73.71	7.19	69.61	2.68	59.39
	0.10	2.95	73.20	12.29	69.63	4.25	60.23
	0.20	5.16	72.75	20.90	69.55	6.79	61.00
	0.50	10.78	72.10	42.09	69.21	12.72	61.83
	1.00	18.80	71.47	71.14	68.72	20.54	62.30
	2.00	32.59	70.64	120.07	68.00	33.39	62.50
	3.00	44.95	70.02	162.47	67.43	44.38	62.52
	4.00	56.29	69.54	200.65	66.98	54.37	62.44
	5.00	66.98	69.12	236.33	66.57	63.50	62.35
	10.00	113.93	67.55	390.43	65.09	103.37	61.79
	25.00	227.48	64.77	745.11	62.57	194.85	60.46
54.4°C	0.01	0.03	79.36	0.15	76.75	0.09	68.59
	0.02	0.06	80.60	0.26	75.81	0.16	66.99
	0.05	0.13	79.04	0.55	74.61	0.31	65.38
	0.10	0.23	77.71	0.97	73.80	0.51	64.47
	0.20	0.41	76.61	1.68	73.15	0.83	63.81
	0.50	0.89	75.48	3.49	72.59	1.57	63.41
	1.00	1.58	74.80	6.05	72.36	2.55	63.36
	2.00	2.79	74.30	10.47	72.20	4.15	63.50
	3.00	3.91	73.94	14.45	72.16	5.51	63.58
	4.00	4.96	73.46	18.18	72.10	6.76	63.58
	5.00	5.98	73.27	21.70	72.06	7.94	63.67
	10.00	10.69	72.10	37.55	72.08	13.13	63.85
	25.00	23.79	68.89	78.53	71.80	26.70	62.68

Table B3
ITS test results for unaged mixtures at 25°C and 40°C

Mix Type	Test Temperatures									
	25°C					40°C				
	Parameters		Test Results			Parameters		Test Results		
	Sample ID	Air Voids	ITS (psi)	Strain (%)	TI	Sample ID	Air Voids	ITS (psi)	Strain (%)	TI
64CO	64C1	6.9	179.7	0.45	0.669	64C19	7.2	70.0	0.73	0.804
	64C5	6.5	182.8	0.47	0.704	64C24	7.5	60.9	0.69	0.772
	64C9	7.6	170.9	0.49	0.727	64C25	6.5	64.7	0.61	0.717
	Average		177.8	0.47	0.70	Average		65.2	0.68	0.76
	St. Dev.		6.2	0.02	0.03	St. Dev.		4.6	0.06	0.04
	CV (%)		3.5	3.7	4.1	CV (%)		7.0	9.2	5.7
64LS	64LS4	6.5	131.3	0.42	0.651	64LS16	7.2	46.0	0.58	0.711
	64LS5	7.2	143.9	0.40	0.702	64LS17	6.7	52.2	0.56	0.660
	64LS9	6.9	138.9	0.40	0.652	64LS18	6.8	49.7	0.56	0.728
	Average		138.0	0.41	0.67	Average		49.3	0.57	0.70
	St. Dev.		6.3	0.01	0.03	St. Dev.		3.1	0.01	0.04
	CV (%)		4.6	3.5	4.4	CV (%)		6.4	2.6	5.1
64LM	64LM1	7.0	180.4	0.26	0.664	64LM6	7.1	69.2	0.67	0.796
	64LM21	7.5	169.8	0.38	0.661	64LM12	7.5	64.6	0.45	0.696
	64LM7	7.1	176.3	0.30	0.642	64LM18	7.0	73.3	0.55	0.694
	Average		175.5	0.32	0.66	Average		69.1	0.56	0.73
	St. Dev.		5.4	0.06	0.01	St. Dev.		4.4	0.11	0.06
	CV (%)		3.1	18.7	1.9	CV (%)		6.3	19.2	8.0
70CO	70C4	6.4	158.4	1.04	0.899	70C6	6.7	56.2	1.04	0.996
	70C7	6.8	143.1	0.98	0.943	70C14	7.0	59.4	0.95	0.981
	70C12	7.4	147.4	0.81	0.913	70C17	6.8	67.8	0.79	0.868
	Average		149.7	0.94	0.92	Average		61.1	0.93	0.95
	St. Dev.		7.9	0.12	0.02	St. Dev.		6.0	0.12	0.07
	CV (%)		5.3	12.7	2.4	CV (%)		9.8	13.4	7.4
70LS	70LS1	6.7	163.6	0.54	0.759	70LS10	7.1	67.7	0.84	0.834
	70LS2	6.8	165.9	0.55	0.839	70LS13	6.5	70.7	0.59	0.790
	70LS3	6.7	153.6	0.56	0.766	70LS25	6.4	62.8	0.71	0.883
	Average		161.0	0.55	0.79	Average		67.1	0.71	0.84
	St. Dev.		6.6	0.01	0.04	St. Dev.		4.0	0.13	0.05
	CV (%)		4.1	2.0	5.6	CV (%)		5.9	17.9	5.6

Table B3
ITS test results for unaged mixtures at 25°C and 40°C (continued)

Mix Type	Test Temperatures									
	25°C					40°C				
	Parameters		Test Results			Parameters		Test Results		
	Sample ID	Air Voids	ITS (psi)	Strain (%)	TI	Sample ID	Air Voids	ITS (psi)	Strain (%)	TI
70LM	70LM4	7.3	167.6	0.42	0.740	70LM1	7.1	61.2	0.97	0.887
	70LM12	7.2	156.5	0.34	0.727	70LM7	7.5	62.5	0.74	0.909
	70LM21	7.4	160.0	0.37	0.739	70LM18	7.4	71.8	0.73	0.740
	Average		161.4	0.38	0.74	Average		65.2	0.82	0.84
	St. Dev.		5.7	0.04	0.01	St. Dev.		5.8	0.14	0.09
	CV (%)		3.5	10.8	1.0	CV (%)		8.9	16.9	10.9
76CO	76C1	7.0	164.2	1.25	1.058	76C7	6.8	74.2	1.20	1.021
	76C9	6.5	167.2	1.31	0.975	76C8	7.2	70.4	1.44	0.983
	76C24	7.4	159.1	1.33	0.969	76C30	7.1	70.2	1.02	0.943
	Average		163.5	1.30	1.00	Average		71.6	1.22	0.98
	St. Dev.		4.1	0.04	0.05	St. Dev.		2.3	0.21	0.04
	CV (%)		2.5	3.0	5.0	CV (%)		3.2	17.5	4.0
76LS	76LS1	6.7	181.7	0.56	0.848	76LS4	6.9	92.2	0.57	0.842
	76LS2	7.1	184.4	0.43	0.815	76LS21	7.4	88.5	0.66	0.848
	76LS7	7.2	186.1	0.47	0.711	76LS23	6.6	87.5	0.64	0.803
	Average		184.0	0.48	0.79	Average		89.4	0.62	0.83
	St. Dev.		2.2	0.07	0.07	St. Dev.		2.5	0.05	0.02
	CV (%)		1.2	14.0	9.0	CV (%)		2.8	7.8	3.0
76LM	76LM15	6.5	177.6	0.52	0.834	76LM4	6.5	84.4	0.53	0.818
	76LM17	6.7	182.0	0.47	0.769	76LM8	7.0	96.1	0.60	0.807
	76LM18	6.6	185.5	0.43	0.873	76LM11	6.7	97.5	0.55	0.833
	Average		181.7	0.48	0.83	Average		92.7	0.56	0.82
	St. Dev.		4.0	0.05	0.05	St. Dev.		7.2	0.03	0.01
	CV (%)		2.2	9.5	6.4	CV (%)		7.7	5.9	1.6

Note: St. Dev: Standard Deviation
 %CV: Coefficient of Variance (%)

Table B4
ITS test results for aged mixtures at 25°C and 40°C

Mix Type	Test Temperatures									
	25°C					40°C				
	Parameters		Test Results			Parameters		Test Results		
	Sample ID	Air Voids	ITS (psi)	Strain (%)	TI	Sample ID	Air Voids	ITS (psi)	Strain (%)	TI
64CO	64C3	6.7	203.9	0.32	0.655	64C12	6.5	82.4	0.62	0.742
	64C4	6.5	206.7	0.22	0.669	64C17	6.9	82.3	0.57	0.826
	64C13	7.3	210.2	0.25	0.684	64C22	6.5	81.8	0.59	0.783
	Average		206.9	0.26	0.67	Average		82.2	0.59	0.78
	St. Dev.		3.2	0.05	0.01	St. Dev.		0.3	0.03	0.04
	CV (%)		1.5	18.6	2.2	CV (%)		0.4	4.3	5.3
64LS	64LS2	7.5	155.5	0.27	0.575	64LS10	6.8	64.7	0.37	0.652
	64LS7	6.8	181.0	0.36	0.594	64LS11	7.5	68.7	0.36	0.645
	64LS8	6.5	157.1	0.28	0.597	64LS12	6.6	71.5	0.38	0.642
	Average		164.5	0.30	0.59	Average		68.3	0.37	0.65
	St. Dev.		14.3	0.05	0.01	St. Dev.		3.4	0.01	0.01
	CV (%)		8.7	15.2	2.1	CV (%)		5.0	2.7	0.8
64LM	64LM9	7.1	181.4	0.32	0.633	64LM3	6.8	98.5	0.37	0.636
	64LM10	6.7	188.9	0.27	0.611	64LM5	6.7	104.8	0.43	0.609
	64LM11	6.5	184.1	0.22	0.537	64LM8	7.1	89.2	0.33	0.675
	Average		184.8	0.27	0.59	Average		97.5	0.38	0.64
	St. Dev.		3.8	0.05	0.05	St. Dev.		7.9	0.05	0.03
	CV (%)		2.1	17.9	8.5	CV (%)		8.1	14.0	5.2
70CO	70C3	7.7	169.3	0.44	0.768	70C10	6.5	65.3	0.75	0.856
	70C20	6.8	167.2	0.53	0.842	70C15	6.4	67.5	0.78	0.885
	70C24	7.2	153.6	0.60	0.838	70C21	6.7	69.1	0.73	0.866
	Average		163.4	0.53	0.82	Average		67.3	0.75	0.87
	St. Dev.		8.5	0.08	0.04	St. Dev.		1.9	0.03	0.01
	CV (%)		5.2	15.3	5.1	CV (%)		2.9	3.9	1.7
70LS	70LS3	7.0	181.3	0.55	0.725	70LS1	7.1	73.2	0.52	0.760
	70LS5	7.2	177.2	0.50	0.748	70LS2	6.4	77.7	0.53	0.804
	70LS31	7.5	177.6	0.39	0.680	70LS4	7.5	65.1	0.65	0.849
	Average		178.7	0.48	0.72	Average		72.0	0.57	0.80
	St. Dev.		2.3	0.08	0.03	St. Dev.		6.4	0.07	0.04
	CV (%)		1.3	16.5	4.8	CV (%)		8.9	13.1	5.5

Table B4
ITS test results for aged mixtures at 25°C and 40°C (continued)

Mix Type	Test Temperatures									
	25°C					40°C				
	Parameters		Test Results			Parameters		Test Results		
	Sample ID	Air Voids	ITS (psi)	Strain (%)	TI	Sample ID	Air Voids	ITS (psi)	Strain (%)	TI
70LM	70LM16	7.6	170.7	0.39	0.772	70LM3	7.4	71.3	0.55	0.849
	70LM20	7.4	168.3	0.32	0.720	70LM9	6.9	80.6	0.61	0.736
	70LM22	6.9	172.0	0.28	0.699	70LM17	6.4	72.3	0.54	0.781
	Average		170.3	0.33	0.73	Average		74.7	0.57	0.79
	St. Dev.		1.9	0.06	0.04	St. Dev.		5.1	0.04	0.06
	CV (%)		1.1	17.8	5.2	CV (%)		6.8	7.1	7.2
76CO	76C26	6.9	187.1	0.77	0.872	76C1	6.7	82.2	0.78	0.892
	76C27	6.4	186.1	0.59	0.850	76C4	7.2	71.7	1.03	0.886
	76C28	6.5	189.0	0.54	0.849	76C11	6.4	76.4	1.10	0.941
	Average		187.4	0.63	0.86	Average		76.8	0.97	0.91
	St. Dev.		1.5	0.12	0.01	St. Dev.		5.2	0.17	0.03
	CV (%)		0.8	19.5	1.5	CV (%)		6.8	17.0	3.4
76LS	76LS5	7.0	186.3	0.39	0.694	76LS6	6.7	91.3	0.40	0.773
	76LS19	7.2	209.4	0.48	0.589	76LS20	7.6	89.0	0.52	0.818
	76LS23	6.6	194.7	0.37	0.702	76LS24	7.3	92.2	0.39	0.722
	Average		196.8	0.41	0.66	Average		90.8	0.44	0.77
	St. Dev.		11.7	0.05	0.06	St. Dev.		1.7	0.07	0.05
	CV (%)		5.9	13.2	9.6	CV (%)		1.8	16.2	6.2
76LM	76LM7	6.9	208.6	0.45	0.698	76LM1	7.4	96.4	0.48	0.850
	76LM9	6.4	215.5	0.34	0.724	76LM3	6.9	103.7	0.51	0.771
	76LM19	6.8	178.0	0.45	0.743	76LM5	7.4	90.0	0.62	0.813
	Average		200.7	0.41	0.72	Average		96.7	0.54	0.81
	St. Dev.		19.9	0.07	0.02	St. Dev.		6.8	0.08	0.04
	CV (%)		9.9	16.0	3.1	CV (%)		7.1	14.2	4.9

Note: St. Dev: Standard Deviation
 %CV: Coefficient of Variance (%)

Table B5
DCSE test data—resilient modulus of asphalt mixtures

Mix Type	Sample ID	Air Voids (%)	Resilient Modulus, M_r (Gpa)				Mean M_r (Gpa)	St. Dev.	CV (%)
			1 st Cycle	2 nd Cycle	3 rd Cycle	4 th Cycle			
64CO	64CO5	6.9	11.37	11.40	11.44	11.46	11.42	0.04	0.4
	64CO9	7.0	13.11	13.00	13.43	13.36	13.23	0.20	1.5
64LS	64LS2	7.0	13.31	13.10	13.31	13.35	13.27	0.11	0.9
	64LS4	7.2	15.70	15.69	15.82	15.71	15.73	0.06	0.4
64LM	64LM9	6.5	15.55	15.36	15.40	15.54	15.46	0.10	0.6
	64LM11	6.6	16.78	16.75	16.82	16.74	16.77	0.04	0.2
	64LM12	7.2	19.66	19.33	19.52	19.16	19.42	0.22	1.1
70CO	70CO3	7.6	11.44	11.32	11.15	11.09	11.25	0.16	1.4
	70CO4	6.6	11.73	11.59	11.50	11.47	11.58	0.12	1.0
	70CO11	7.4	15.89	15.69	15.67	15.62	15.72	0.12	0.8
70LS	70LS3	6.4	10.33	10.05	10.13	9.90	10.10	0.18	1.7
	70LS5	6.9	13.06	12.87	12.77	12.81	12.88	0.13	1.0
	70LS6	6.4	21.29	21.02	21.11	20.96	21.10	0.14	0.7
70LM	70LM13	6.8	14.33	13.86	13.59	13.74	13.88	0.32	2.3
	70LM14	7.4	17.07	16.88	16.85	16.73	16.88	0.14	0.8
	70LM15	6.4	18.62	18.26	18.23	18.26	18.34	0.19	1.0
76CO	76CO12	7.0	7.06	6.92	6.86	6.79	6.91	0.11	1.6
	76CO13	7.2	11.51	10.95	10.92	10.99	11.09	0.28	2.5
	76CO14	6.8	14.11	13.56	13.44	13.35	13.62	0.34	2.5
76LS	76LS12	7.1	10.68	10.59	10.53	10.46	10.57	0.09	0.9
	76LS13	6.5	10.23	10.08	10.15	10.12	10.14	0.06	0.6
	76LS14	6.8	12.83	12.76	12.71	12.66	12.74	0.07	0.6
76LM	76LM2	7.5	11.50	11.34	11.32	11.27	11.35	0.10	0.9
	76LM3	7.6	9.60	9.39	9.20	9.30	9.37	0.17	1.8
	76LM15	7.1	13.17	12.76	12.69	12.69	12.83	0.23	1.7

*Note: St. Dev.: Standard Deviation
%CV: Coefficient of Variance (%)*

Table B6
DCSE test results

Mix Type	Sample ID	Air Voids (%)	Resilient Modulus (Gpa)	Failure Strain (M.strain)	ITS (Mpa)	Initial Strain (M.strain)	Elastic Energy (KJ/m ³)	Fracture Energy (KJ/m ³)	DCSE (KJ/m ³)
64CO	64CO5	6.9	11.42	1422	2.25	1225	0.22	1.60	1.38
	64CO9	7.0	13.23	1153	2.14	991	0.17	1.23	1.06
	Average		12.32	1288	2.20	1108	0.20	1.42	1.22
	St. Dev.		1.3	190.2	0.1	165.3	0.0	0.3	0.2
	CV (%)		10.4	14.8	3.5	14.9	17.4	18.3	18.4
64LS	64LS2	7.0	13.27	1828	3.15	1591	0.37	2.88	2.51
	64LS4	7.2	15.73	2152	3.11	1954	0.31	3.35	3.04
	Average		14.50	1990	3.13	1772	0.34	3.11	2.77
	St. Dev.		1.7	229.1	0.0	257.2	0.0	0.3	0.4
	CV (%)		12.0	11.5	0.9	14.5	13.8	10.6	13.6
64LM	64LM9	6.5	15.46	1094	2.67	921	0.23	1.46	1.23
	64LM11	6.6	16.77	1321	3.16	1133	0.30	2.09	1.79
	64LM12	7.2	19.42	1368	2.93	1217	0.22	2.00	1.78
	Average		17.22	1261	2.92	1090	0.25	1.85	1.60
	St. Dev.		2.0	146.5	0.2	152.3	0.0	0.3	0.3
	CV (%)		11.7	11.6	8.4	14.0	16.7	18.4	20.1
70CO	70CO3	7.6	11.25	2097	2.34	1889	0.24	2.46	2.21
	70CO4	6.6	11.58	2255	2.38	2049	0.25	2.69	2.44
	70CO11	7.4	15.72	2465	2.53	2305	0.20	3.12	2.91
	Average		12.85	2272	2.42	2081	0.23	2.75	2.52
	St. Dev.		2.5	184.8	0.1	209.7	0.0	0.3	0.4
	CV (%)		19.4	8.1	4.0	10.1	10.4	12.2	14.2
70LS	70LS3	6.4	10.10	1816	2.72	1546	0.37	2.47	2.11
	70LS5	6.9	12.88	1525	2.64	1321	0.27	2.01	1.74
	70LS6	6.4	21.10	1548	2.67	1422	0.17	2.06	1.89
	Average		14.69	1630	2.68	1429	0.27	2.18	1.91
	St. Dev.		5.7	161.5	0.0	113.0	0.1	0.3	0.2
	CV (%)		38.9	9.9	1.7	7.9	37.0	11.6	9.6

Note: St. Dev: Standard Deviation, %CV: Coefficient of Variance (%)
M.strain : Microstrain

Table B6
DCSE test results (Continued)

Mix Type	Sample ID	Air Voids (%)	Resilient Modulus (Gpa)	Failure Strain (M.strain)	ITS (Mpa)	Initial Strain (M.strain)	Elastic Energy (KJ/m ³)	Fracture Energy (KJ/m ³)	DCSE (KJ/m ³)
70LM	70LM13	6.8	13.88	1599	2.25	1437	0.18	1.80	1.61
	70LM14	7.4	16.88	1699	2.18	1570	0.14	1.85	1.71
	70LM15	6.4	18.34	1383	2.96	1222	0.24	2.04	1.81
	Average		16.37	1560	2.46	1409	0.19	1.90	1.71
	St. Dev.		2.3	161.4	0.4	175.6	0.05	0.13	0.10
	CV (%)		13.9	10.3	17.5	12.5	26.2	6.9	5.6
76CO	76CO12	7.0	6.91	4336	2.16	4024	0.34	4.67	4.34
	76CO13	7.2	11.09	3766	2.64	3528	0.31	4.97	4.65
	76CO14	6.8	13.62	3375	2.25	3209	0.19	3.80	3.61
	Average		10.54	3826	2.35	3587	0.28	4.48	4.20
	St. Dev.		3.4	483.6	0.3	410.7	0.1	0.6	0.5
	CV (%)		32.1	12.6	10.9	11.4	29.1	13.6	12.7
76LS	76LS12	7.1	10.57	1488	2.86	1218	0.39	2.13	1.74
	76LS13	6.5	10.14	2410	2.36	2177	0.27	2.85	2.57
	76LS14	6.8	12.74	2395	2.30	2215	0.21	2.75	2.54
	Average		11.15	2098	2.51	1870	0.29	2.57	2.28
	St. Dev.		1.4	527.8	0.3	565.1	0.1	0.4	0.5
	CV (%)		12.5	25.2	12.3	30.2	31.4	15.1	20.6
76LM	76LM2	7.5	11.35	3433	2.18	3241	0.21	3.73	3.53
	76LM3	7.6	9.37	2320	2.14	2092	0.24	2.48	2.23
	76LM15	7.1	12.83	3099	2.26	2923	0.20	3.50	3.30
	Average		11.19	2951	2.19	2752	0.22	3.24	3.02
	St. Dev.		1.7	571.0	0.1	593.2	0.0	0.7	0.7
	CV (%)		15.5	19.4	2.8	21.6	10.8	20.6	22.9

Note: St. Dev: Standard Deviation, %CV: Coefficient of Variance (%)
M.strain : Microstrain

Table B7
SCB test results

Mix Type	Aging Property	Strain Energy for different notch depths(mm)			Jc (Kj/m ²)	Aging Index
		25.4	31.8	38.0		
64CO	Unaged	0.77	0.45	0.37	0.57	0.88
	Aged	0.69	0.61	0.33	0.50	
64LS	Unaged	0.70	0.41	0.28	0.59	0.86
	Aged	0.56	0.43	0.19	0.51	
64LM	Unaged	0.70	0.36	0.28	0.59	0.92
	Aged	0.55	0.46	0.16	0.54	
70CO	Unaged	1.02	0.58	0.34	0.96	0.96
	Aged	1.02	0.59	0.36	0.92	
70LS	Unaged	0.89	0.48	0.38	0.71	0.80
	Aged	0.80	0.52	0.39	0.57	
70LM	Unaged	0.89	0.46	0.41	0.68	0.91
	Aged	0.85	0.51	0.41	0.62	
76CO	Unaged	1.13	0.75	0.45	0.95	0.98
	Aged	1.11	0.72	0.44	0.93	
76LS	Unaged	0.82	0.61	0.27	0.77	0.91
	Aged	0.81	0.41	0.31	0.70	
76LM	Unaged	0.97	0.58	0.39	0.82	0.85

Table B8
Dynamic modulus (E*) test results of 64CO mixture

Temperature	Sample ID	Air Voids (%)	E* (Ksi) values at different frequencies (Hz)					
			25 Hz	10 Hz	5 Hz	1 Hz	0.5 Hz	0.1 Hz
-10°C	64CO-5	6.9	3962	3846	3732	3410	3259	2874
	64CO-6	7.2	3782	3696	3595	3303	3173	2852
	64CO-8	6.6	4126	3988	3879	3559	3410	3042
	Average		3957	3844	3735	3424	3281	2922
	St. Dev.		172	146	142	128	120	104
	CV%		4.4	3.8	3.8	3.7	3.7	3.6
4.4°C	64CO-5	6.9	2927	2739	2546	2049	1834	1315
	64CO-6	7.2	3280	3022	2853	2380	2141	1634
	64CO-8	6.6	3138	2912	2741	2229	2027	1559
	Average		3115	2891	2713	2219	2001	1503
	St. Dev.		178.0	142.8	155.3	165.7	155.5	166.6
	CV%		5.7	4.9	5.7	7.5	7.8	11.1
25°C	64CO-5	6.9	1045	779	615	322	238	115
	64CO-6	7.2	1175	889	704	364	261	123
	64CO-8	6.6	1319	1030	804	438	316	150
	Average		1180	899	707	375	272	130
	St. Dev.		137.4	125.5	94.6	58.7	40.2	18.2
	CV%		11.6	14.0	13.4	15.7	14.8	14.0
37.8°C	64CO-5	6.9	370	243	171	80	60	35
	64CO-6	7.2	417	265	186	75	56	33
	64CO-8	6.6	434	279	198	93	69	39
	Average		407	262	185	82	62	36
	St. Dev.		32.8	18.5	13.5	9.3	6.7	3.0
	CV%		8.0	7.1	7.3	11.3	10.8	8.4
54.4°C	64CO-5	6.9	73	48	36	23	20	15
	64CO-6	7.2	69	53	38	24	19	14
	64CO-8	6.6	98	62	46	28	23	17
	Average		80	54	40	25	20	15
	St. Dev.		15.7	7.1	5.3	2.9	2.2	1.1
	CV%		19.5	13.1	13.2	11.7	10.6	7.4

Note: St. Dev.: Standard Deviation
%CV: Coefficient of Variance (%)

Table B9
Dynamic modulus (E*) test results of 64LS mixture

Temperature	Sample ID	Air Voids (%)	E* (Ksi) values at different frequencies (Hz)					
			25 Hz	10 Hz	5 Hz	1 Hz	0.5 Hz	0.1 Hz
-10°C	64LS-1	6.9	4039	3917	3810	3505	3363	2997
	64LS-2	6.5	4349	4226	4122	3804	3650	3287
	64LS-3	7.4	4213	4091	3966	3641	3474	3082
	Average		4201	4078	3966	3650	3495	3122
	St. Dev.		156	155	156	150	145	149
	CV%		3.7	3.8	3.9	4.1	4.1	4.8
4.4°C	64LS-1	6.9	3052	2821	2640	2163	1953	1480
	64LS-2	6.5	3252	3053	2900	2365	2149	1628
	64LS-3	7.4	3137	2916	2722	2218	1991	1463
	Average		3147	2930	2754	2248	2031	1524
	St. Dev.		100.1	116.8	133.2	104.4	103.7	90.8
	CV%		3.2	4.0	4.8	4.6	5.1	6.0
25°C	64LS-1	6.9	1094	791	597	281	201	97
	64LS-2	6.5	1361	1031	781	377	268	117
	64LS-3	7.4	1224	893	681	328	235	105
	Average		1226	905	686	329	235	106
	St. Dev.		133.8	120.6	92.1	48.2	33.5	10.2
	CV%		10.9	13.3	13.4	14.7	14.3	9.6
37.8°C	64LS-1	6.9	374	228	153	66	48	28
	64LS-2	6.5	382	233	161	75	56	34
	64LS-3	7.4	376	231	156	68	52	33
	Average		377	231	157	69	52	31
	St. Dev.		3.9	2.4	3.9	4.7	3.9	3.2
	CV%		1.0	1.0	2.5	6.7	7.6	10.1
54.4°C	64LS-1	6.9	76	45	33	20	18	14
	64LS-2	6.5	76	49	37	25	21	18
	64LS-3	7.4	69	41	32	22	18	15
	Average		74	45	34	22	19	16
	St. Dev.		3.9	3.9	2.7	2.6	2.0	2.1
	CV%		5.4	8.6	7.9	11.7	10.7	13.2

Note: St. Dev.: Standard Deviation
%CV: Coefficient of Variance (%)

Table B10
Dynamic modulus (E*) test results of 64LM mixture

Temperature	Sample ID	Air Voids (%)	E* (Ksi) values at different frequencies (Hz)					
			25 Hz	10 Hz	5 Hz	1 Hz	0.5 Hz	0.1 Hz
-10°C	64LM-1	7.3	3871	3689	3559	3261	3122	2783
	64LM-3	7.4	3811	3717	3631	3372	3244	2940
	64LM-4	7.5	4061	3924	3815	3515	3371	3049
	Average		3914	3777	3669	3383	3246	2924
	St. Dev.		131	128	132	127	125	134
	CV%		3.3	3.4	3.6	3.8	3.8	4.6
4.4°C	64LM-1	7.3	2895	2700	2534	2111	1923	1527
	64LM-3	7.4	2927	2716	2536	2095	1897	1450
	64LM-4	7.5	2980	2811	2649	2222	2034	1622
	Average		2934	2742	2573	2142	1951	1533
	St. Dev.		42.8	60.1	65.8	69.1	72.6	86.0
	CV%		1.5	2.2	2.6	3.2	3.7	5.6
25°C	64LM-1	7.3	1240	979	773	418	308	146
	64LM-3	7.4	1280	970	773	399	294	134
	64LM-4	7.5	1317	991	774	407	292	134
	Average		1279	980	774	408	298	138
	St. Dev.		38.7	10.4	0.8	9.8	8.9	7.1
	CV%		3.0	1.1	0.1	2.4	3.0	5.2
37.8°C	64LM-1	7.3	471	319	225	108	80	45
	64LM-3	7.4	461	296	206	91	71	40
	64LM-4	7.5	419	268	187	85	65	39
	Average		450	294	206	95	72	41
	St. Dev.		27.8	25.1	19.1	11.7	7.4	3.0
	CV%		6.2	8.5	9.3	12.3	10.3	7.3
54.4°C	64LM-1	7.3	95	59	44	26	21	15
	64LM-3	7.4	90	59	44	27	23	18
	64LM-4	7.5	81	53	41	27	22	18
	Average		89	57	43	27	22	17
	St. Dev.		6.7	3.3	1.5	0.4	0.9	1.6
	CV%		7.6	5.8	3.5	1.6	4.3	9.5

Note: St. Dev.: Standard Deviation
%CV: Coefficient of Variance (%)

Table B11
Dynamic modulus (E*) test results of 70CO mixture

Temperature	Sample ID	Air Voids (%)	E* (Ksi) values at different frequencies (Hz)					
			25 Hz	10 Hz	5 Hz	1 Hz	0.5 Hz	0.1 Hz
-10°C	70CO-1	7.5	3393	3219	3106	2803	2661	2327
	70CO-2	6.4	3902	3744	3622	3289	3141	2760
	70CO-11	6.9	3669	3524	3392	3055	2914	2546
	Average		3655	3496	3374	3049	2905	2544
	St. Dev.		255	264	259	243	240	216
	CV%		7.0	7.5	7.7	8.0	8.3	8.5
4.4°C	70CO-1	7.5	2282	2053	1869	1449	1277	912
	70CO-2	6.4	2607	2318	2118	1668	1485	1093
	70CO-11	6.9	2559	2367	2180	1721	1539	1149
	Average		2483	2246	2056	1613	1434	1051
	St. Dev.		175.4	169.0	164.6	144.7	138.0	123.6
	CV%		7.1	7.5	8.0	9.0	9.6	11.8
25°C	70CO-1	7.5	873	679	551	300	240	128
	70CO-2	6.4	1024	819	652	380	289	165
	70CO-11	6.9	901	693	556	298	234	123
	Average		933	730	586	326	254	139
	St. Dev.		80.3	77.3	56.7	46.6	30.0	22.5
	CV%		8.6	10.6	9.7	14.3	11.8	16.2
37.8°C	70CO-1	7.5	328	225	168	86	66	41
	70CO-2	6.4	421	286	217	113	86	53
	70CO-11	6.9	352	233	178	95	74	46
	Average		367	248	188	98	75	47
	St. Dev.		48.3	33.7	26.0	14.0	10.1	6.4
	CV%		13.2	13.6	13.8	14.3	13.4	13.7
54.4°C	70CO-1	7.5	70	51	39	23	21	16
	70CO-2	6.4	88	60	47	31	27	21
	70CO-11	6.9	92	63	51	32	26	24
	Average		84	58	46	29	25	21
	St. Dev.		11.6	6.1	6.0	4.8	3.5	3.8
	CV%		13.9	10.5	13.2	16.8	14.3	18.6

Note: St. Dev.: Standard Deviation
%CV: Coefficient of Variance (%)

Table B12
Dynamic modulus (E*) test results of 70LS mixture

Temperature	Sample ID	Air Voids (%)	E* (Ksi) values at different frequencies (Hz)					
			25 Hz	10 Hz	5 Hz	1 Hz	0.5 Hz	0.1 Hz
-10°C	70LS-1	6.8	3663	3556	3455	3197	3085	2795
	70LS-2	6.5	4348	4191	4064	3737	3573	3167
	70LS-5	6.7	3869	3675	3539	3225	3064	2691
	Average		3960	3808	3686	3386	3241	2884
	St. Dev.		352	338	330	304	288	250
	CV%		8.9	8.9	9.0	9.0	8.9	8.7
4.4°C	70LS-1	6.8	2737	2508	2350	1959	1792	1418
	70LS-2	6.5	3024	2752	2551	2079	1881	1445
	70LS-5	6.7	2798	2600	2440	2034	1855	1458
	Average		2853	2620	2447	2024	1843	1440
	St. Dev.		151.0	122.8	100.3	60.8	45.7	20.2
	CV%		5.3	4.7	4.1	3.0	2.5	1.4
25°C	70LS-1	6.8	1219	1007	848	515	404	233
	70LS-2	6.5	1310	1016	873	500	390	223
	70LS-5	6.7	1132	940	795	492	390	238
	Average		1220	987	839	502	395	232
	St. Dev.		88.8	41.3	40.1	12.2	8.1	7.8
	CV%		7.3	4.2	4.8	2.4	2.1	3.4
37.8°C	70LS-1	6.8	494	353	272	151	114	73
	70LS-2	6.5	547	397	304	165	129	81
	70LS-5	6.7	428	314	240	133	107	74
	Average		489	355	272	150	117	76
	St. Dev.		59.4	41.3	31.6	15.8	10.9	4.5
	CV%		12.1	11.6	11.6	10.5	9.4	5.9
54.4°C	70LS-1	6.8	128	95	76	53	46	39
	70LS-2	6.5	154	113	90	60	53	42
	70LS-5	6.7	140	105	85	61	55	46
	Average		141	104	84	58	51	42
	St. Dev.		13.0	9.0	7.0	4.4	4.6	3.5
	CV%		9.2	8.7	8.3	7.6	9.0	8.3

Note: St. Dev.: Standard Deviation
%CV: Coefficient of Variance (%)

Table B13
Dynamic modulus (E*) test results of 70LM mixture

Temperature	Sample ID	Air Voids (%)	E* (Ksi) values at different frequencies (Hz)					
			25 Hz	10 Hz	5 Hz	1 Hz	0.5 Hz	0.1 Hz
-10°C	70LM-1	7.3	4255	3873	3722	3446	3314	2974
	70LM-7	7.1	4040	3886	3745	3396	3234	2834
	70LM-9	7.1	4343	4231	4117	3794	3639	3267
	Average		4213	3997	3861	3545	3396	3025
	St. Dev.		156	203	221	217	215	221
	CV%		3.7	5.1	5.7	6.1	6.3	7.3
4.4°C	70LM-1	7.3	2882	2631	2458	2021	1832	1402
	70LM-7	7.1	2982	2740	2543	2040	1830	1348
	70LM-9	7.1	2953	2743	2615	2216	2043	1636
	Average		2939	2705	2539	2092	1901	1462
	St. Dev.		51.8	63.9	78.8	107.6	122.3	153.2
	CV%		1.8	2.4	3.1	5.1	6.4	10.5
25°C	70LM-1	7.3	1163	895	728	401	304	166
	70LM-7	7.1	1084	873	709	402	297	165
	70LM-9	7.1	1376	1104	910	543	417	234
	Average		1208	957	782	449	339	188
	St. Dev.		151.2	127.2	110.5	81.4	66.9	39.2
	CV%		12.5	13.3	14.1	18.2	19.7	20.8
37.8°C	70LM-1	7.3	432	290	213	113	87	60
	70LM-7	7.1	372	250	188	102	79	53
	70LM-9	7.1	526	372	287	152	117	75
	Average		444	304	229	123	94	62
	St. Dev.		77.6	62.5	51.5	26.3	19.8	10.9
	CV%		17.5	20.5	22.4	21.4	21.0	17.5
54.4°C	70LM-1	7.3	106	77	58	41	37	32
	70LM-7	7.1	100	70	56	40	36	31
	70LM-9	7.1	127	93	71	48	42	38
	Average		111	80	62	43	38	34
	St. Dev.		14.2	11.8	8.2	4.1	3.6	3.7
	CV%		12.8	14.7	13.3	9.5	9.3	11.1

Note: St. Dev.: Standard Deviation
%CV: Coefficient of Variance (%)

Table B14
Dynamic modulus (E*) test results of 76CO mixture

Temperature	Sample ID	Air Voids (%)	E* (Ksi) values at different frequencies (Hz)					
			25 Hz	10 Hz	5 Hz	1 Hz	0.5 Hz	0.1 Hz
-10°C	76CO-1	7.4	3813	3691	3569	3253	3032	2667
	76CO-2	6.5	3729	3598	3481	3191	3057	2714
	76CO-9	7.3	3339	3219	3107	2818	2621	2369
	Average		3627	3502	3386	3088	2903	2583
	St. Dev.		253	250	245	235	244	187
	CV%		7.0	7.1	7.2	7.6	8.4	7.2
4.4°C	76CO-1	7.4	2637	2421	2241	1801	1618	1213
	76CO-2	6.5	2577	2401	2242	1827	1663	1305
	76CO-9	7.3	2558	2286	2098	1730	1565	1196
	Average		2591	2369	2194	1786	1615	1238
	St. Dev.		41.5	72.8	82.8	50.4	48.9	58.8
	CV%		1.6	3.1	3.8	2.8	3.0	4.7
25°C	76CO-1	7.4	1084	864	696	391	292	152
	76CO-2	6.5	1124	904	739	423	342	190
	76CO-9	7.3	983	789	652	398	310	189
	Average		1064	852	696	404	315	177
	St. Dev.		72.6	58.5	43.8	17.1	25.5	21.4
	CV%		6.8	6.9	6.3	4.2	8.1	12.1
37.8°C	76CO-1	7.4	439	303	231	114	89	55
	76CO-2	6.5	459	323	247	128	97	57
	76CO-9	7.3	354	251	202	120	92	63
	Average		417	292	227	121	93	58
	St. Dev.		55.8	37.2	22.5	6.9	4.3	3.9
	CV%		13.4	12.7	9.9	5.7	4.6	6.6
54.4°C	76CO-1	7.4	105	74	58	37	34	27
	76CO-2	6.5	111	76	61	40	37	32
	76CO-9	7.3	115	84	69	47	42	34
	Average		110	78	62	41	38	31
	St. Dev.		5.2	5.2	5.8	5.4	4.3	3.8
	CV%		4.7	6.7	9.3	13.1	11.5	12.2

Note: St. Dev.: Standard Deviation
%CV: Coefficient of Variance (%)

Table B15
Dynamic modulus (E*) test results of 76LS mixture

Temperature	Sample ID	Air Voids (%)	E* (Ksi) values at different frequencies (Hz)					
			25 Hz	10 Hz	5 Hz	1 Hz	0.5 Hz	0.1 Hz
-10°C	76LS-2	7.4	4228	4076	3958	3666	3531	3175
	76LS-3	7.1	3873	3739	3629	3344	3211	2886
	76LS-5	7.1	3813	3684	3571	3270	3135	2802
	Average		3971	3833	3719	3427	3293	2954
	St. Dev.		224	212	209	210	210	196
	CV%		5.6	5.5	5.6	6.1	6.4	6.6
4.4°C	76LS-2	7.4	3176	2978	2808	2385	2204	1772
	76LS-3	7.1	2692	2485	2316	1896	1734	1357
	76LS-5	7.1	2648	2435	2261	1839	1660	1279
	Average		2839	2633	2462	2040	1866	1469
	St. Dev.		292.9	299.8	301.3	300.4	295.2	265.3
	CV%		10.3	11.4	12.2	14.7	15.8	18.1
25°C	76LS-2	7.4	1316	1127	952	607	493	310
	76LS-3	7.1	1225	984	827	496	394	232
	76LS-5	7.1	1141	938	763	454	352	206
	Average		1227	1016	848	519	413	249
	St. Dev.		88.0	99.0	96.2	79.3	72.7	54.4
	CV%		7.2	9.7	11.4	15.3	17.6	21.8
37.8°C	76LS-2	7.4	578	423	339	188	147	94
	76LS-3	7.1	473	336	262	142	113	74
	76LS-5	7.1	474	349	271	145	114	73
	Average		508	370	291	158	125	80
	St. Dev.		60.5	47.0	41.8	25.6	19.1	12.1
	CV%		11.9	12.7	14.4	16.1	15.4	15.1
54.4°C	76LS-2	7.4	181	132	107	70	60	46
	76LS-3	7.1	168	125	98	61	53	41
	76LS-5	7.1	150	107	87	56	51	41
	Average		166	121	97	62	54	42
	St. Dev.		15.3	12.5	9.8	7.0	4.8	2.9
	CV%		9.2	10.3	10.0	11.3	8.8	6.9

Note: St. Dev.: Standard Deviation
%CV: Coefficient of Variance (%)

Table B16
Dynamic modulus (E*) test results of 76LM mixture

Temperature	Sample ID	Air Voids (%)	E* (Ksi) values at different frequencies (Hz)					
			25 Hz	10 Hz	5 Hz	1 Hz	0.5 Hz	0.1 Hz
-10°C	76LM-3	7.1	4149	4007	3900	3591	3442	3081
	76LM-4	6.9	3969	3847	3737	3455	3323	2987
	76LM-5	7.4	4404	4282	4170	3854	3706	3323
	Average		4174	4046	3936	3633	3490	3130
	St. Dev.		219	220	218	203	196	173
	CV%		5.2	5.4	5.5	5.6	5.6	5.5
4.4°C	76LM-3	7.1	2832	2609	2431	1981	1793	1387
	76LM-4	6.9	2858	2649	2479	2055	1873	1471
	76LM-5	7.4	3181	2952	2747	2247	2035	1575
	Average		2957	2737	2553	2094	1900	1478
	St. Dev.		194.5	187.8	170.4	137.6	123.2	94.2
	CV%		6.6	6.9	6.7	6.6	6.5	6.4
25°C	76LM-3	7.1	1346	1103	900	537	425	239
	76LM-4	6.9	1244	1000	827	480	381	215
	76LM-5	7.4	1250	976	804	453	349	192
	Average		1280	1026	844	490	385	215
	St. Dev.		57.4	67.8	50.2	42.7	38.2	23.6
	CV%		4.5	6.6	5.9	8.7	9.9	11.0
37.8°C	76LM-3	7.1	606	428	328	171	129	75
	76LM-4	6.9	507	368	298	154	118	71
	76LM-5	7.4	483	360	246	127	99	60
	Average		532	385	291	151	115	69
	St. Dev.		64.8	37.3	41.2	22.3	15.4	7.5
	CV%		12.2	9.7	14.2	14.8	13.4	10.9
54.4°C	76LM-3	7.1	144	100	78	46	41	31
	76LM-4	6.9	136	92	73	43	37	30
	76LM-5	7.4	126	86	67	41	36	29
	Average		135	93	73	43	38	30
	St. Dev.		9.2	7.0	5.2	2.4	2.5	1.2
	CV%		6.8	7.5	7.2	5.5	6.5	3.9

Note: St. Dev.: Standard Deviation
%CV: Coefficient of Variance (%)

Table B17
Phase angle test results of 64CO mixture

Temperature	Sample ID	Air Voids (%)	Phase Angle (Degrees) values at different frequencies (Hz)					
			25 Hz	10 Hz	5 Hz	1 Hz	0.5 Hz	0.1 Hz
-10°C	64CO-5	6.9	0.97	3.14	4.10	5.88	6.59	8.54
	64CO-6	7.2	0.88	2.97	3.83	5.57	6.15	7.93
	64CO-8	6.6	0.59	2.79	3.83	5.43	6.19	7.86
	Average		0.8	3.0	3.9	5.6	6.3	8.1
	St. Dev.		0.2	0.2	0.2	0.2	0.2	0.4
	CV%		24.4	5.9	4.0	4.1	3.9	4.6
4.4°C	64CO-5	6.9	6.14	9.2	10.9	14.81	16.65	20.82
	64CO-6	7.2	4.58	7.4	8.83	12.07	13.95	18.19
	64CO-8	6.6	5.42	8.39	10.02	13.81	15.46	20.03
	Average		5.4	8.3	9.9	13.6	15.4	19.7
	St. Dev.		0.8	0.9	1.0	1.4	1.4	1.3
	CV%		14.5	10.8	10.5	10.2	8.8	6.9
25°C	64CO-5	6.9	22.12	27.3	30.33	35.45	36.45	35.26
	64CO-6	7.2	20.78	25.45	28.7	34.82	36.91	36.1
	64CO-8	6.6	19.9	24.31	27.63	33.93	36.1	35.57
	Average		20.9	25.7	28.9	34.7	36.5	35.6
	St. Dev.		1.1	1.5	1.4	0.8	0.4	0.4
	CV%		5.3	5.9	4.7	2.2	1.1	1.2
37.8°C	64CO-5	6.9	33.38	35.56	37.29	35.41	32.53	24.86
	64CO-6	7.2	32.54	35.98	36.9	37.34	34.67	26.88
	64CO-8	6.6	32.89	35.66	36.88	35.5	33.1	25.56
	Average		32.9	35.7	37.0	36.1	33.4	25.8
	St. Dev.		0.4	0.2	0.2	1.1	1.1	1.0
	CV%		1.3	0.6	0.6	3.0	3.3	4.0
54.4°C	64CO-5	6.9	33.11	30.24	27.24	21.54	20.4	17.95
	64CO-6	7.2	37.99	34.36	31.98	26.27	22.4	17.56
	64CO-8	6.6	35.54	33.64	31.34	24.69	23.13	17.19
	Average		35.5	32.7	30.2	24.2	22.0	17.6
	St. Dev.		2.4	2.2	2.6	2.4	1.4	0.4
	CV%		6.9	6.7	8.5	10.0	6.4	2.2

Note: St. Dev.: Standard Deviation
%CV: Coefficient of Variance (%)

Table B18
Phase angle test results of 64LS mixture

Temperature	Sample ID	Air Voids (%)	Phase Angle (Degrees) values at different frequencies (Hz)					
			25 Hz	10 Hz	5 Hz	1 Hz	0.5 Hz	0.1 Hz
-10°C	64LS-1	6.9	0.56	2.88	3.84	5.55	6.23	8.16
	64LS-2	6.5	0.66	2.80	3.83	5.48	6.17	7.90
	64LS-3	7.4	0.39	2.62	3.73	5.48	6.10	8.16
	Average		0.5	2.8	3.8	5.5	6.2	8.1
	St. Dev.		0.1	0.1	0.1	0.0	0.1	0.2
	CV%		25.4	4.8	1.6	0.7	1.1	1.9
4.4°C	64LS-1	6.9	5.6	8.51	10.1	14.9	15.74	20.71
	64LS-2	6.5	5.19	8.12	9.78	13.77	15.65	20.54
	64LS-3	7.4	5.16	8.23	9.89	13.99	15.89	20.63
	Average		5.3	8.3	9.9	14.2	15.8	20.6
	St. Dev.		0.2	0.2	0.2	0.6	0.1	0.1
	CV%		4.6	2.4	1.6	4.2	0.8	0.4
25°C	64LS-1	6.9	23.84	29.26	32.67	39.07	39.62	37.17
	64LS-2	6.5	21.67	26.61	30.38	37.64	39.11	37.65
	64LS-3	7.4	22.66	28.11	31.34	37.77	38.46	36.2
	Average		22.7	28.0	31.5	38.2	39.1	37.0
	St. Dev.		1.1	1.3	1.1	0.8	0.6	0.7
	CV%		4.8	4.7	3.7	2.1	1.5	2.0
37.8°C	64LS-1	6.9	36.07	39.96	41.07	40.46	37.44	28.14
	64LS-2	6.5	36.38	39.85	40.79	36.78	33.55	24.33
	64LS-3	7.4	35.79	38.64	39.2	36.14	32.76	23.43
	Average		36.1	39.5	40.4	37.8	34.6	25.3
	St. Dev.		0.3	0.7	1.0	2.3	2.5	2.5
	CV%		0.8	1.9	2.5	6.2	7.2	9.9
54.4°C	64LS-1	6.9	38.45	35.9	32.26	24.09	20.54	14.41
	64LS-2	6.5	37.05	33.75	29.02	21.01	18.18	12.91
	64LS-3	7.4	35.45	31.78	28.88	22.28	19.53	13.98
	Average		37.0	33.8	30.1	22.5	19.4	13.8
	St. Dev.		1.5	2.1	1.9	1.5	1.2	0.8
	CV%		4.1	6.1	6.4	6.9	6.1	5.6

Note: St. Dev.: Standard Deviation
%CV: Coefficient of Variance (%)

Table B19
Phase angle test results of 64LM mixture

Temperature	Sample ID	Air Voids (%)	Phase Angle (Degrees) values at different frequencies (Hz)					
			25 Hz	10 Hz	5 Hz	1 Hz	0.5 Hz	0.1 Hz
-10°C	64LM-1	7.3	0.59	2.71	3.72	5.42	6.08	7.81
	64LM-3	7.4	0.34	2.42	3.35	4.85	5.48	7.16
	64LM-4	7.5	0.60	2.81	3.77	5.42	6.07	7.78
	Average		0.5	2.6	3.6	5.2	5.9	7.6
	St. Dev.		0.1	0.2	0.2	0.3	0.3	0.4
	CV%		28.9	7.7	6.3	6.3	5.8	4.8
4.4°C	64LM-1	7.3	4.64	7.44	8.95	12.24	13.82	17.81
	64LM-3	7.4	4.88	7.88	9.45	13.2	14.88	19.54
	64LM-4	7.5	4.28	7.18	8.72	12.16	13.79	18.16
	Average		4.6	7.5	9.0	12.5	14.2	18.5
	St. Dev.		0.3	0.4	0.4	0.6	0.6	0.9
	CV%		6.6	4.7	4.1	4.6	4.4	4.9
25°C	64LM-1	7.3	19.15	23.45	26.53	32.82	34.87	34.32
	64LM-3	7.4	20.4	25.45	28.89	35.67	37.25	36.73
	64LM-4	7.5	20.46	25.08	28.62	35.45	37.04	37.1
	Average		20.0	24.7	28.0	34.6	36.4	36.1
	St. Dev.		0.7	1.1	1.3	1.6	1.3	1.5
	CV%		3.7	4.3	4.6	4.6	3.6	4.2
37.8°C	64LM-1	7.3	30.48	34.04	35.57	34.31	32.04	25.42
	64LM-3	7.4	33.44	37.14	38.14	36.9	32.82	24.91
	64LM-4	7.5	33.65	36.73	37.97	36.59	33.54	25.33
	Average		32.5	36.0	37.2	35.9	32.8	25.2
	St. Dev.		1.8	1.7	1.4	1.4	0.8	0.3
	CV%		5.5	4.7	3.9	3.9	2.3	1.1
54.4°C	64LM-1	7.3	36.89	34.99	32.53	24.35	21.82	15.76
	64LM-3	7.4	36.98	34.16	31.18	22.89	20.59	15.58
	64LM-4	7.5	35.33	33.08	29.73	22.21	20.67	18.95
	Average		36.4	34.1	31.1	23.2	21.0	16.8
	St. Dev.		0.9	1.0	1.4	1.1	0.7	1.9
	CV%		2.5	2.8	4.5	4.7	3.3	11.3

Note: St. Dev.: Standard Deviation
%CV: Coefficient of Variance (%)

Table B20
Phase angle test results of 70CO mixture

Temperature	Sample ID	Air Voids (%)	Phase Angle (Degrees) values at different frequencies (Hz)					
			25 Hz	10 Hz	5 Hz	1 Hz	0.5 Hz	0.1 Hz
-10°C	70CO-1	7.5	1.58	3.71	4.80	6.49	7.14	8.92
	70CO-2	6.4	1.55	3.69	4.66	6.26	6.92	8.62
	70CO-11	6.9	1.48	3.70	4.74	6.49	7.14	8.98
	Average		1.5	3.7	4.7	6.4	7.1	8.8
	St. Dev.		0.1	0.0	0.1	0.1	0.1	0.2
	CV%		3.3	0.3	1.5	2.1	1.8	2.2
4.4°C	70CO-1	7.5	8.23	11.2	12.9	16.87	18.5	22.48
	70CO-2	6.4	7.35	10.49	12.13	15.93	17.58	21.38
	70CO-11	6.9	6.76	9.79	11.42	15.01	16.68	20.3
	Average		7.4	10.5	12.2	15.9	17.6	21.4
	St. Dev.		0.7	0.7	0.7	0.9	0.9	1.1
	CV%		9.9	6.7	6.1	5.8	5.2	5.1
25°C	70CO-1	7.5	21.29	24.8	27.1	32.36	32.5	32.09
	70CO-2	6.4	20.48	23.55	25.6	30.47	31.87	30.47
	70CO-11	6.9	22.39	25.49	27.41	32.55	32.24	30.85
	Average		21.4	24.6	26.7	31.8	32.2	31.1
	St. Dev.		1.0	1.0	1.0	1.1	0.3	0.8
	CV%		4.5	4.0	3.6	3.6	1.0	2.7
37.8°C	70CO-1	7.5	29.67	31.92	32.48	32.5	31.19	25.97
	70CO-2	6.4	28.7	31.37	31.8	31.8	30.79	25.35
	70CO-11	6.9	29.97	31.41	31.7	30.16	28.78	23.06
	Average		29.4	31.6	32.0	31.5	30.3	24.8
	St. Dev.		0.7	0.3	0.4	1.2	1.3	1.5
	CV%		2.3	1.0	1.3	3.8	4.3	6.2
54.4°C	70CO-1	7.5	33.4	31.84	30.23	25.62	22.75	17.04
	70CO-2	6.4	31.38	28.97	27.31	23.42	22.18	17.74
	70CO-11	6.9	31.29	29.63	27.57	22.53	20.67	15.13
	Average		32.0	30.1	28.4	23.9	21.9	16.6
	St. Dev.		1.2	1.5	1.6	1.6	1.1	1.4
	CV%		3.7	5.0	5.7	6.7	4.9	8.1

Note: St. Dev.: Standard Deviation
%CV: Coefficient of Variance (%)

Table B21
Phase angle test results of 70LS mixture

Temperature	Sample ID	Air Voids (%)	Phase Angle (Degrees) values at different frequencies (Hz)					
			25 Hz	10 Hz	5 Hz	1 Hz	0.5 Hz	0.1 Hz
-10°C	70LS-1	6.8	0.33	2.42	3.29	4.72	5.13	6.56
	70LS-2	6.5	0.97	3.03	3.87	5.26	5.92	7.58
	70LS-5	6.7	0.28	2.15	3.03	4.21	4.88	6.18
	Average		0.5	2.5	3.4	4.7	5.3	6.8
	St. Dev.		0.4	0.5	0.4	0.5	0.5	0.7
	CV%		73.1	17.8	12.7	11.1	10.2	10.7
4.4°C	70LS-1	6.8	5.92	7.52	8.98	11.97	13.28	16.72
	70LS-2	6.5	5.19	8.18	9.72	13.2	14.67	17.9
	70LS-5	6.7	5.81	7.12	8.53	11.57	13	16.82
	Average		5.6	7.6	9.1	12.2	13.7	17.1
	St. Dev.		0.4	0.5	0.6	0.8	0.9	0.7
	CV%		7.0	7.0	6.6	6.9	6.6	3.8
25°C	70LS-1	6.8	17.35	21.32	23.68	29.04	30.73	31.46
	70LS-2	6.5	16.68	22.11	24.59	30.24	32.07	32.11
	70LS-5	6.7	16.97	22.09	24.74	30.03	31.76	32.48
	Average		17.0	21.8	24.3	29.8	31.5	32.0
	St. Dev.		0.3	0.5	0.6	0.6	0.7	0.5
	CV%		2.0	2.1	2.4	2.2	2.2	1.6
37.8°C	70LS-1	6.8	27.63	30.42	31.34	30.67	30.18	25.09
	70LS-2	6.5	28.23	30.76	31.57	31.93	30.9	25.97
	70LS-5	6.7	29.48	31.94	32.31	31.42	30.24	24.1
	Average		28.4	31.0	31.7	31.3	30.4	25.1
	St. Dev.		0.9	0.8	0.5	0.6	0.4	0.9
	CV%		3.3	2.6	1.6	2.0	1.3	3.7
54.4°C	70LS-1	6.8	31.17	28.55	26.57	21.82	19.67	15.08
	70LS-2	6.5	32.24	30.15	28.37	23.71	21.01	16.63
	70LS-5	6.7	31.11	28.78	26.13	20.93	18.48	13.72
	Average		31.5	29.2	27.0	22.2	19.7	15.1
	St. Dev.		0.6	0.9	1.2	1.4	1.3	1.5
	CV%		2.0	3.0	4.4	6.4	6.4	9.6

Note: St. Dev.: Standard Deviation
%CV: Coefficient of Variance (%)

Table B22
Phase angle test results of 70LM mixture

Temperature	Sample ID	Air Voids (%)	Phase Angle (Degrees) values at different frequencies (Hz)					
			25 Hz	10 Hz	5 Hz	1 Hz	0.5 Hz	0.1 Hz
-10°C	70LM-1	7.3	2.03	2.05	3.65	5.14	5.78	7.46
	70LM-7	7.1	1.27	3.45	4.49	6.27	6.84	8.67
	70LM-9	7.1	0.97	2.89	3.89	5.37	6.04	7.79
	Average		1.4	2.8	4.0	5.6	6.2	8.0
	St. Dev.		0.5	0.7	0.4	0.6	0.6	0.6
	CV%		38.4	25.2	10.8	10.7	8.9	7.8
4.4°C	70LM-1	7.3	2.85	8.01	9.62	13.27	15.00	19.23
	70LM-7	7.1	5.97	8.82	10.43	14.09	15.57	19.57
	70LM-9	7.1	3.96	6.81	8.16	11.07	12.43	15.95
	Average		4.3	7.9	9.4	12.8	14.3	18.3
	St. Dev.		1.6	1.0	1.2	1.6	1.7	2.0
	CV%		37.1	12.8	12.2	12.2	11.7	11.0
25°C	70LM-1	7.3	19.85	25.09	27.82	33.30	34.29	32.27
	70LM-7	7.1	20.79	24.66	27.23	32.47	34.07	32.91
	70LM-9	7.1	17.16	21.72	24.54	30.36	32.26	32.66
	Average		19.3	23.8	26.5	32.0	33.5	32.6
	St. Dev.		1.9	1.8	1.7	1.5	1.1	0.3
	CV%		9.8	7.7	6.6	4.7	3.3	1.0
37.8°C	70LM-1	7.3	30.91	32.78	33.22	30.63	28.90	22.14
	70LM-7	7.1	31.53	33.51	33.82	30.74	29.02	22.65
	70LM-9	7.1	29.05	31.81	32.4	31.72	30.81	24.81
	Average		30.5	32.7	33.1	31.0	29.6	23.2
	St. Dev.		1.3	0.9	0.7	0.6	1.1	1.4
	CV%		4.2	2.6	2.2	1.9	3.6	6.1
54.4°C	70LM-1	7.3	31.73	28.36	26.75	20.73	18.04	13.42
	70LM-7	7.1	31.22	28.92	26.73	21.03	18.64	14.04
	70LM-9	7.1	33.69	30.25	27.01	23.14	20.21	14.38
	Average		32.2	29.2	26.8	21.6	19.0	13.9
	St. Dev.		1.3	1.0	0.2	1.3	1.1	0.5
	CV%		4.0	3.3	0.6	6.1	5.9	3.5

Note: St. Dev.: Standard Deviation
%CV: Coefficient of Variance (%)

Table B23
Phase angle test results of 76CO mixture

Temperature	Sample ID	Air Voids (%)	Phase Angle values at different frequencies (Hz)					
			25 Hz	10 Hz	5 Hz	1 Hz	0.5 Hz	0.1 Hz
-10°C	76CO-1	7.4	1.30	3.19	4.20	5.80	6.67	8.38
	76CO-2	6.5	0.81	3.01	3.92	5.48	6.01	7.65
	76CO-9	7.3	1.48	3.61	4.60	6.22	8.84	9.11
	Average		1.2	3.3	4.2	5.8	7.2	8.4
	St. Dev.		0.3	0.3	0.3	0.4	1.5	0.7
	CV%		29.0	9.4	8.1	6.4	20.6	8.7
4.4°C	76CO-1	7.4	6.14	8.99	10.61	14.12	15.76	19.11
	76CO-2	6.5	6.04	8.92	10.56	14.12	15.7	19.35
	76CO-9	7.3	4.73	8.5	9.97	13.12	14.54	17.93
	Average		5.6	8.8	10.4	13.8	15.3	18.8
	St. Dev.		0.8	0.3	0.4	0.6	0.7	0.8
	CV%		14.0	3.0	3.4	4.2	4.5	4.0
25°C	76CO-1	7.4	20.17	23.5	26.2	31.24	32.76	33.22
	76CO-2	6.5	19.25	22.59	25.03	29.68	30.42	30.79
	76CO-9	7.3	18.48	22.26	24.43	28.64	30.24	30.09
	Average		19.3	22.8	25.2	29.9	31.1	31.4
	St. Dev.		0.8	0.6	0.9	1.3	1.4	1.6
	CV%		4.4	2.8	3.6	4.4	4.5	5.2
37.8°C	76CO-1	7.4	28.24	31.04	31.79	32.79	30.92	25.58
	76CO-2	6.5	28.23	30.6	31.57	32.35	31.43	27.3
	76CO-9	7.3	26.63	28.82	28.69	27.4	26.96	22.5
	Average		27.7	30.2	30.7	30.8	29.8	25.1
	St. Dev.		0.9	1.2	1.7	3.0	2.4	2.4
	CV%		3.3	3.9	5.6	9.7	8.2	9.7
54.4°C	76CO-1	7.4	31.09	29.79	28.28	23.93	21.16	16.47
	76CO-2	6.5	29.68	28.39	26.9	22.13	19.12	14.22
	76CO-9	7.3	26.6	25.32	24.35	20.82	19.46	15.96
	Average		29.1	27.8	26.5	22.3	19.9	15.6
	St. Dev.		2.3	2.3	2.0	1.6	1.1	1.2
	CV%		7.9	8.2	7.5	7.0	5.5	7.6

Note: St. Dev.: Standard Deviation
%CV: Coefficient of Variance (%)

Table B24
Phase angle test results of 76LS mixture

Temperature	Sample ID	Air Voids (%)	Phase Angle values at different frequencies (Hz)					
			25 Hz	10 Hz	5 Hz	1 Hz	0.5 Hz	0.1 Hz
-10°C	76LS-2	7.4	0.09	2.55	3.42	4.90	5.47	6.86
	76LS-3	7.1	0.03	3.05	3.90	5.30	5.93	7.45
	76LS-5	7.1	1.01	3.23	4.18	5.65	6.21	7.74
	Average		0.4	2.9	3.8	5.3	5.9	7.4
	St. Dev.		0.5	0.4	0.4	0.4	0.4	0.4
	CV%		14.8	12.0	10.0	7.1	6.4	6.1
4.4°C	76LS-2	7.4	3.56	6.68	8.02	10.68	11.89	15.05
	76LS-3	7.1	5.29	8.45	9.9	13.19	14.52	17.51
	76LS-5	7.1	5.64	9.09	10.63	13.96	15.43	18.46
	Average		4.8	8.1	9.5	12.6	13.9	17.0
	St. Dev.		1.1	1.2	1.3	1.7	1.8	1.8
	CV%		23.1	15.5	14.1	13.6	13.2	10.3
25°C	76LS-2	7.4	16.79	19.48	22.0	27.37	28.97	30.12
	76LS-3	7.1	16.51	20.93	23.33	28.87	30.37	31.22
	76LS-5	7.1	17.6	21.83	24.4	30	31.96	31.8
	Average		17.0	20.7	23.2	28.7	30.4	31.0
	St. Dev.		0.6	1.2	1.2	1.3	1.5	0.9
	CV%		3.3	5.7	5.2	4.6	4.9	2.7
37.8°C	76LS-2	7.4	25.42	27.75	28.64	30.46	30.54	26.48
	76LS-3	7.1	28.41	30.6	31.14	32.13	31.06	26.86
	76LS-5	7.1	28.4	30.65	31.26	32.16	31.23	26.28
	Average		27.4	29.7	30.3	31.6	30.9	26.5
	St. Dev.		1.7	1.7	1.5	1.0	0.4	0.3
	CV%		6.3	5.6	4.9	3.1	1.2	1.1
54.4°C	76LS-2	7.4	30.35	29.23	28.36	25.13	23.41	18.78
	76LS-3	7.1	31.03	29.22	27.87	25.31	23.1	18.61
	76LS-5	7.1	30.5	28.55	26.95	23.43	20.69	16.19
	Average		30.6	29.0	27.7	24.6	22.4	17.9
	St. Dev.		0.4	0.4	0.7	1.0	1.5	1.4
	CV%		1.2	1.3	2.6	4.2	6.6	8.1

Note: St. Dev.: Standard Deviation
%CV: Coefficient of Variance (%)

Table B25
Phase angle test results of 76LM mixture

Temperature	Sample ID	Air Voids (%)	Phase Angle values at different frequencies (Hz)					
			25 Hz	10 Hz	5 Hz	1 Hz	0.5 Hz	0.1 Hz
-10°C	76LM-3	7.1	0.77	2.79	3.77	5.25	5.82	7.37
	76LM-4	6.9	0.63	2.69	3.59	5.04	5.56	7.02
	76LM-5	7.4	0.64	2.70	3.61	4.98	5.58	7.08
	Average		0.7	2.7	3.7	5.1	5.7	7.2
	St. Dev.		0.1	0.1	0.1	0.1	0.1	0.2
	CV%		11.5	2.0	2.7	2.8	2.6	2.6
4.4°C	76LM-3	7.1	5.83	8.63	10.16	13.63	15.04	18.53
	76LM-4	6.9	5.02	7.81	9.21	12.31	13.68	16.95
	76LM-5	7.4	5.46	8.24	9.76	13.18	14.71	18.14
	Average		5.4	8.2	9.7	13.0	14.5	17.9
	St. Dev.		0.4	0.4	0.5	0.7	0.7	0.8
	CV%		7.5	5.0	4.9	5.1	4.9	4.6
25°C	76LM-3	7.1	17.36	20.82	23.18	29.47	30.97	31.45
	76LM-4	6.9	17.76	21.4	23.73	29.76	30.89	31.72
	76LM-5	7.4	19.13	22.31	25.00	30.81	32.45	32.83
	Average		18.1	21.5	24.0	30.0	31.4	32.0
	St. Dev.		0.9	0.8	0.9	0.7	0.9	0.7
	CV%		5.1	3.5	3.9	2.3	2.8	2.3
37.8°C	76LM-3	7.1	26.35	29.66	30.74	33.21	32.82	29.06
	76LM-4	6.9	28.03	30.54	31.54	33.5	32.69	29.00
	76LM-5	7.4	29.49	31.56	33.68	34.55	33.55	29.38
	Average		28.0	30.6	32.0	33.8	33.0	29.1
	St. Dev.		1.6	1.0	1.5	0.7	0.5	0.2
	CV%		5.6	3.1	4.8	2.1	1.4	0.7
54.4°C	76LM-3	7.1	31.54	30.6	29.56	26.68	23.78	18.24
	76LM-4	6.9	32.23	31.52	29.91	27.17	24.48	18.36
	76LM-5	7.4	31.96	31.12	29.94	25.6	23.19	17.83
	Average		31.9	31.1	29.8	26.5	23.8	18.1
	St. Dev.		0.3	0.5	0.2	0.8	0.6	0.3
	CV%		1.1	1.5	0.7	3.0	2.7	1.5

Note: St. Dev.: Standard Deviation
%CV: Coefficient of Variance (%)